Principles and Basics of InSAR

Irena Hajnsek

*Earth Observation and Remote Sensing,
Institute of Environmental Engineering, ETH Zürich
*Microwaves and Radar Institut,
German Aerospace Center, Oberpfaffenhofen

Earth Observation and Remote Sensing

hajnsek@ifu.baug.ethz.ch
irena.hajnsek@dlr.de

ETH
Eidgenössische Technische Hochschule Zürich
Swiss Federal Institute of Technology Zurich

SAR Interferometry

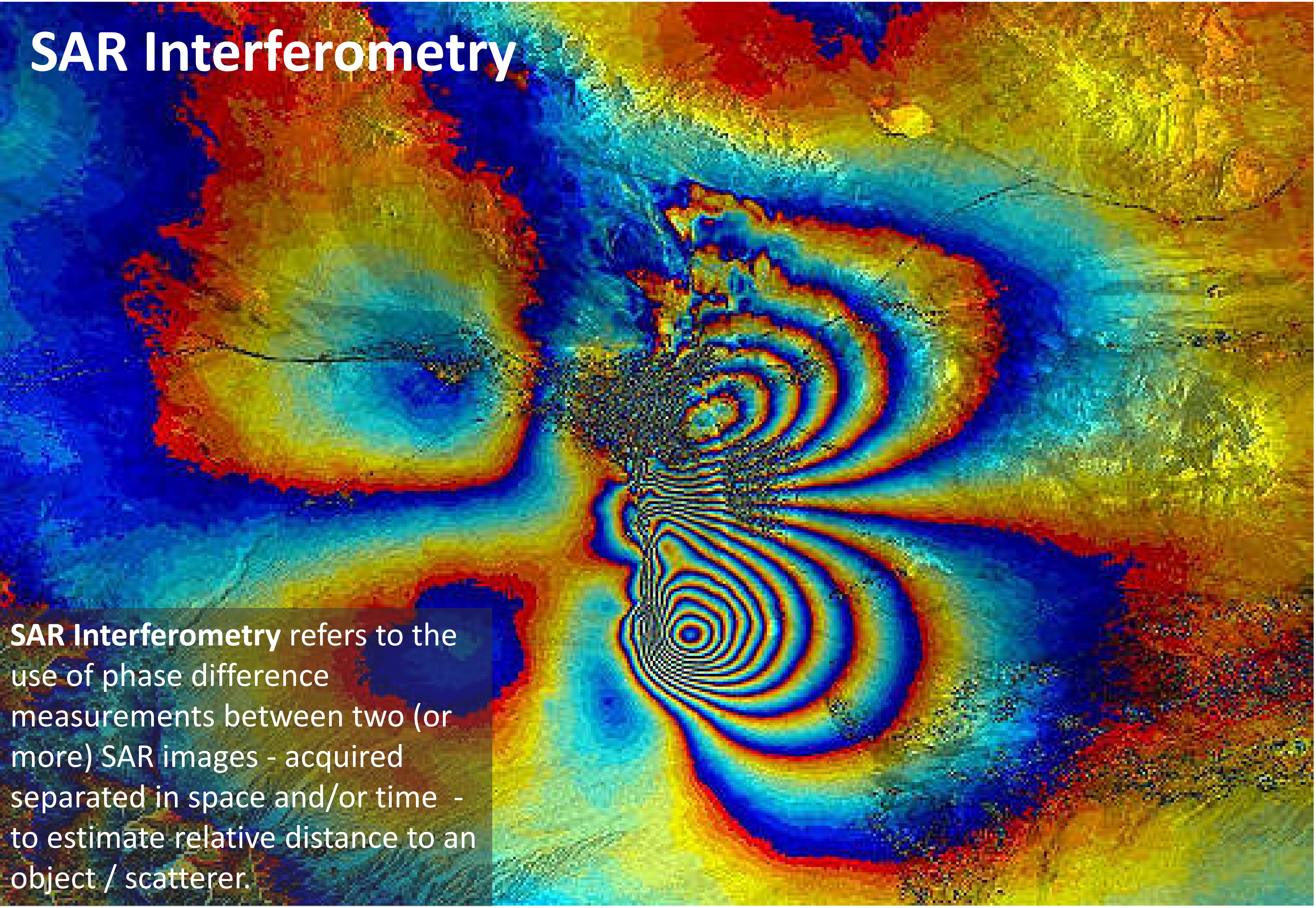

SAR Interferometry refers to the use of phase difference measurements between two (or more) SAR images - acquired separated in space and/or time - to estimate relative distance to an object / scatterer.

SAR Interferometry

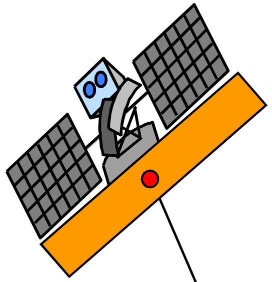

Signal from resolution cell P in Image 1: $i_1 = |i_1| \exp[-i(2\frac{2\pi}{\lambda}R_1) + \varphi_{S1}]$

Phase: $\varphi_1 = \arg(\ i_1) = \boxed{(2\frac{2\pi}{\lambda}R_1)} + \boxed{\varphi_{S1}}$

R_1

Term 1: Deterministic - proportional to the range distance R_1 of P

Term 2: Stochastic - induced by the scatterer (Speckle)

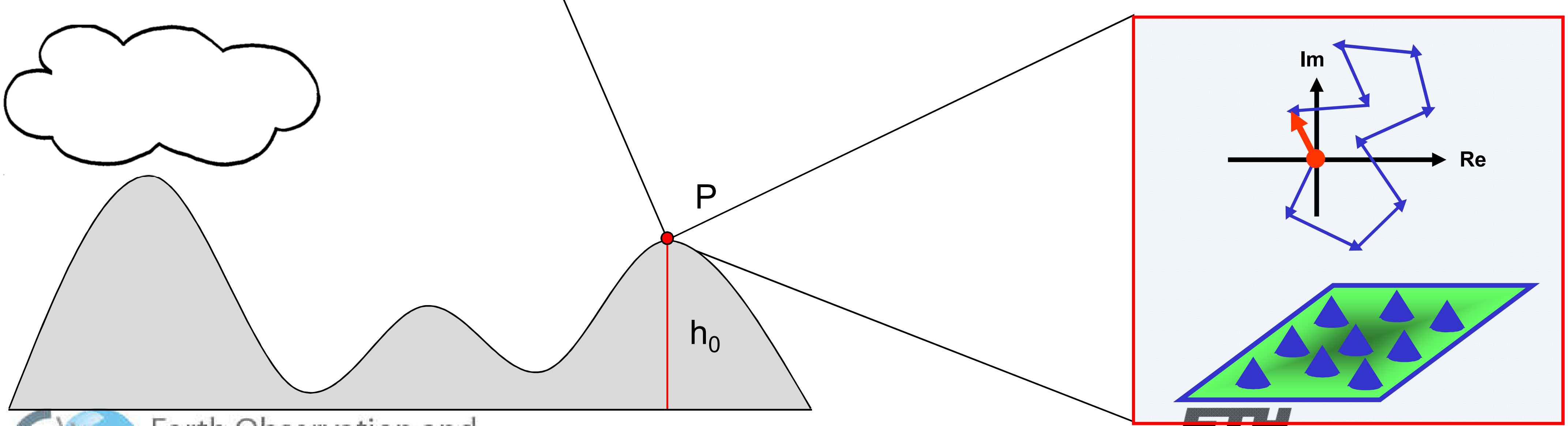

hajnsek@ifu.baug.ethz.ch
irena.hajnsek@dlr.de

ERS – Bachu / China ~ 100 km × 80 km

Amplitude of Image 1

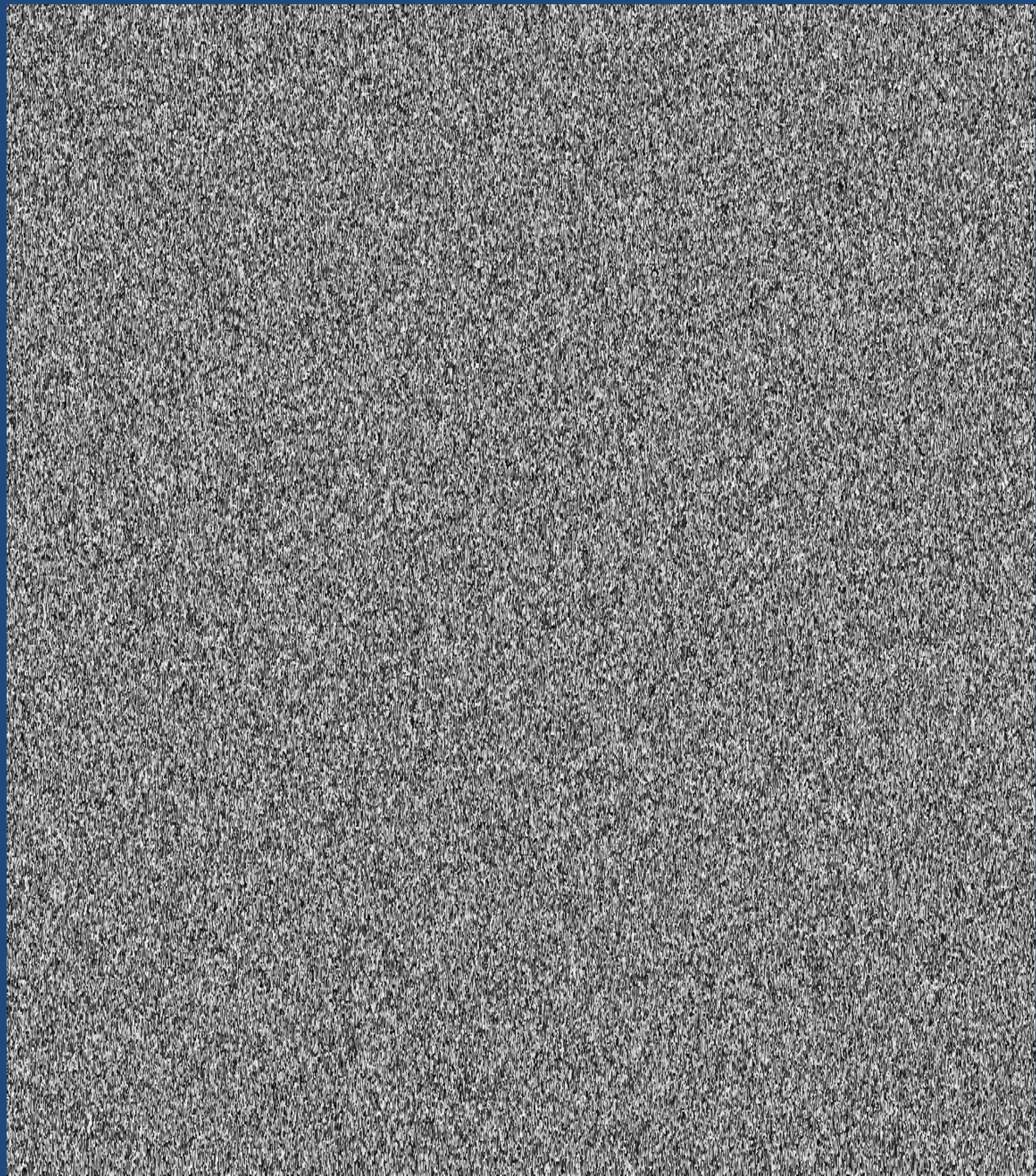

Phase of Image 1

SAR Interferometry

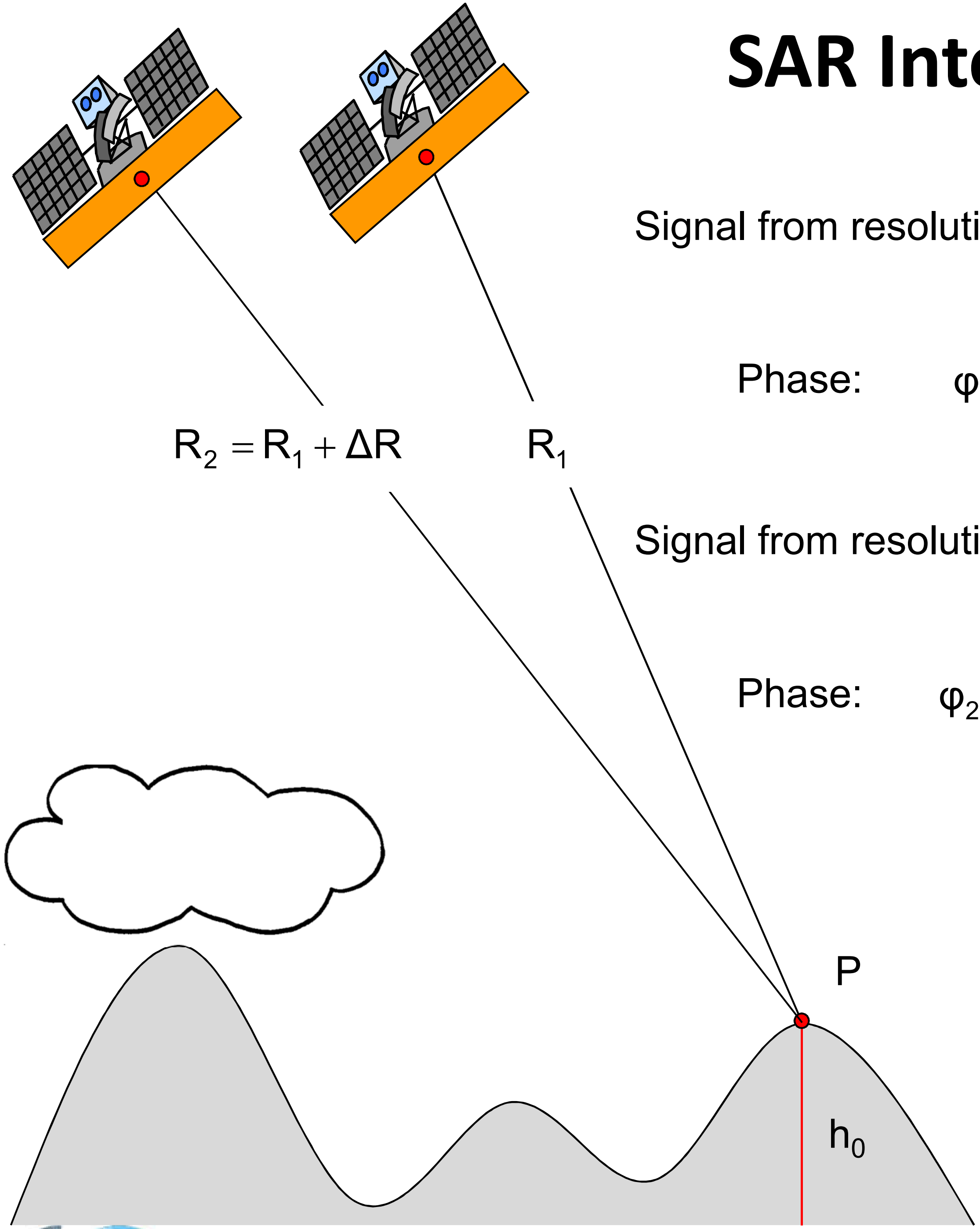

Signal from resolution cell P in Image 1: $i_1 = |i_1| \exp[-i(2\frac{2\pi}{\lambda}R_1) + \varphi_{S1}]$

Phase: $\varphi_1 = \arg(i_1) = \boxed{(2\frac{2\pi}{\lambda}R_1)} + \boxed{\varphi_{S1}}$

Signal from resolution cell P in Image 2: $i_2 = |i_2| \exp[-i(2\frac{2\pi}{\lambda}R_2) + \varphi_{S2}]$

Phase: $\varphi_2 = \arg(i_2) = \boxed{(2\frac{2\pi}{\lambda}R_2)} + \boxed{\varphi_{S2}}$

hajnsek@ifu.baug.ethz.ch
irena.hajnsek@dlr.de

SAR Interferometry

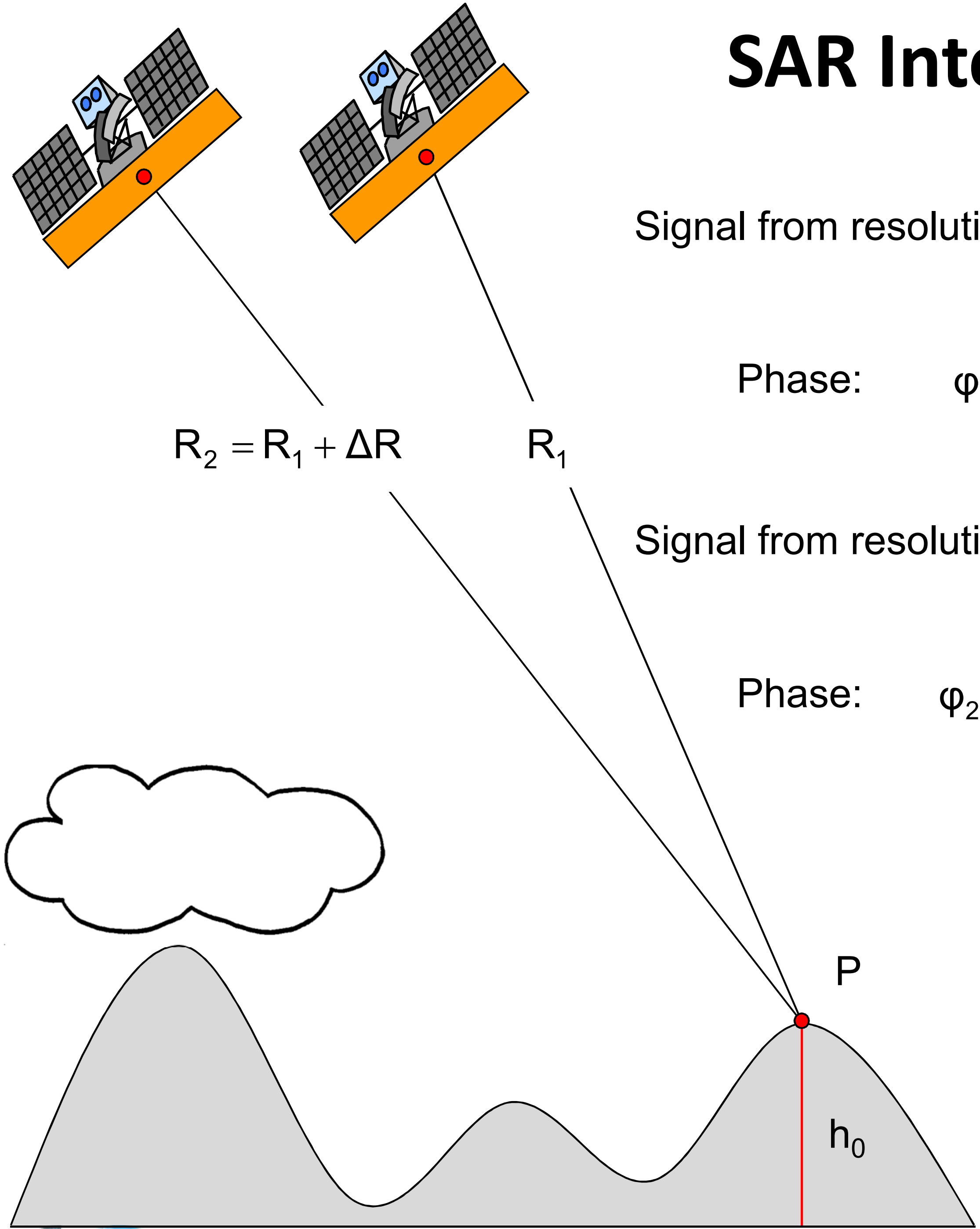

Signal from resolution cell P in Image 1: $i_1 = |i_1| \exp[-i(2\frac{2\pi}{\lambda}R_1) + \varphi_{S1}]$

Phase: $\varphi_1 = \arg(i_1) = \boxed{(2\frac{2\pi}{\lambda}R_1)} + \boxed{\varphi_{S1}}$

Signal from resolution cell P in Image 2: $i_2 = |i_2| \exp[-i(2\frac{2\pi}{\lambda}R_2) + \varphi_{S2}]$

Phase: $\varphi_2 = \arg(i_2) = \boxed{(2\frac{2\pi}{\lambda}R_2)} + \boxed{\varphi_{S2}}$

Assuming $\varphi_{S1} = \varphi_{S2}$!!!

Interferogram: $i_1 i_2^* = |i_1 i_2^*| \exp[-i(2\frac{2\pi}{\lambda}\Delta R)]$

Phase: $\varphi_{Int} = \frac{\mathrm{Re}\{i_1 i_2^*\}}{\mathrm{Im}\{i_1 i_2^*\}} = \boxed{2\frac{2\pi}{\lambda}\Delta R}$

Deterministic !!!

Earth Observation and Remote Sensing

hajnsek@ifu.baug.e
irena.hajnsek@d

ERS – Bachu / China ~ 100 km × 80 km

Amplitude of Image 1

Amplitude of Image 2

ERS – Bachu / China ~ 100 km × 80 km

Amplitude of Image 1

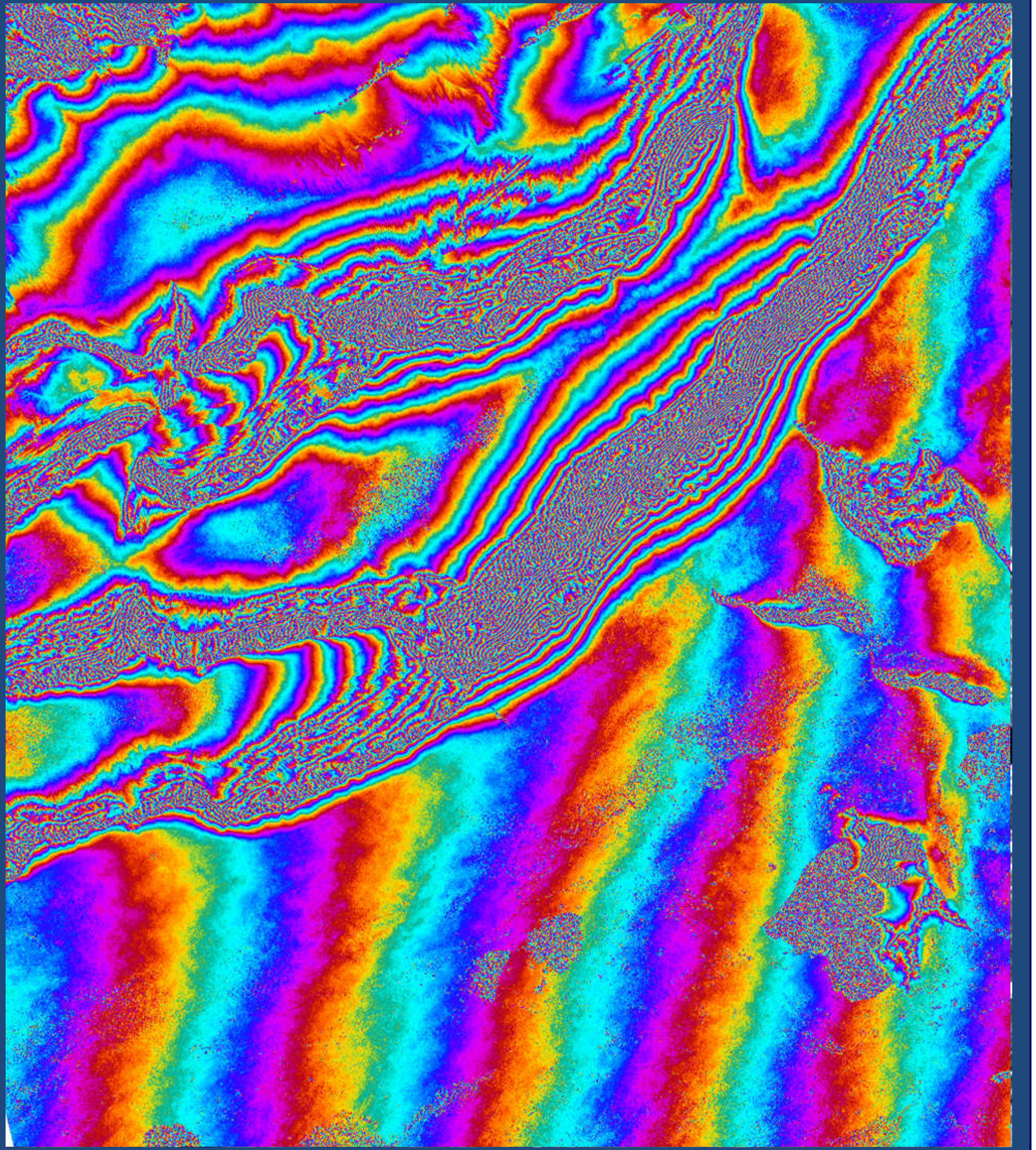

Interferometric Phase Image

SAR Interferometry

Interferometric Phase: $\varphi = 2\frac{2\pi}{\lambda}\boxed{\Delta R}$

The interferometric phase φ is another way to measure the (relative) distance ΔR:

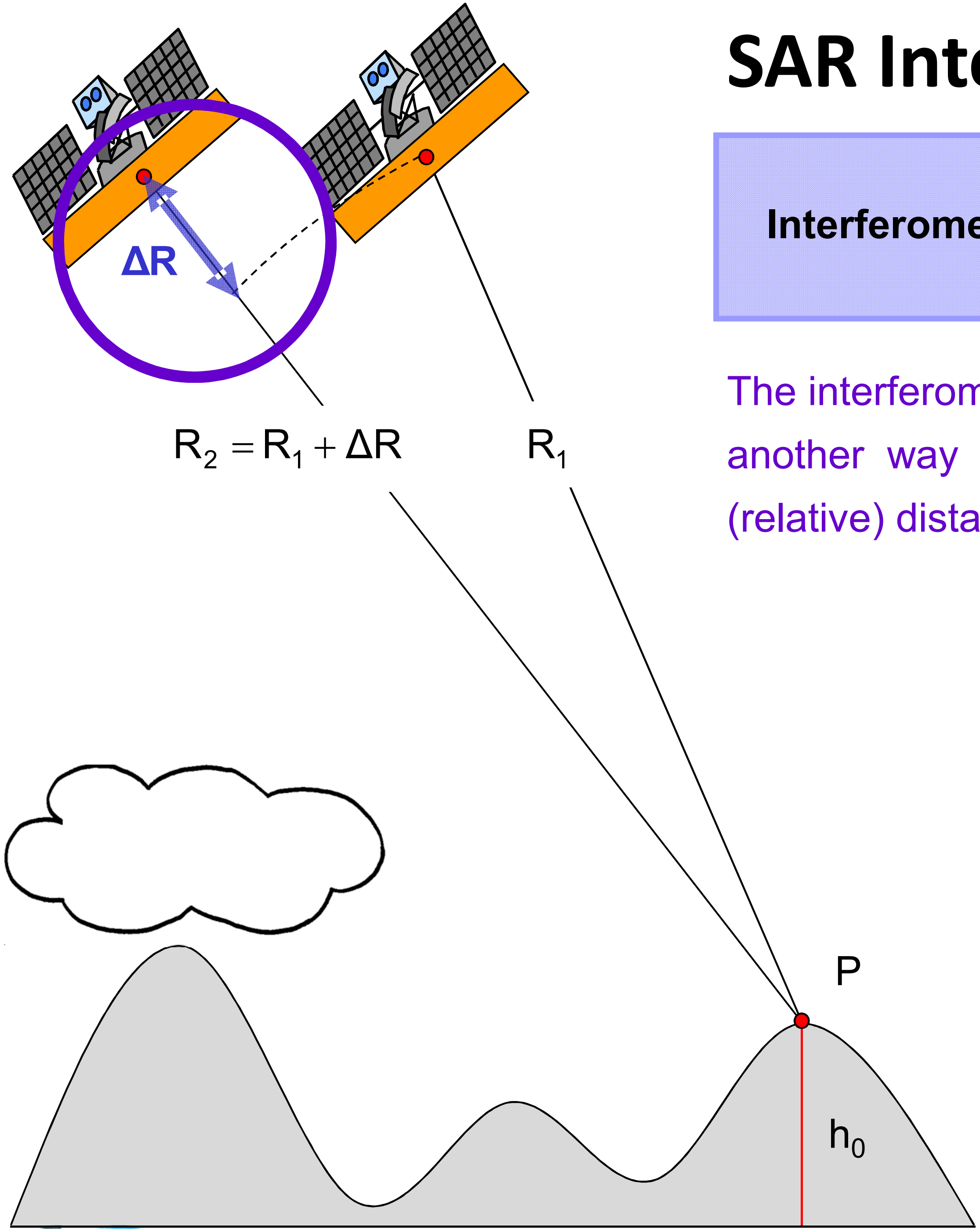

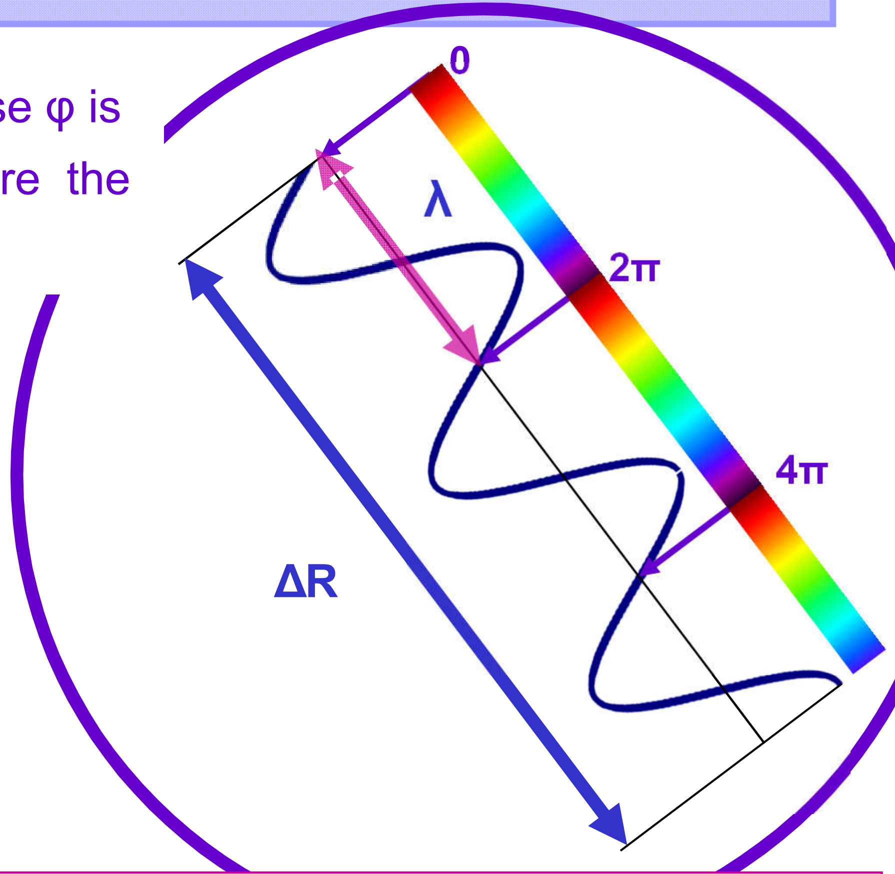

Phase measurements in interferometric systems can be made with a degree level accuracy. At radar wavelengths of 1-90cm (Ku to P-band) this corresponds to millimeter accuracy !!!

Earth Observation and Remote Sensing

hajnsek@ifu.baug.ethz.ch
irena.hajnsek@dlr.de

DEM Generation

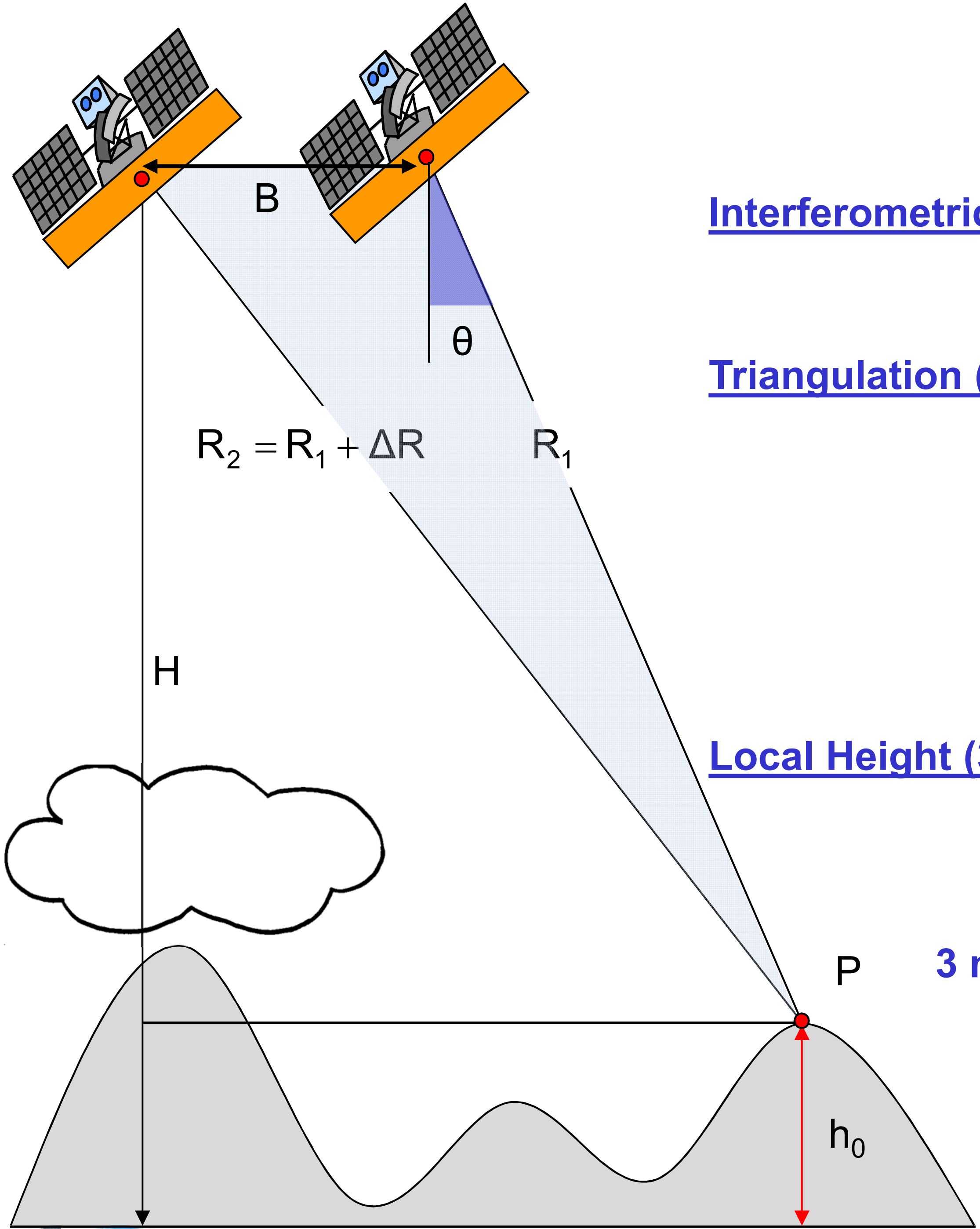

Interferometric Phase (1): $\varphi = 2\frac{2\pi}{\lambda}\Delta R + 2\pi N \quad N = 0, \ \pm 1, \ \pm 2$

Triangulation (2): $(R_1 + \Delta R)^2 = R_1^{\ 2} + B^2 - 2R_1 B\cos(\pi/2 + \theta) \rightarrow$

$$\rightarrow \sin(\theta) = \frac{(R_1 + \Delta R)^2 - R_1^{\ 2} - B^2}{2R_1 B}$$

Local Height (3): $h_0 = H - (R_1 + \Delta R)\cos(\theta)$

3 non-linear equations for 3 unknowns (h_0, θ, ΔR)

B … Spatial baseline and

R_1 … Range distance in Image 1 are known

Critical is the fact that the interferometric phase φ is initially measured modulo 2π ► Phase Unwrapping

Earth Observation and Remote Sensing

hajnsek@ifu.baug.e
irena.hajnsek@d

ERS – Bachu / China ~ 100 km × 80 km

Amplitude Image

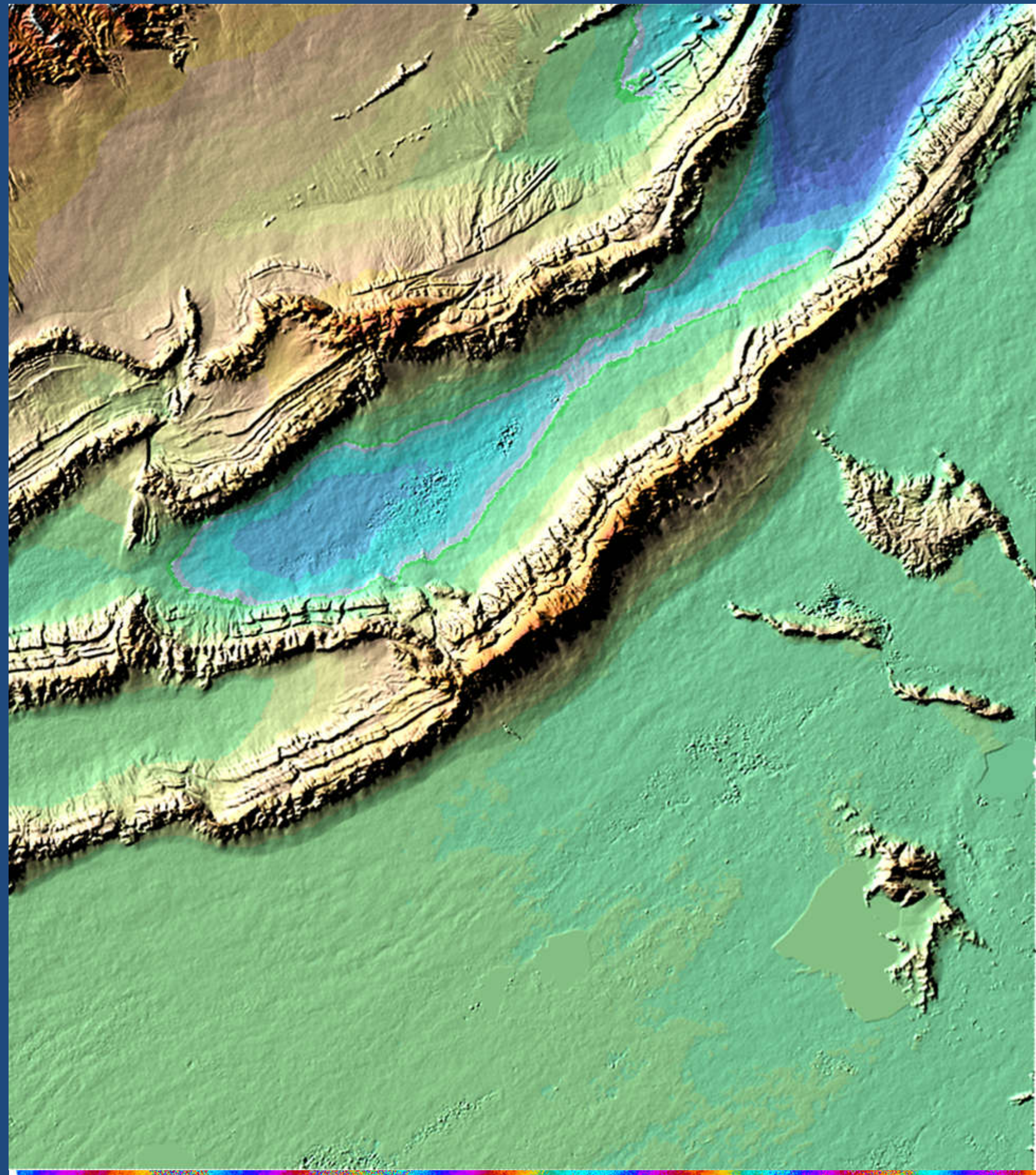

Digital Elevation Model with false colors

ERS – Bachu / China ~ 100 km × 80 km

Amplitude Image

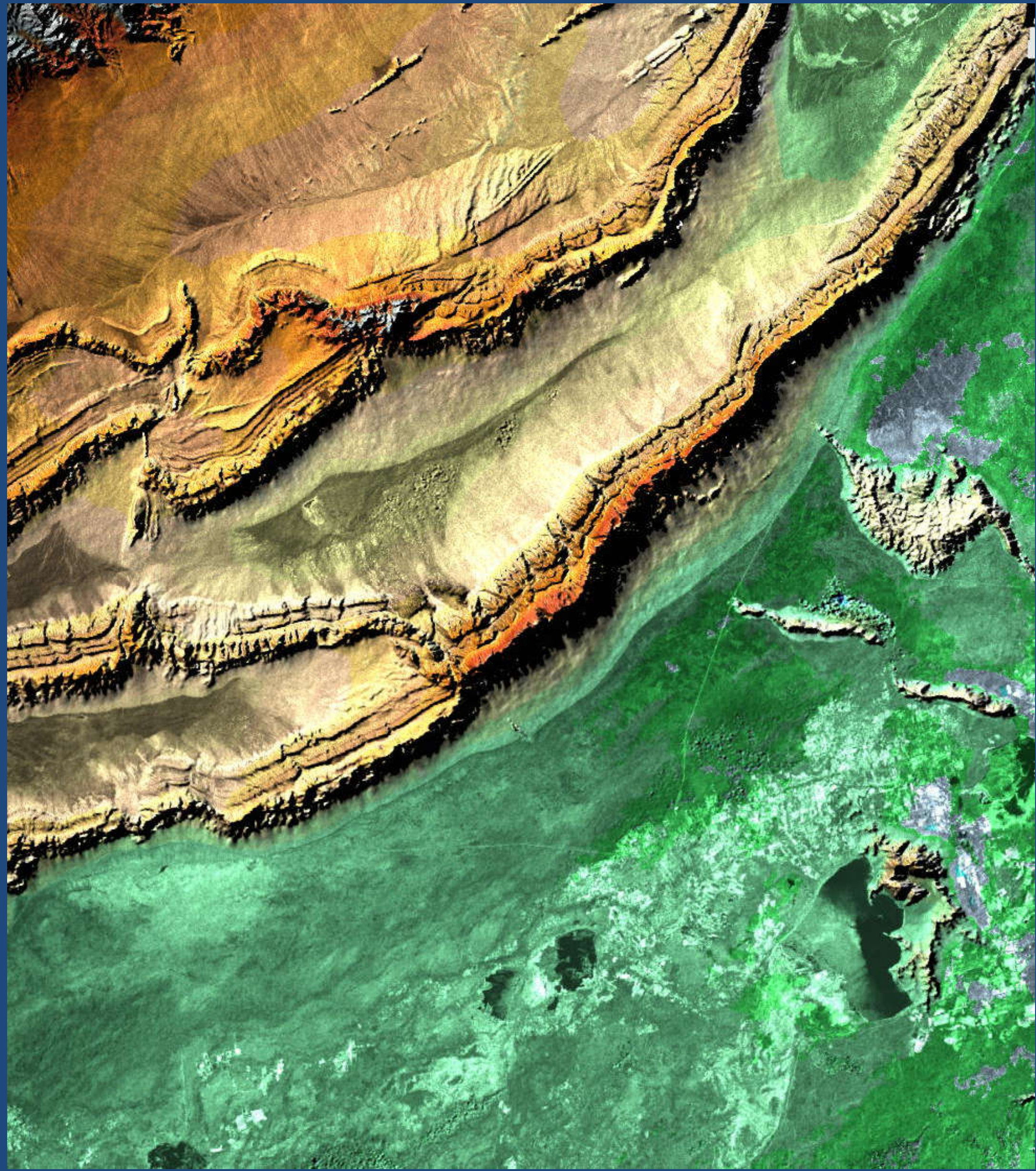

Digital Elevation Model and SAR image

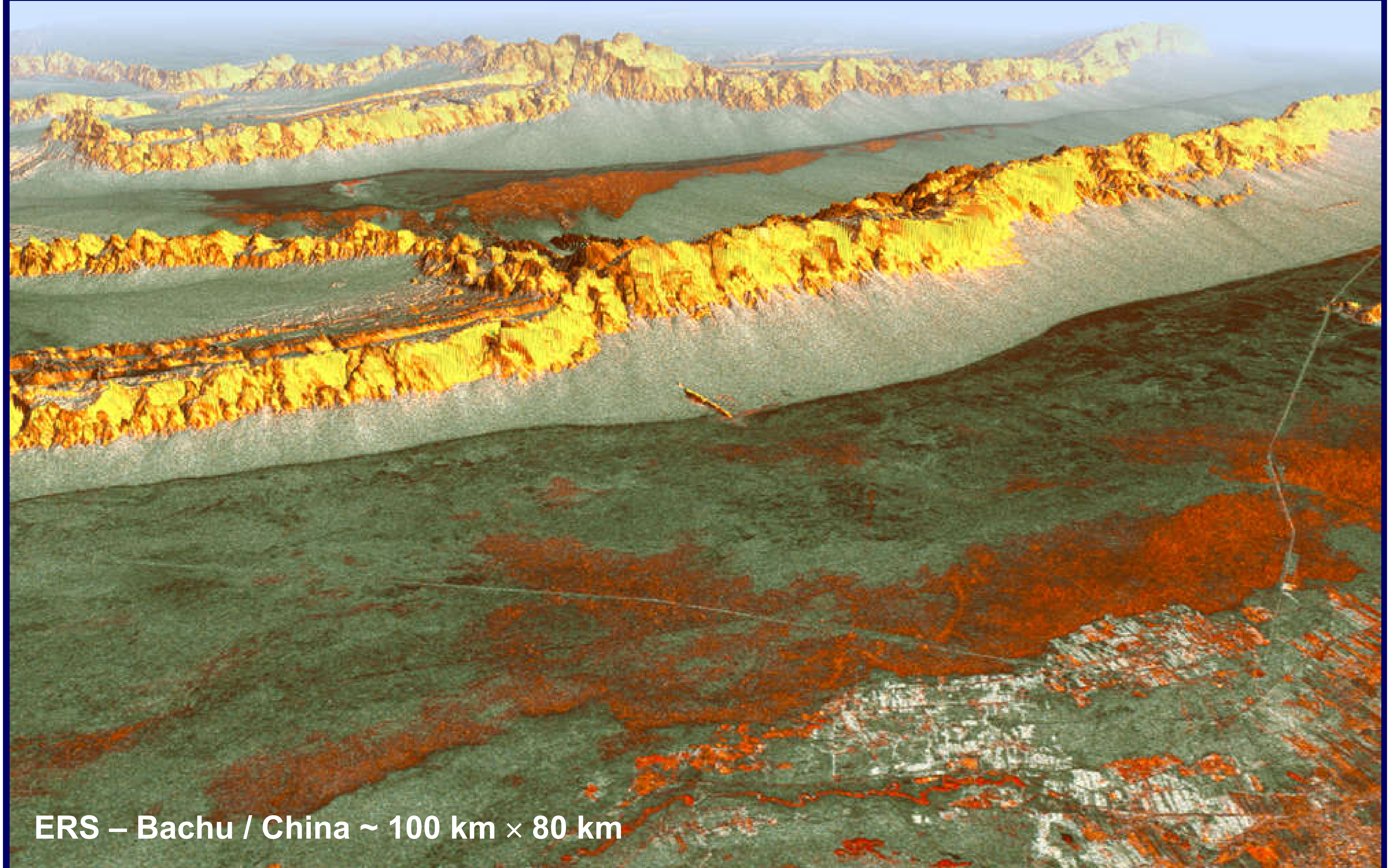
ERS – Bachu / China ~ 100 km × 80 km

InSAR Phase: Height Sensitivity

Interferometric Phase: $\varphi = 2\frac{2\pi}{\lambda}\Delta R + 2\pi N$ where $N = 0, \pm 1, \pm 2$

P_1 & P_2 : Two points at the same range but different heights h_1 & h_2 :

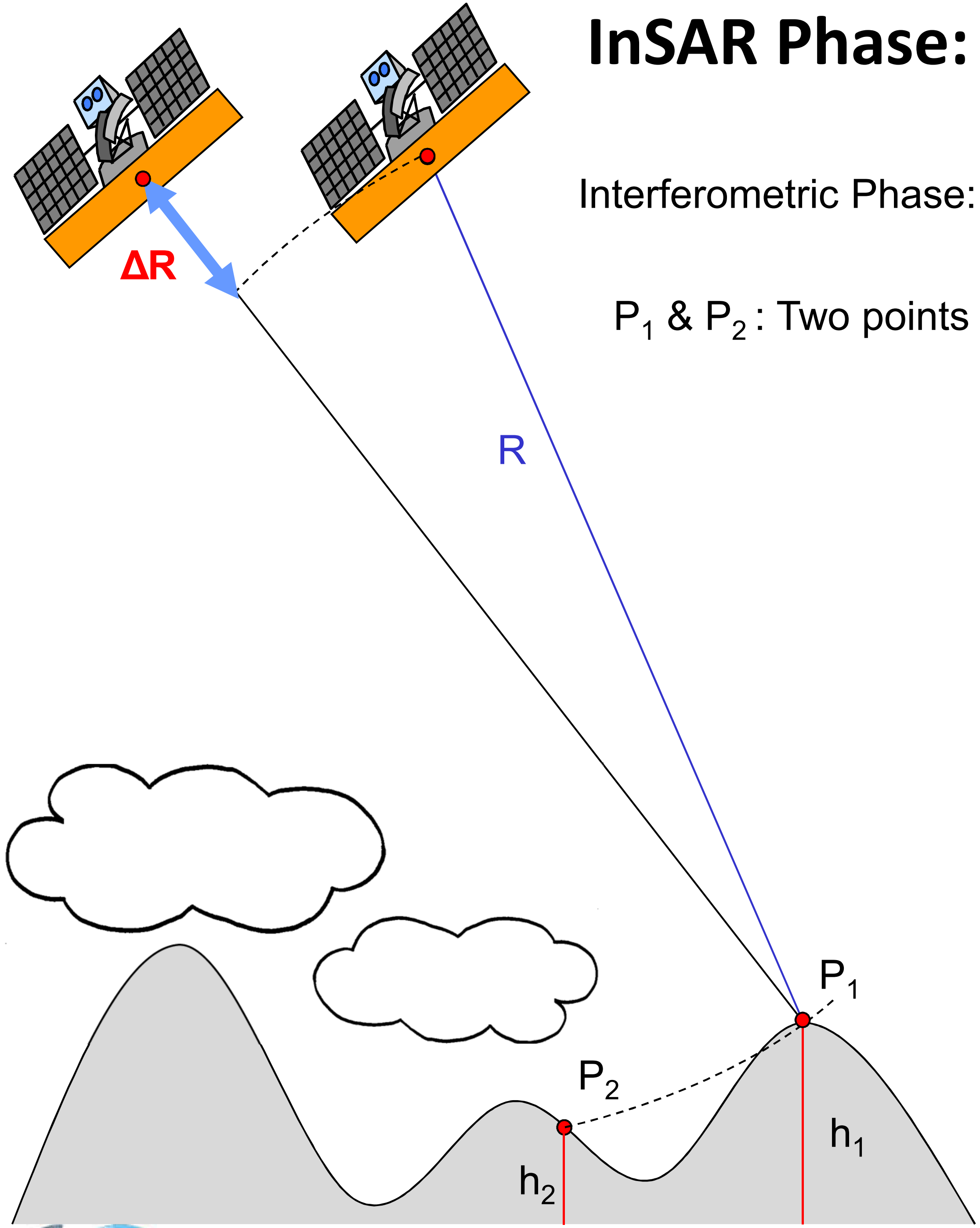

InSAR Phase: Height Sensitivity

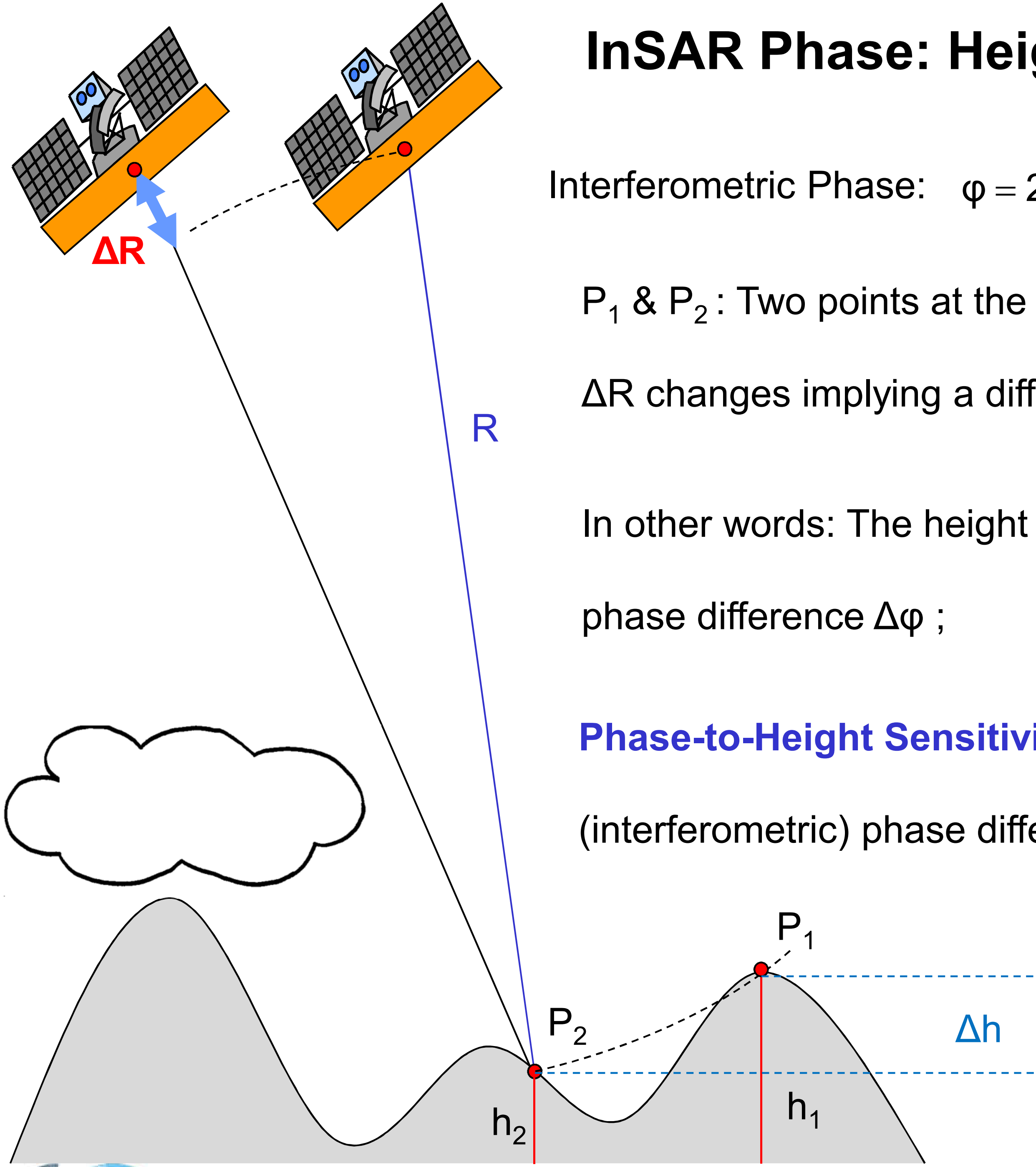

Interferometric Phase: $\varphi = 2\frac{2\pi}{\lambda}\Delta R + 2\pi N$ where $N = 0, \ \pm 1, \ \pm 2$

P_1 & P_2 : Two points at the same range but different heights h_1 & h_2

ΔR changes implying a different interferometric phase at each point

In other words: The height difference $\Delta h = h_1 - h_2$ causes an (interferometric) phase difference $\Delta\varphi$;

Phase-to-Height Sensitivity $\partial\varphi / \partial z$ [rad/m]: is defined by the (interferometric) phase difference caused by a given height difference (1m)

InSAR Phase: Height Sensitivity

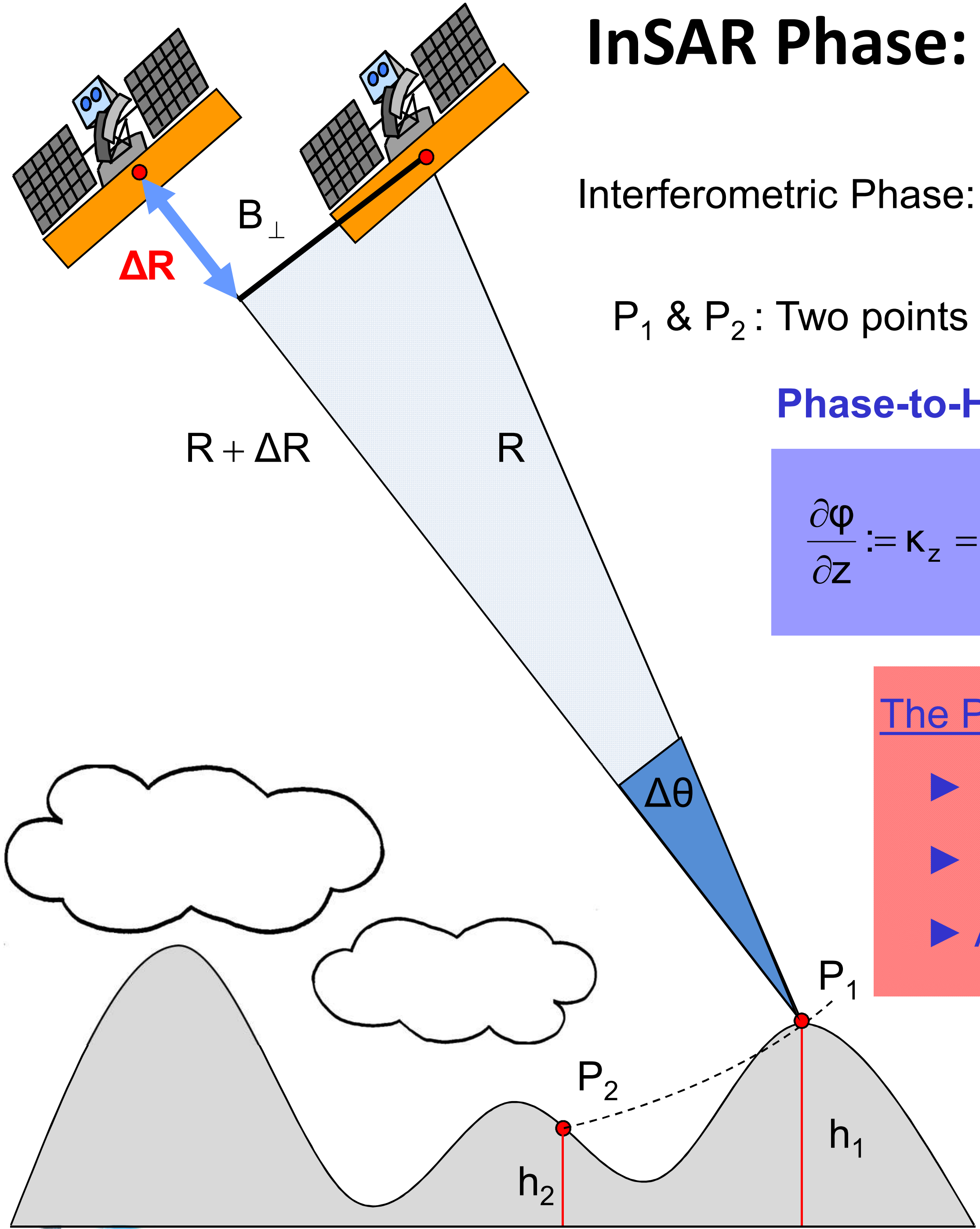

Interferometric Phase: $\varphi = 2\dfrac{2\pi}{\lambda}\boxed{\Delta R} + 2\pi N$ where $N = 0, \pm 1, \pm 2$

P_1 & P_2 : Two points at the same range but different heights h_1 & h_2 :

Phase-to-Height Sensitivity:

$$\frac{\partial\varphi}{\partial z} := \kappa_z = \frac{4\pi}{\lambda}\frac{\Delta\theta}{\sin(\theta)} \approx \frac{4\pi}{\lambda}\frac{B_\perp}{R\sin(\theta)}$$ using $$\Delta\theta \approx \frac{B_\perp}{R}$$

<u>The Phase-to-Height Sensitivity increases with:</u>

- ► Increasing the spatial baseline (i.e. $\Delta\theta$ or B❍);
- ► Increasing the system frequency (<u>i.e. decreasing λ</u>);
- ► At steeper (i.e. smaller) incidence angles θ.

Height of Ambiguity (HoA):

the height that causes a 2π phase difference:

$$HoA = \frac{\lambda}{4\pi}\frac{R\sin(\theta)}{B_\perp}2\pi = \frac{\lambda}{2}\frac{R\sin(\theta)}{B_\perp}$$

Earth Observation and Remote Sensing

hajnsek@ifu.baug.ethz.ch
irena.hajnsek@dlr.de

Swiss Federal Institute of Technology Zurich

InSAR Phase: Height Sensitivity

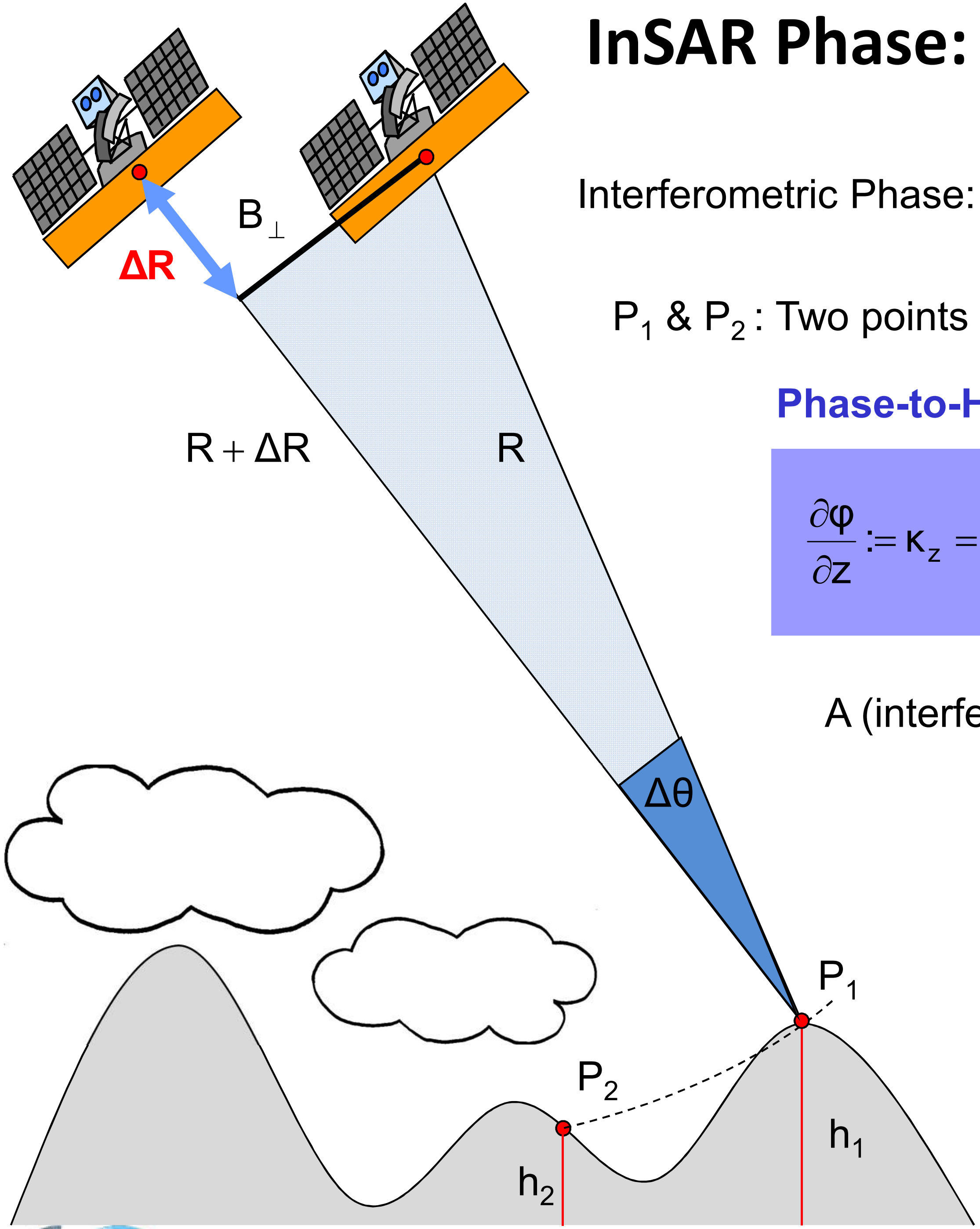

Interferometric Phase: $\varphi = 2\frac{2\pi}{\lambda}\Delta R + 2\pi\, N$ where $N = 0, \ \pm 1, \ \pm 2$

P_1 & P_2 : Two points at the same range but different heights h_1 & h_2 :

Phase-to-Height Sensitivity [rad/m]:

$$\frac{\partial\varphi}{\partial z} := \kappa_z = \frac{4\pi}{\lambda}\frac{\Delta\theta}{\sin(\theta)} \approx \frac{4\pi}{\lambda}\frac{B_\perp}{R\sin(\theta)}$$

using $\Delta\theta \approx \frac{B_\perp}{R}$

A (interferometric) phase error σ_φ induces a **height error σ_z:**

$$\sigma_z = \frac{1}{\partial\varphi/\partial z}\sigma_\varphi = \frac{1}{\kappa_z}\sigma_\varphi \approx \frac{\lambda}{4\pi}\frac{R\sin(\theta)}{B_\perp}\sigma_\varphi$$

For the same (interferometric) phase error σ_φ the induced height error decreases with:

- ► Increasing the spatial baseline;
- ► Increasing the system frequency;
- ► At steeper incidence angles θ.

hajnsek@ifu.baug.e
irena.hajnsek@d

InSAR Phase: Height Sensitivity

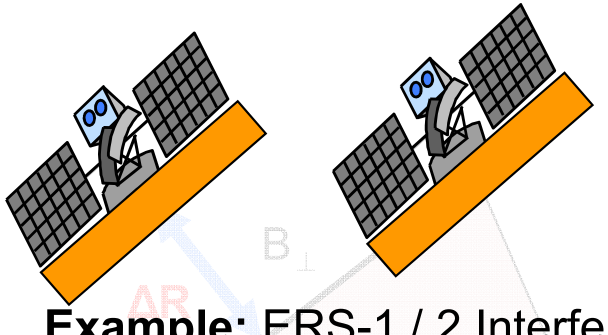

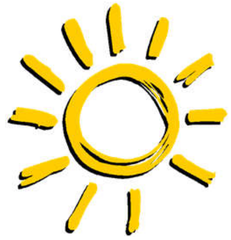

Example: ERS-1 / 2 Interferometry at C-band λ=5.6 cm =0.056m , R=870km, θ=23º=23 π/180 rad

Phase-to-Height Sensitivity: $$\frac{\partial\varphi}{\partial z} = \frac{4\pi}{\lambda}\frac{B_\perp}{R\sin(\theta)} \approx 2\pi\frac{B_\perp}{100^2}$$

$B_\perp$	$\partial\varphi/\partial z$ [rad/m]	HoA
50 m	$\approx$ 0.0314	$\approx$ 200 m
100 m	$\approx$ 0.0628	$\approx$ 100 m
200 m	$\approx$ 0.1256	$\approx$ 50 m

… with increasing $B_\perp$ the Phase-to-Height Sensitivity increases

Height Error: $$\sigma_z = \frac{1}{\partial\varphi/\partial z}\sigma_\varphi \approx \frac{1}{2\pi}\frac{100^2}{B_\perp}\sigma_\varphi$$

Assuming that one can estimate the interferometric phase with an accuracy of 30º (σ_φ=30 π/180 rad)

$B_\perp$	$\partial\varphi/\partial z$ [rad/m]	σ_z
50 m	$\approx$ 0.0314	$\approx$ 16.6 m
100 m	$\approx$ 0.0628	$\approx$ 8.3 m
200 m	$\approx$ 0.1256	$\approx$ 4.2 m

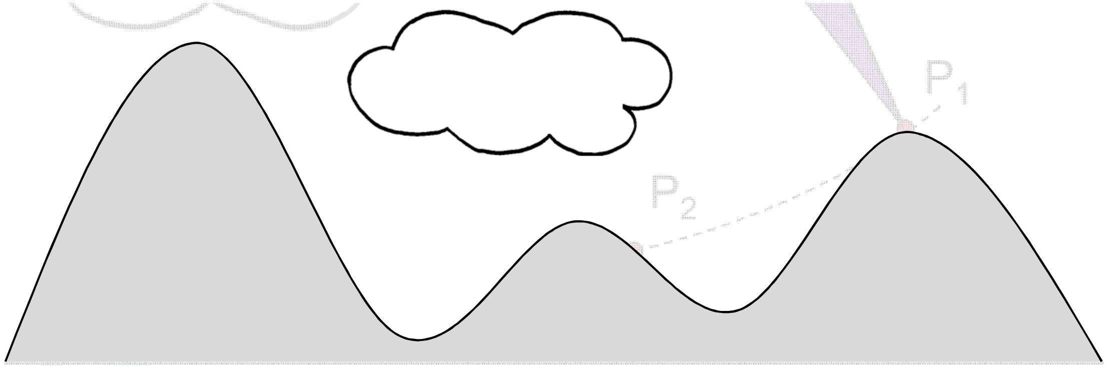

With increasing the spatial baseline ($B_\perp$) the height error decreases !!!

SAR Interferometry (InSAR)

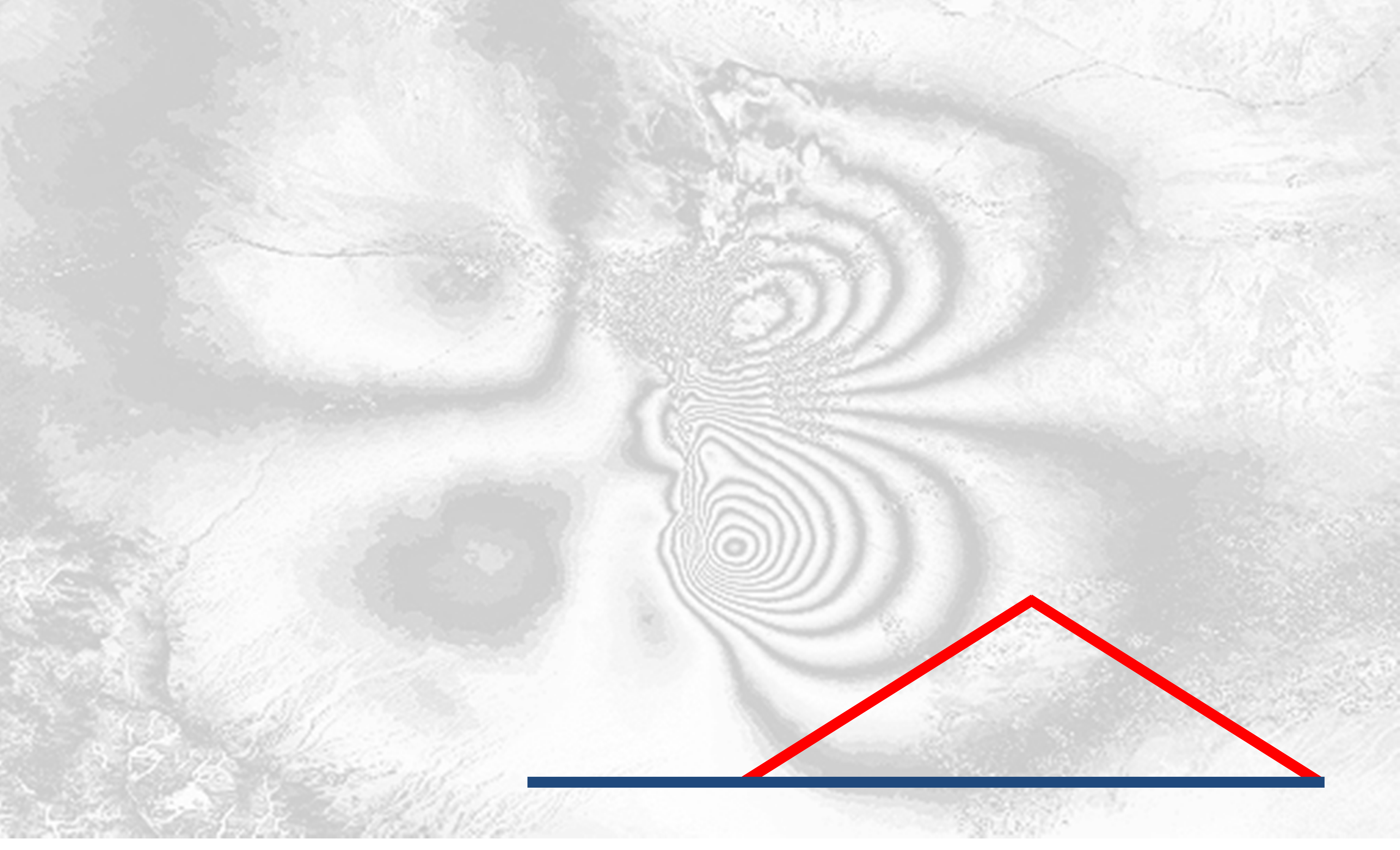

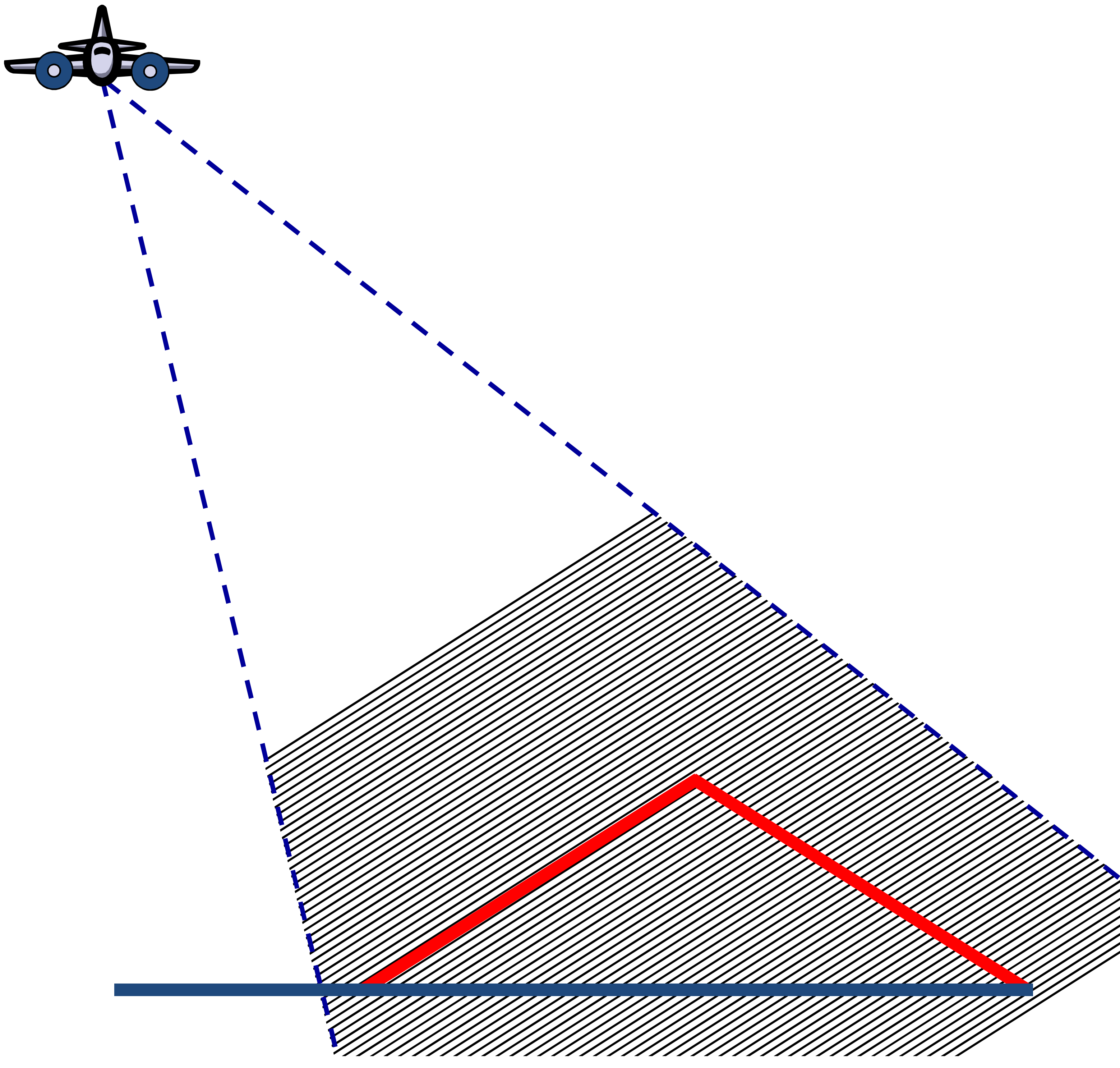

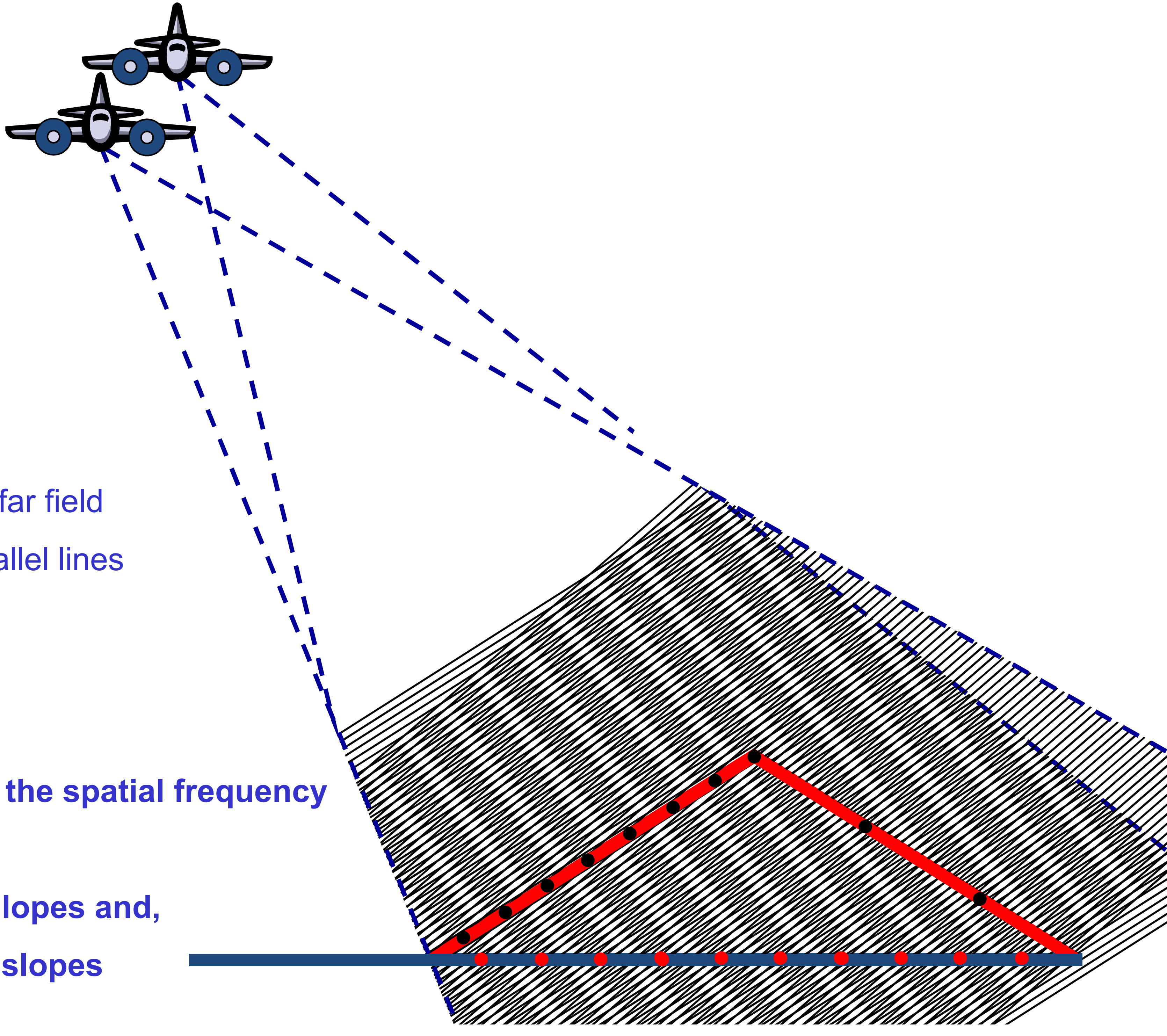

Interference pattern in the far field
consists of equidistant parallel lines
(parallel ray approx.).

With respect to flat terrain, **the spatial frequency** of the interference pattern

- **increases at positive slopes and,**
- **decreases at negative slopes**

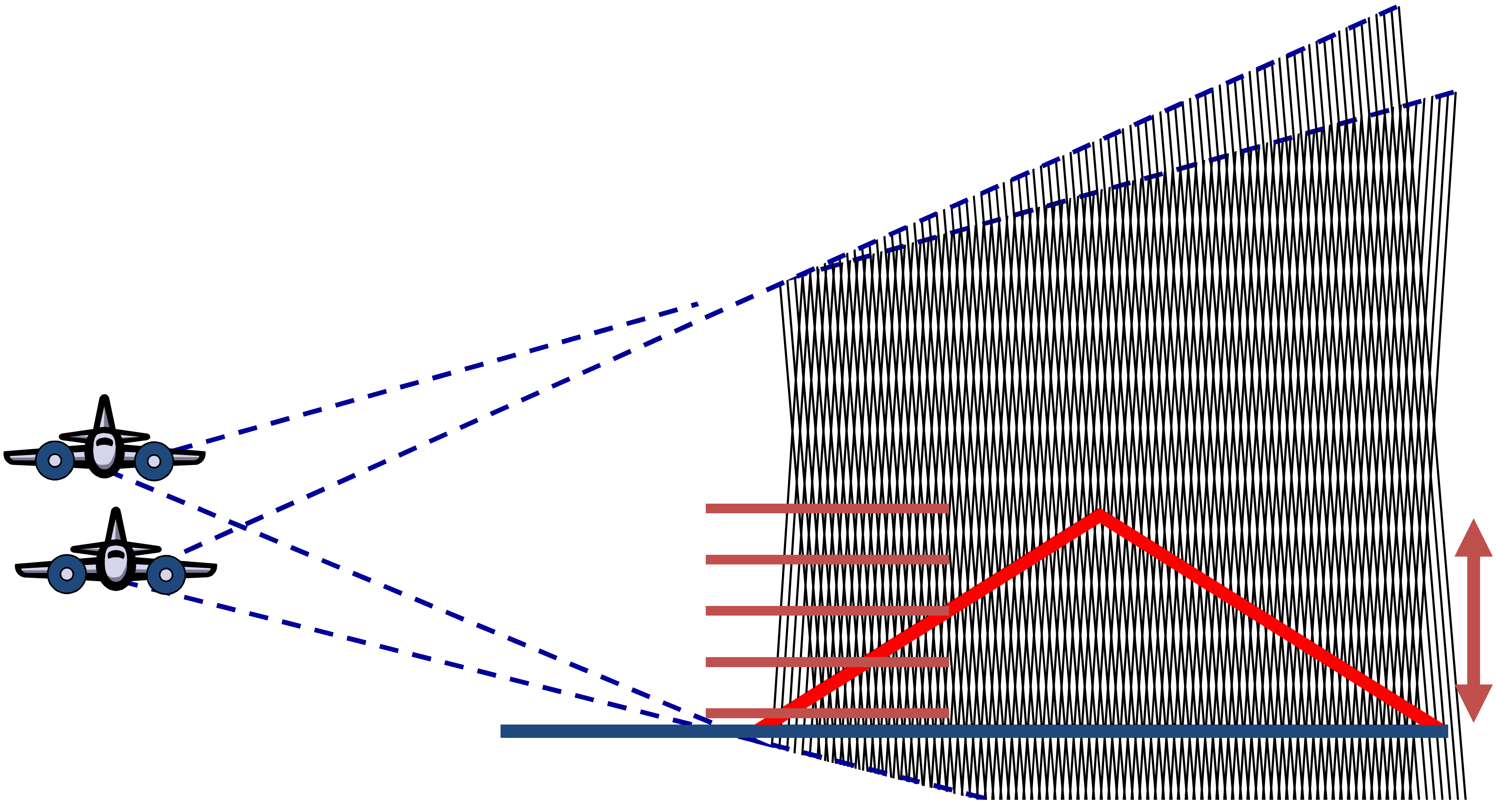

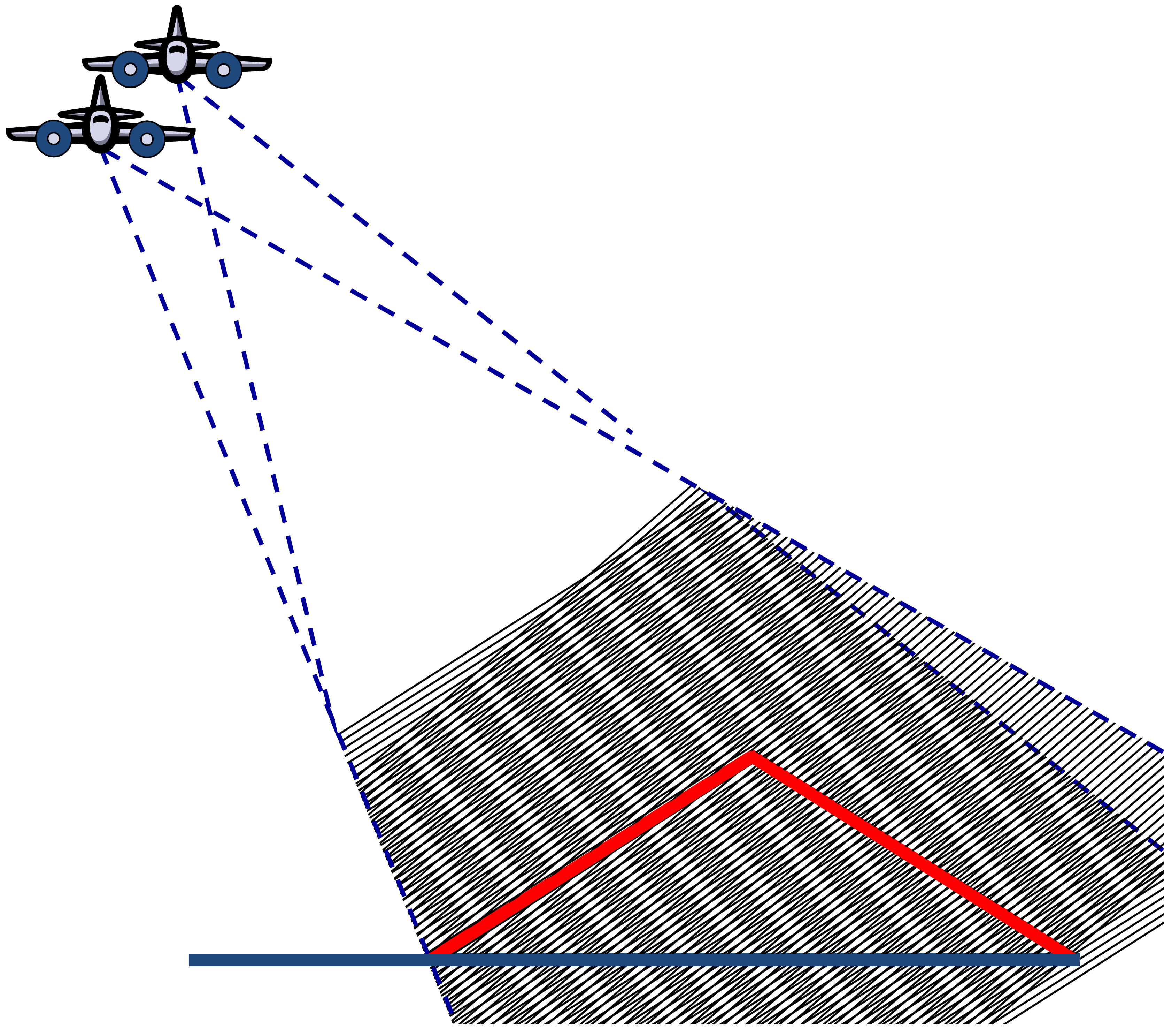

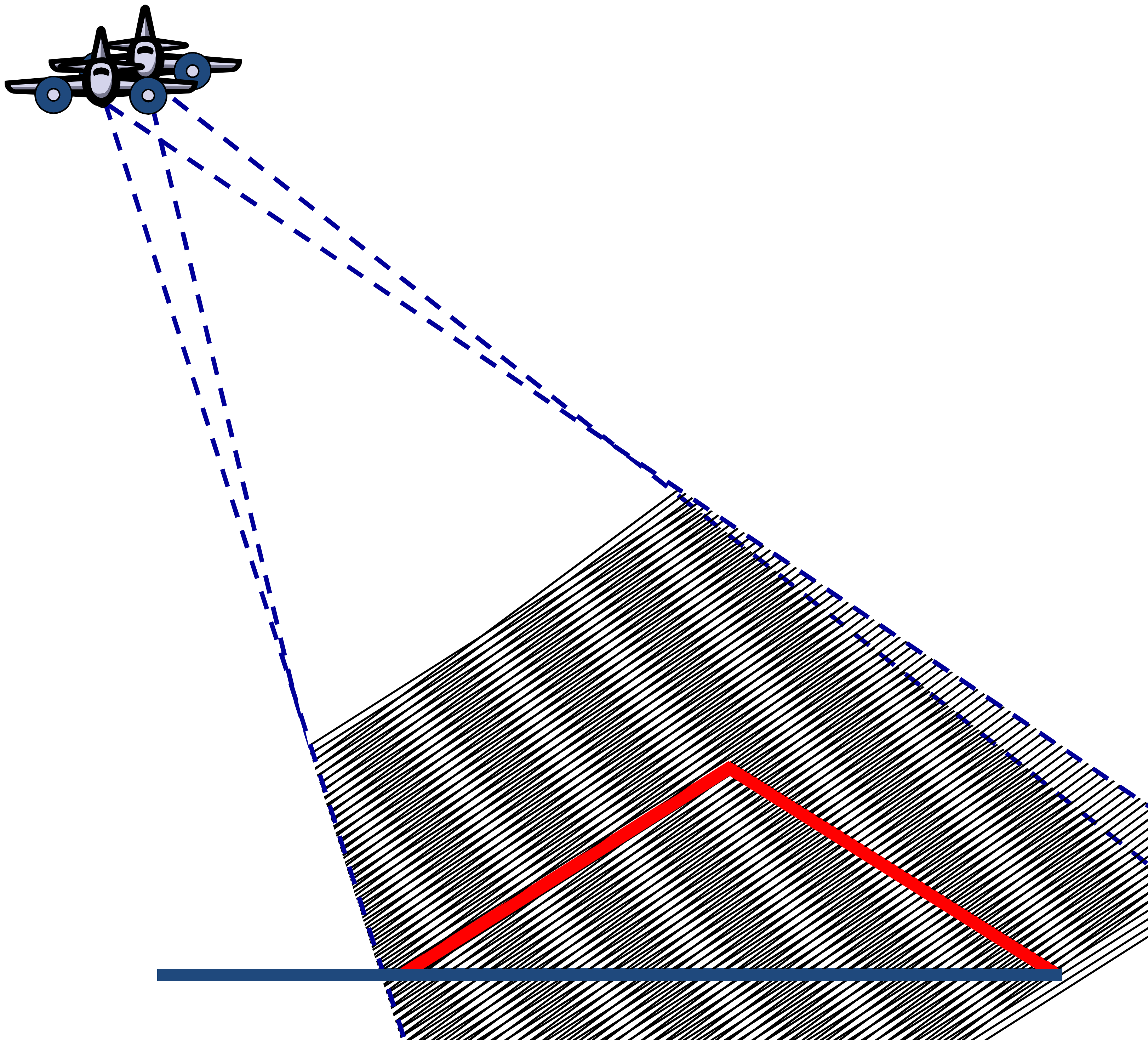

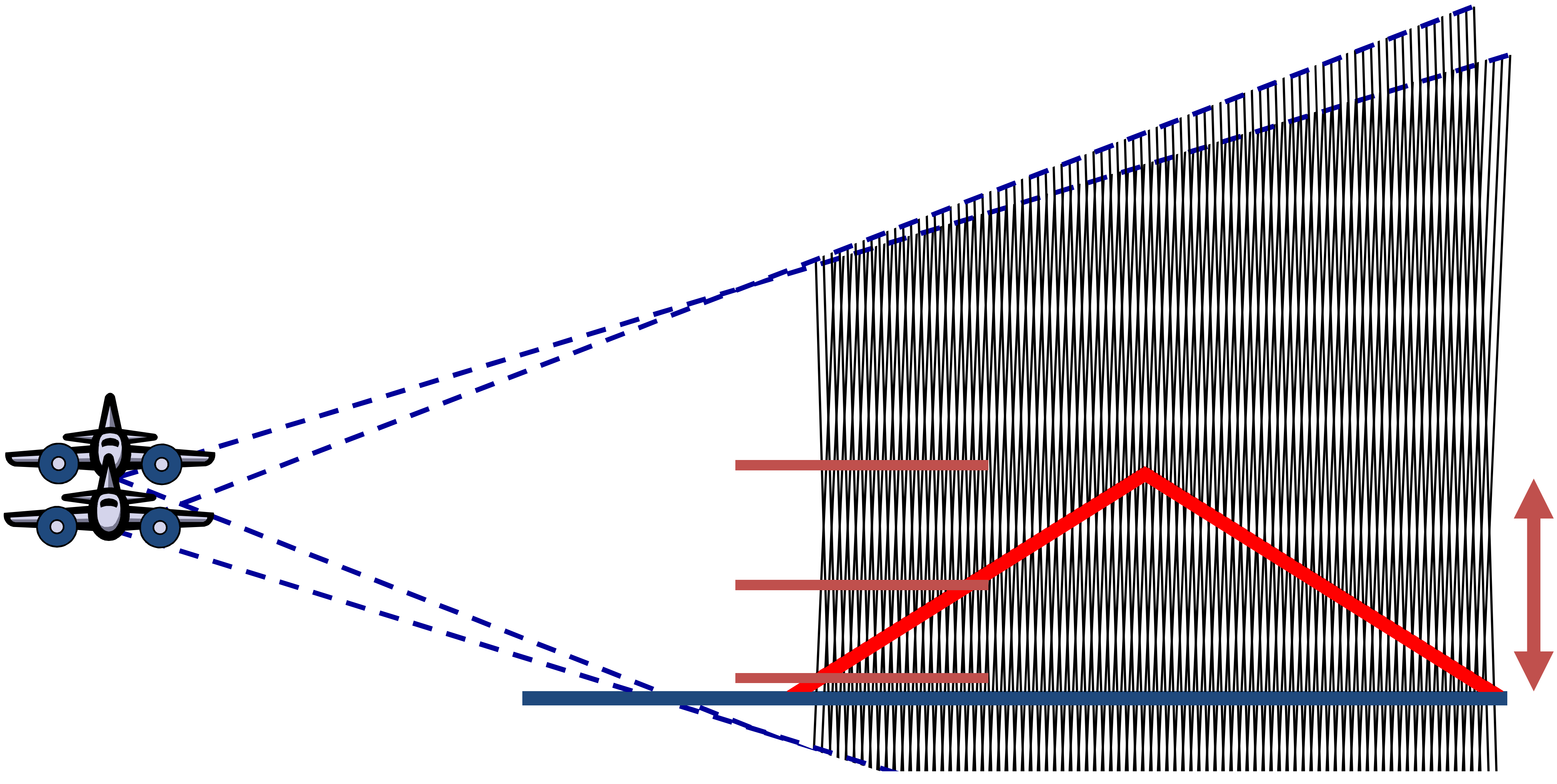

The Phase-to-Height Sensitivity increases with increasing the spatial baseline (i.e. Δθ or B❍);

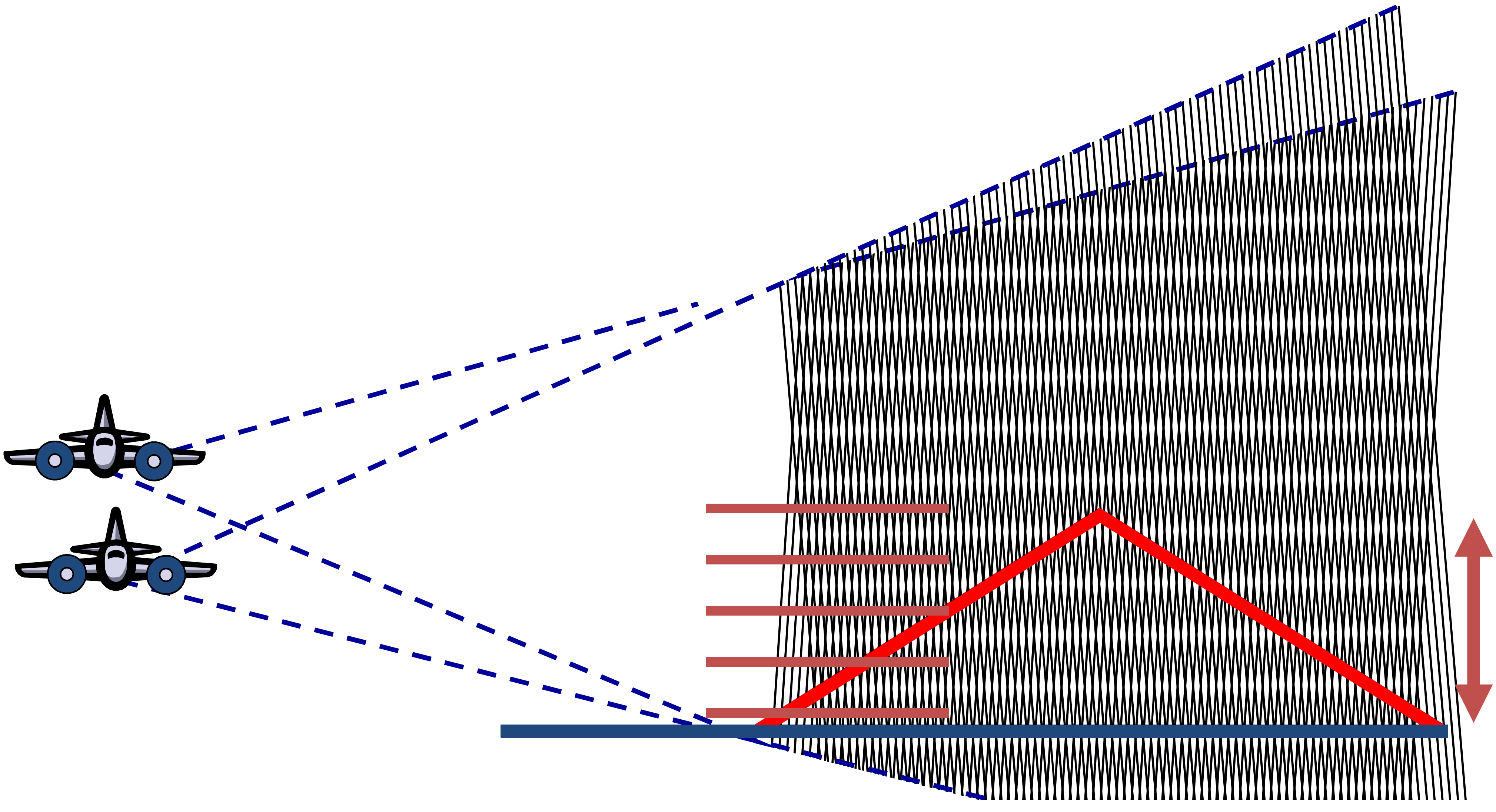

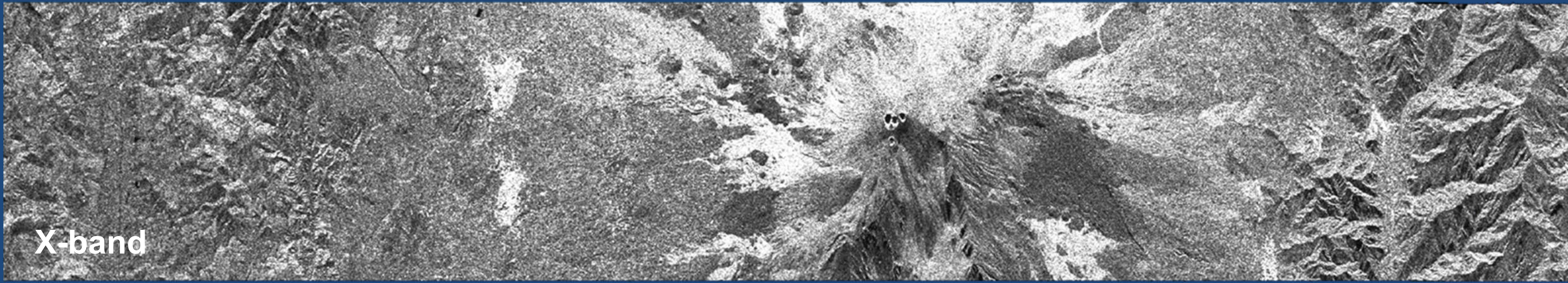

Amplitude Images

24 Hours Temporal Baseline

SIR-C / Test Site: Mt. Etna, Italy

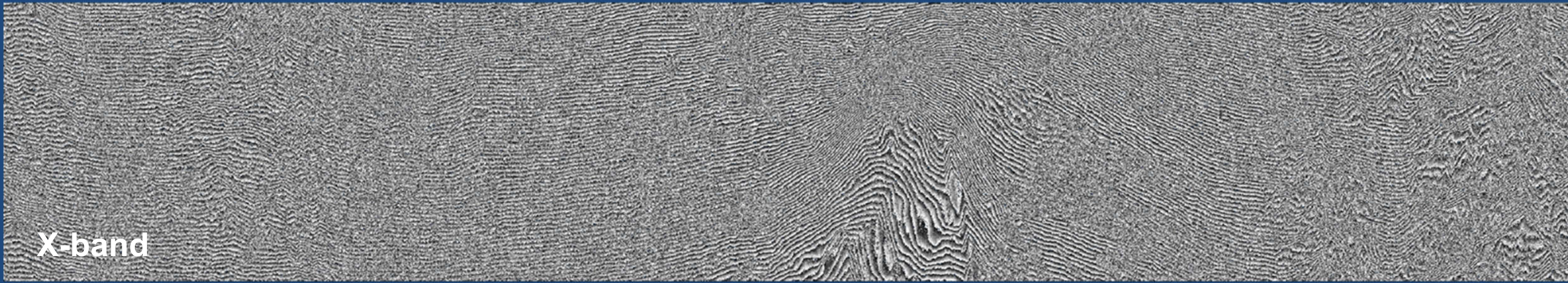

Phase Images

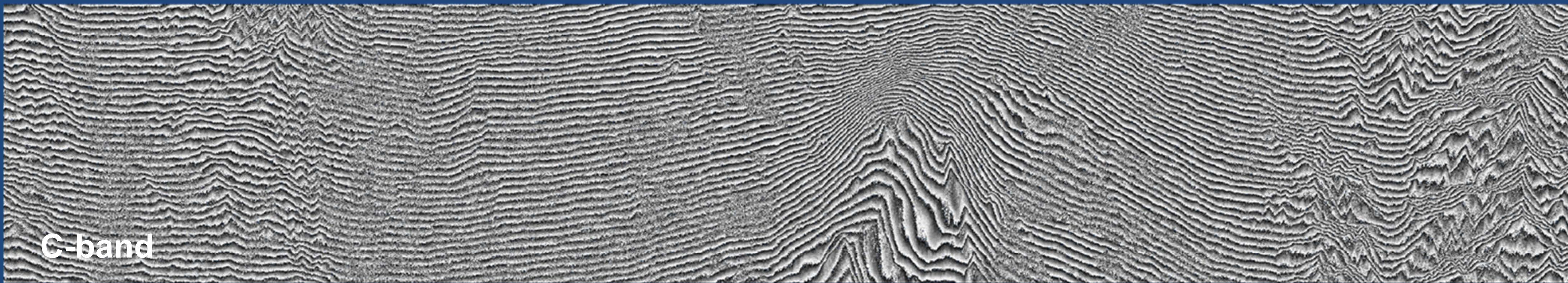

SIR-C / Test Site: Mt. Etna, Italy

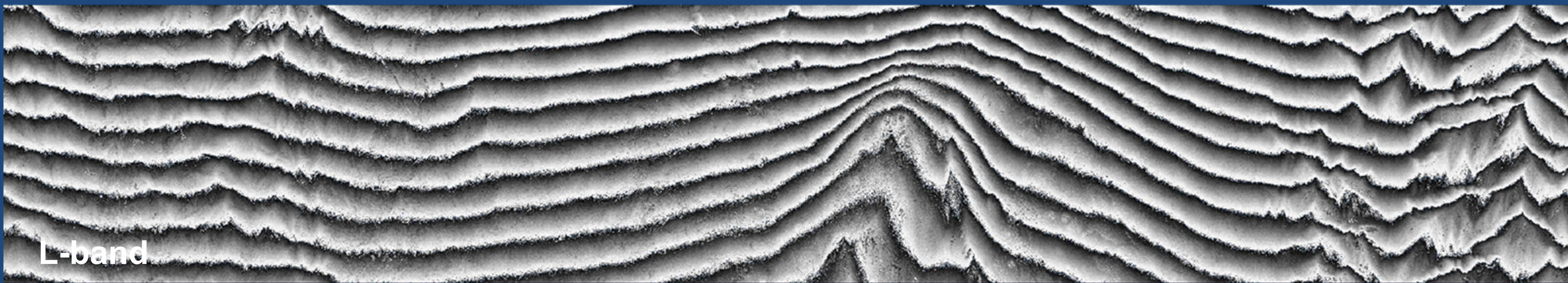

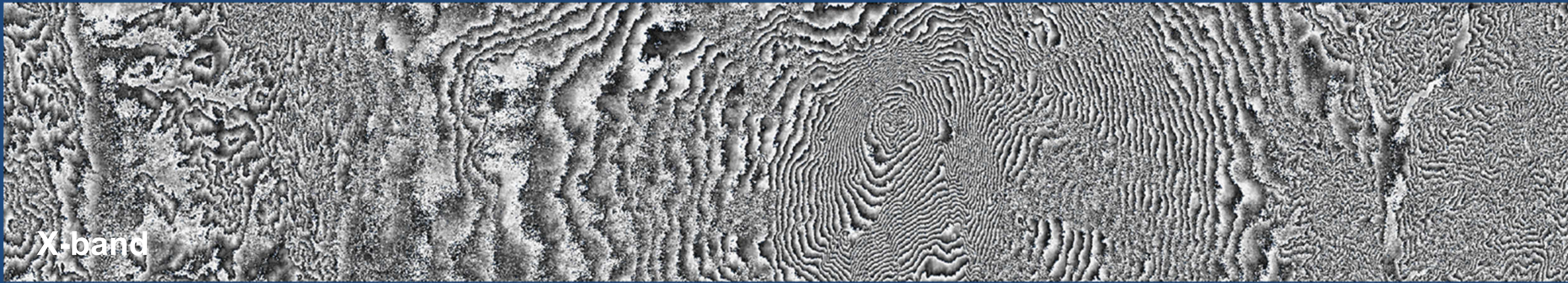

Phase Images

SIR-C / Test Site: Mt. Etna, Italy

Interferometric Coherence

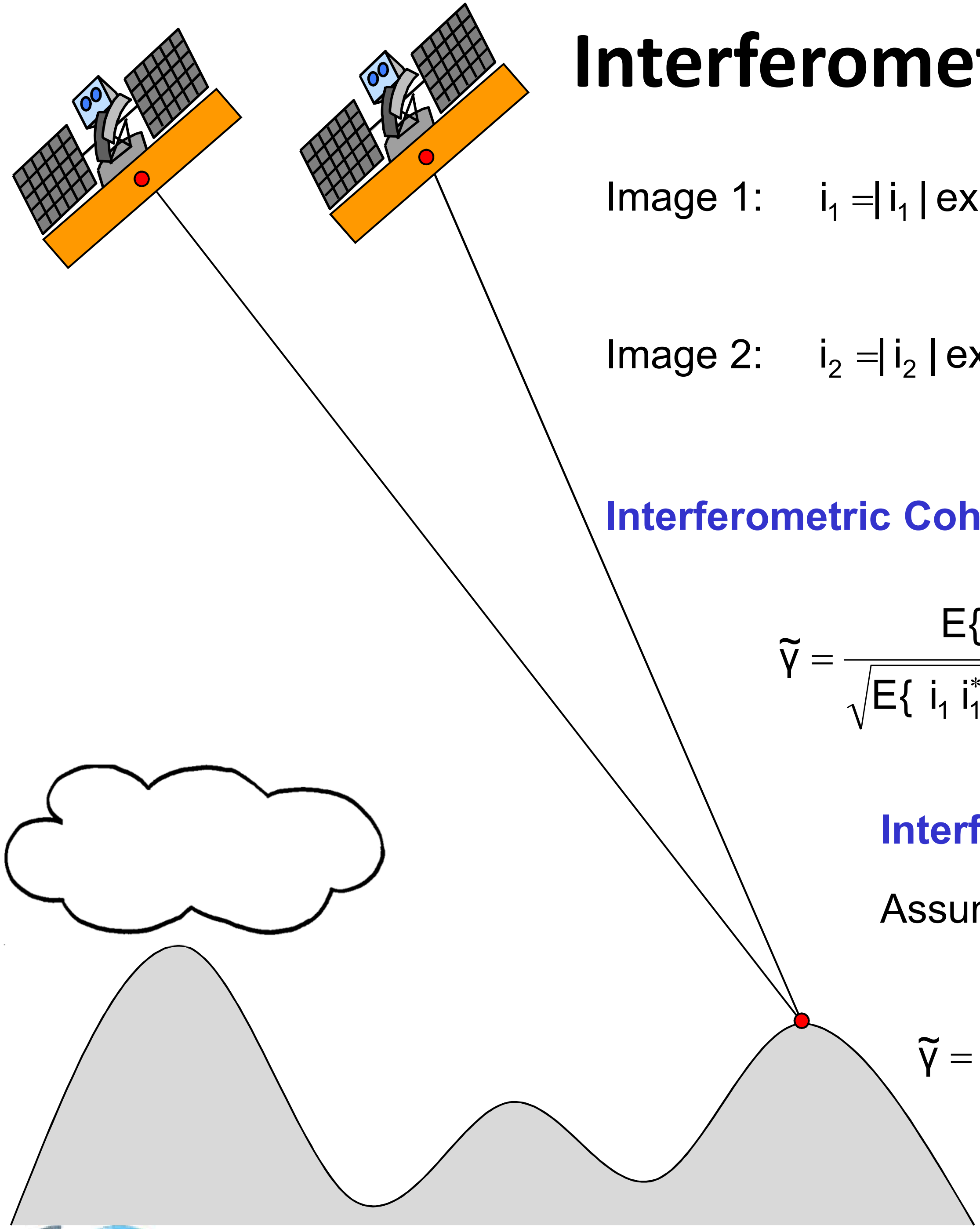

Image 1: $i_1 = |i_1| \exp[-i(2\frac{2\pi}{\lambda}R_1) + \varphi_{S1}]$

Image 2: $i_2 = |i_2| \exp[-i(2\frac{2\pi}{\lambda}R_2) + \varphi_{S2}]$

Interferometric Coherence: Normalised Complex Correlation Coefficient

$$\tilde{\gamma} = \frac{E\{\, i_1\, i_2^* \,\}}{\sqrt{E\{\, i_1\, i_1^* \,\}\; E\{\, i_2\, i_2^* \,\}}} = \frac{|E\{\, i_1\, i_2^* \,\}|\exp(i\varphi)}{\sqrt{E\{|\, i_1\,|^2\}\; E\{|\, i_2\,|^2\}}} \qquad 0 \leq |\,\tilde{\gamma}\,| \leq 1$$

Interferometric Coherence Estimation:

Assuming stationarity within the estimation window:

$$\tilde{\gamma} = \frac{\sum_{W} i_1[i,j]\;\, i_2^*[i,j]}{\sqrt{\sum_{W} |\, i_1[i,j]\,|^2 \sum_{W} |\, i_2[i,j]\,|^2}} = \frac{< i_1\, i_2^* >}{\sqrt{< i_1\, i_1^* > \; < i_2\, i_2^* >}}$$

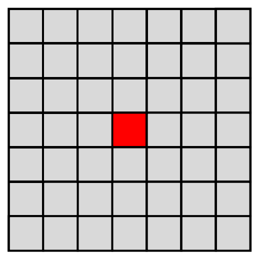

Typical window size: 10 (3x3) – >100 pixels

InSAR Coherence

... is a measure of interferogram quality:

Standard Deviation of the InSAR Phase φ:

$$\sigma_\varphi = \sqrt{\int_{-\pi}^{\pi} \varphi^2 \mathrm{pdf}(\varphi) \cdot d\varphi}$$

depends on ► the underlying coherence &

► the number of looks N.

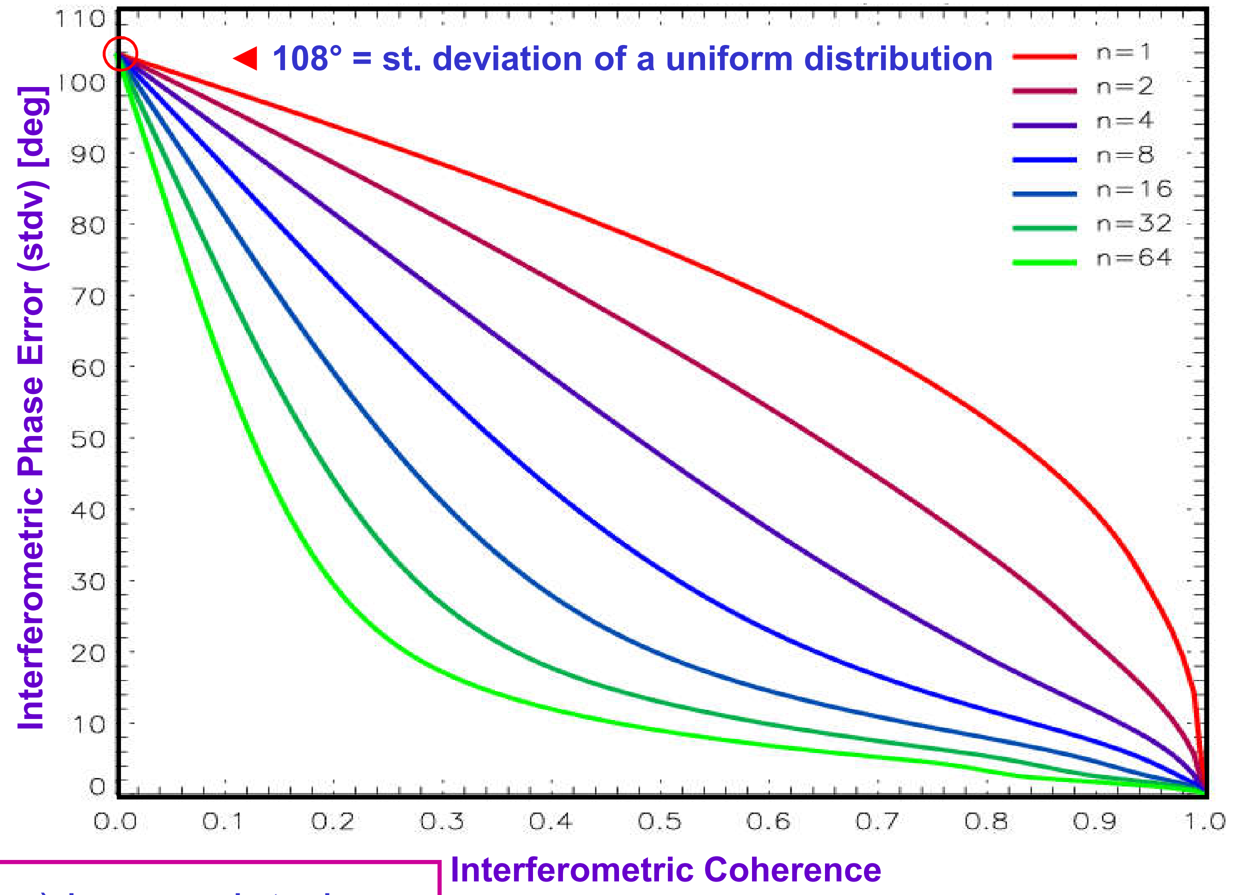

An increase in decorrelation (= loss in coherence) is associated with an increase in the phase variance;

► Increased phase variance leads to increased height errors.

where: $\mathrm{pdf}(\varphi, N) = \frac{\Gamma(N+1/2)(1-|\gamma|^2)^2\beta}{2\sqrt{\pi}\Gamma(N)(1-\beta^2)^{N+1/2}} + \frac{(1-|\gamma|^2)^N}{2\pi} F(N,1;1/2;\beta^2)$

► F is a Gauss hypergeometric function and $\beta = |\gamma|\cos(\varphi - \overline{\varphi})$

► **N is the number of Looks**

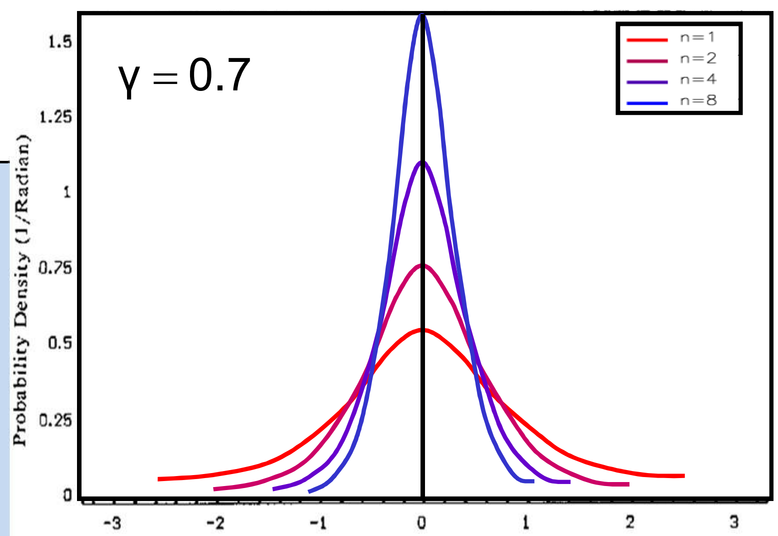

Interferometric Phase Images

Simulation

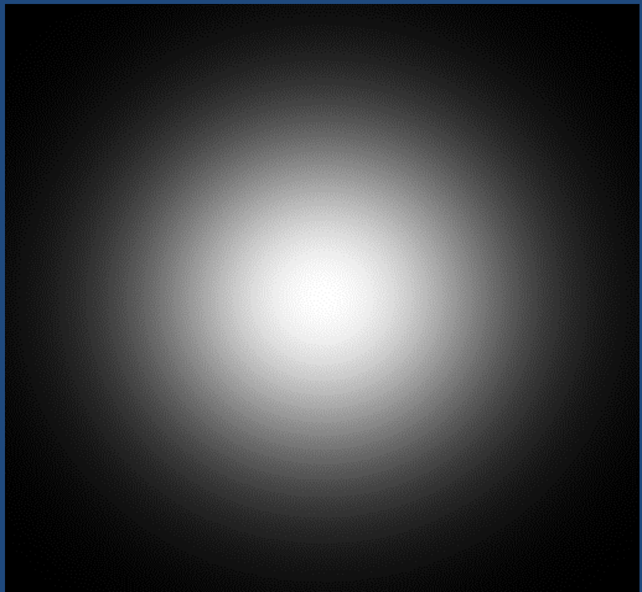

Absolute Phase

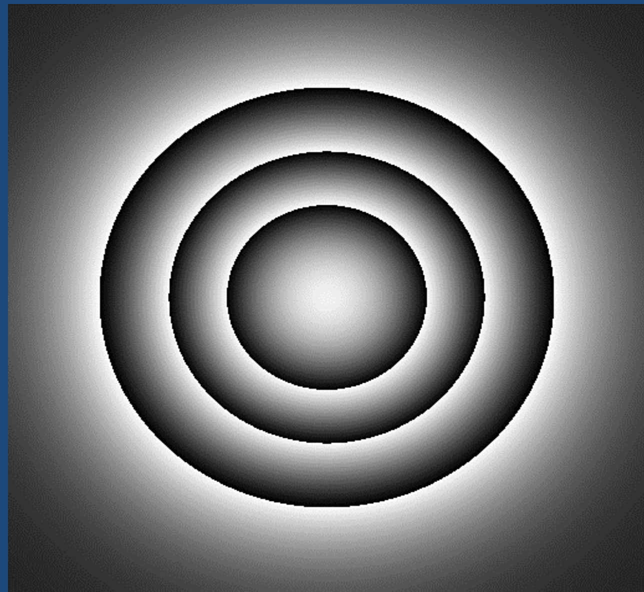

Coherence=1.0 Looks=1

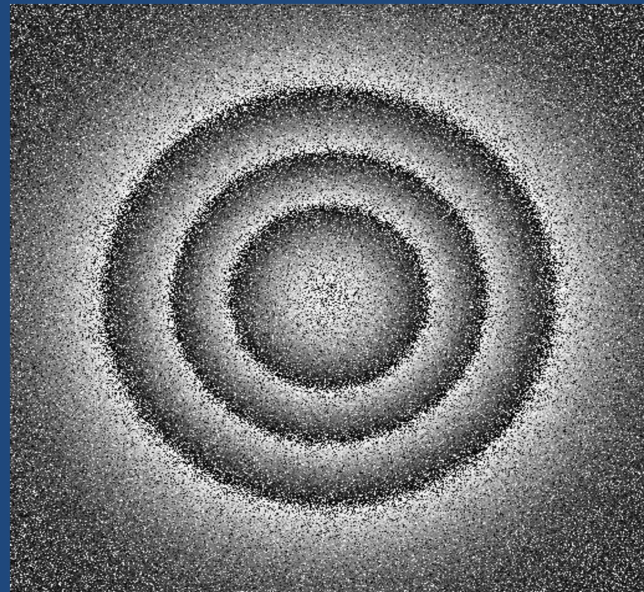

Coherence=0.8 Looks=1

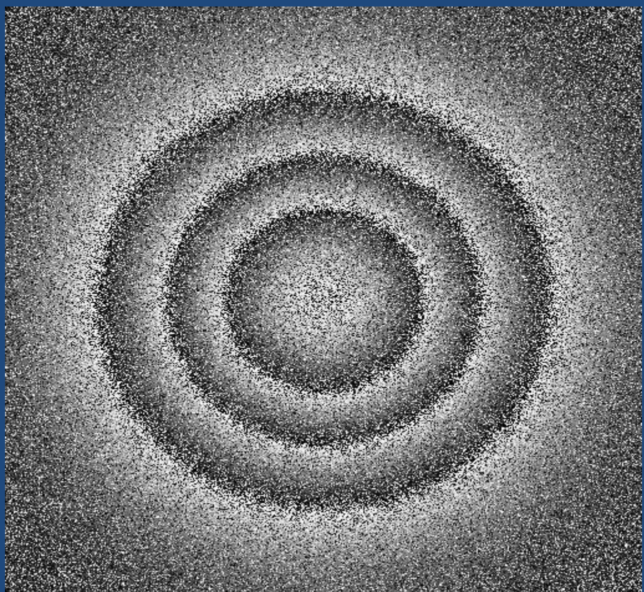

Coherence=0.6 Looks=1

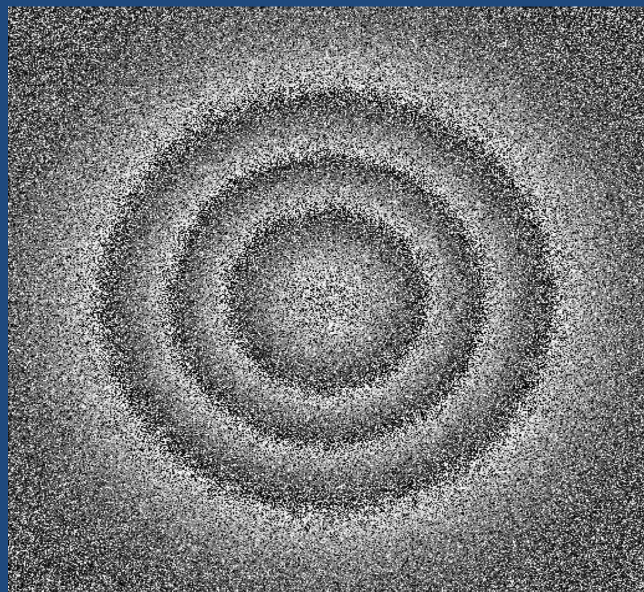

Coherence=0.4 Looks=1

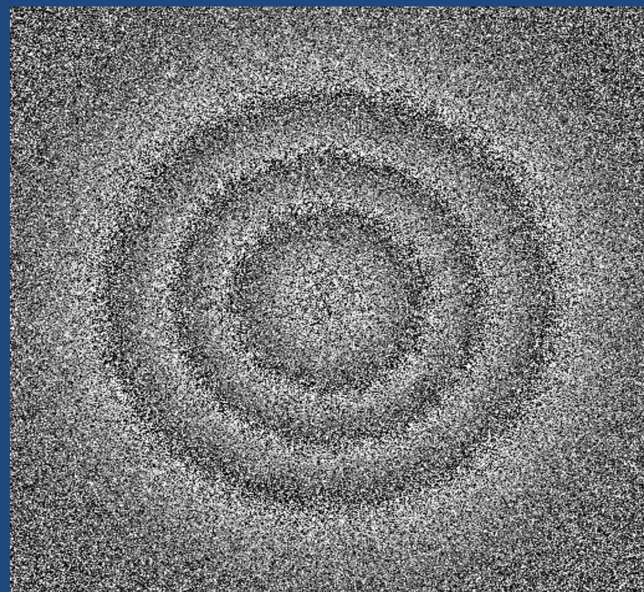

Coherence=0.2 Looks=1

Interferometric Phase Images

Simulation

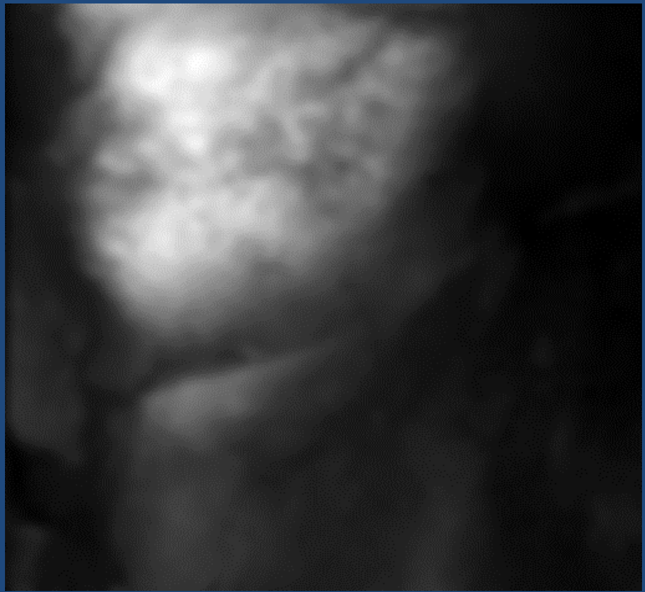

Absolute Phase

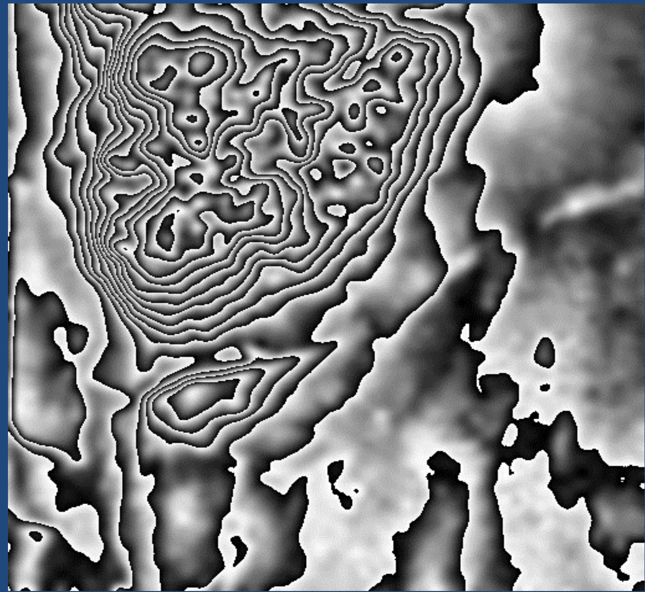

Coherence=1.0 Looks=1

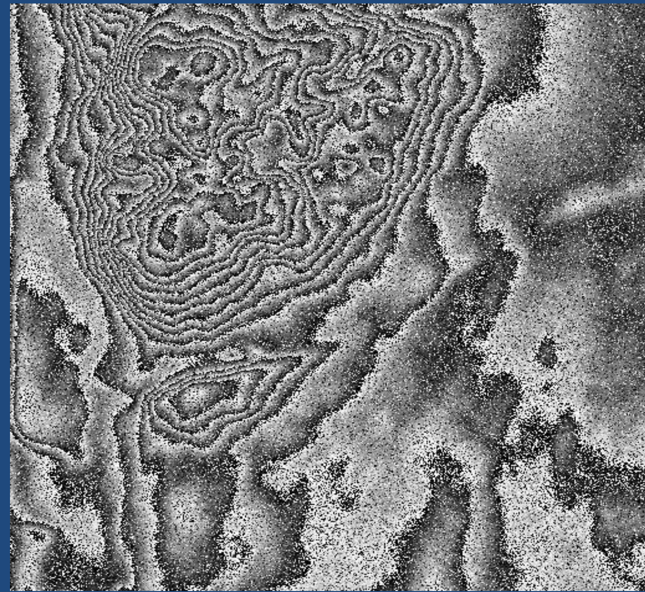

Coherence=0.8 Looks=1

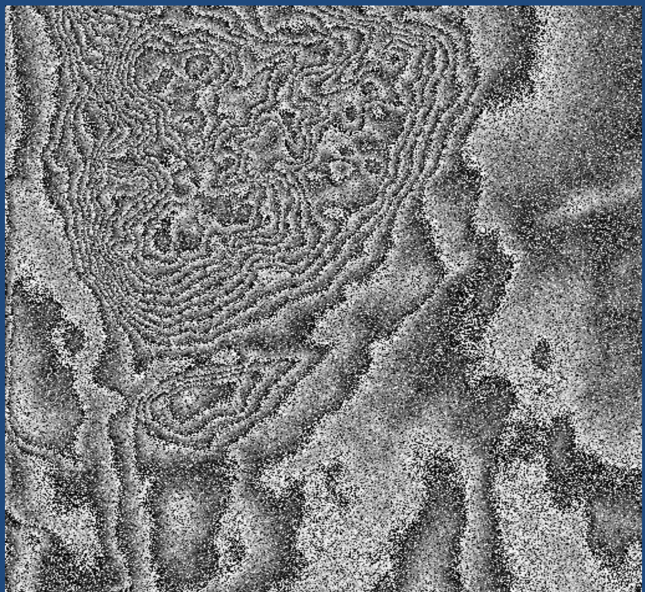

Coherence=0.6 Looks=1

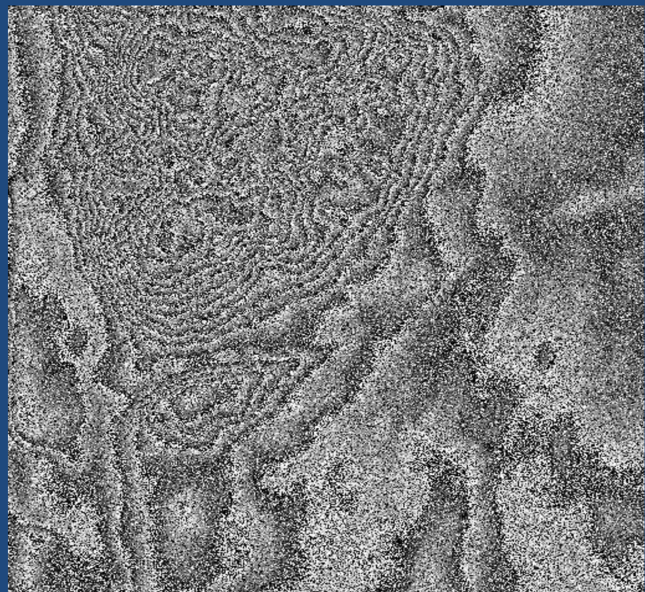

Coherence=0.4 Looks=1

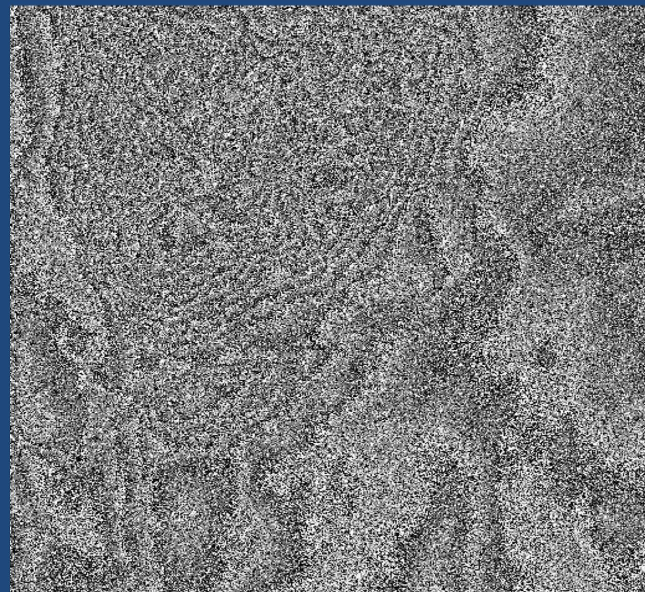

Coherence=0.2 Looks=1

Repeat-Pass SAR Interferometry

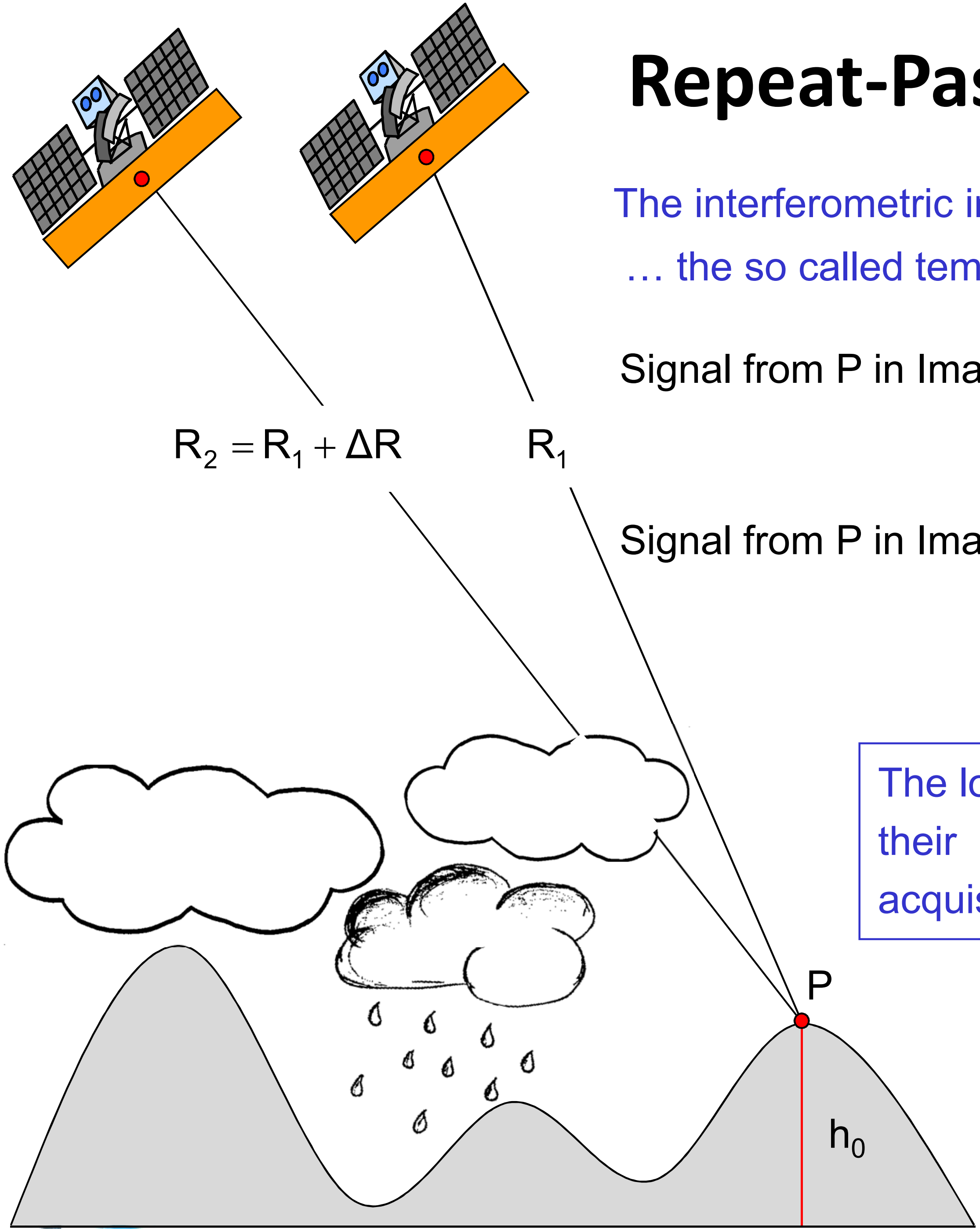

The interferometric images are acquired at different times

… the so called temporal baseline may range from seconds to years

Signal from P in Image 1 @ time t_1:

$$i_1 = |i_1| \exp[-i(2\frac{2\pi}{\lambda}R_1) + \varphi_S(t_1) + \varphi_{Prop}(t_1)]$$

Signal from P in Image 2 @ time t_2:

$$i_2 = |i_2| \exp[-i(2\frac{2\pi}{\lambda}R_2) + \varphi_S(t_2) + \varphi_{Prop}(t_2)]$$

The location of the scatterers in the resolution cell and/or their properties may change in the time between the two acquisitions: $\varphi_S(t_1) \neq \varphi_S(t_2)$ **Temporal decorrelation**

The phase induced by the propagation medium (atmosphere or ionosphere) varies in the time between the two acquisitions: $\varphi_{Prop}(t_1) \neq \varphi_{Prop}(t_2)$

Earth Ob
Remote

Reduced and variable quality but allows displacement measurements

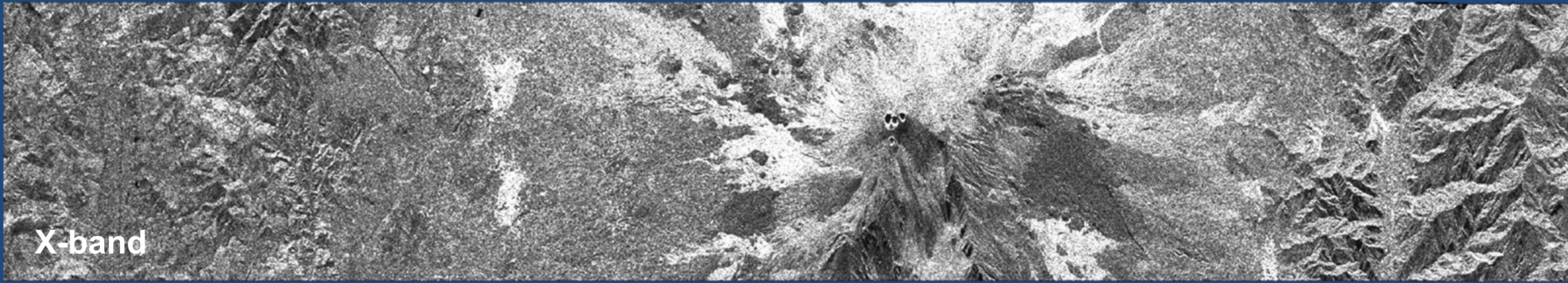

Amplitude Images

24 Hours Temporal Baseline

SIR-C / Test Site: Mt. Etna, Italy

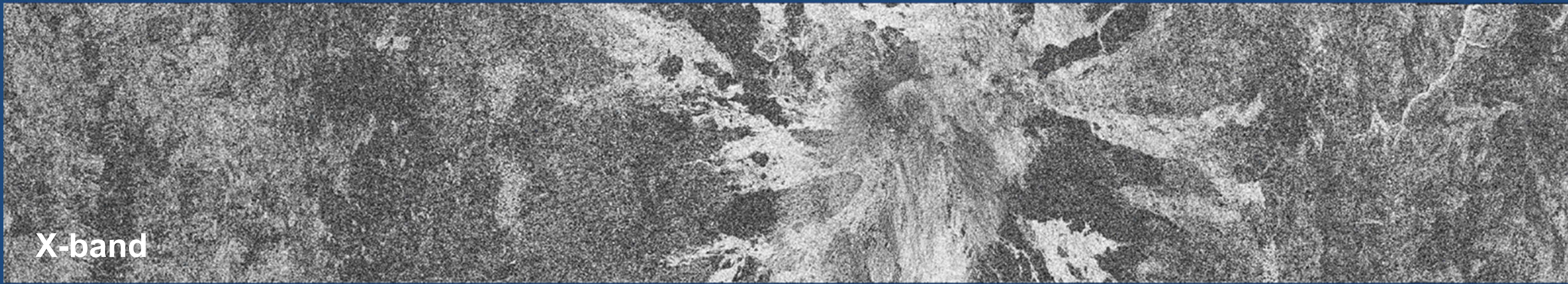

Coherence Images

SIR-C / Test Site: Mt. Etna, Italy

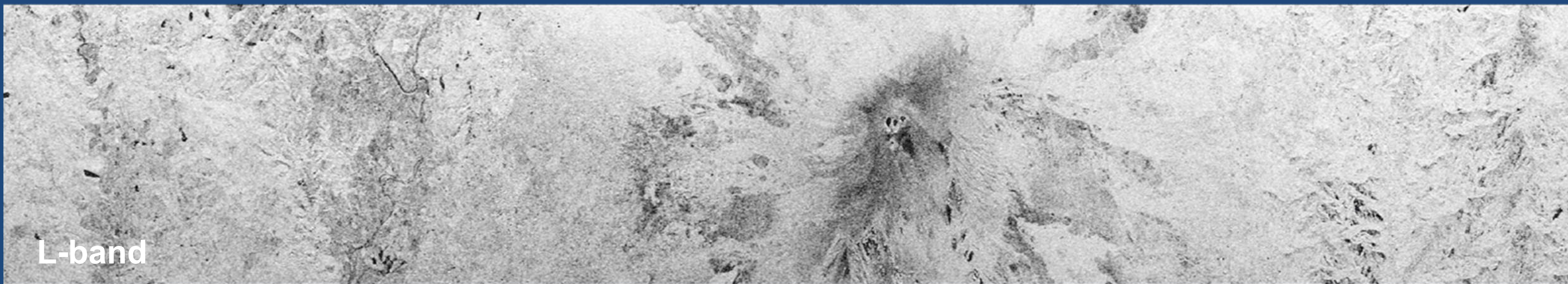

Temporal Decorrelation

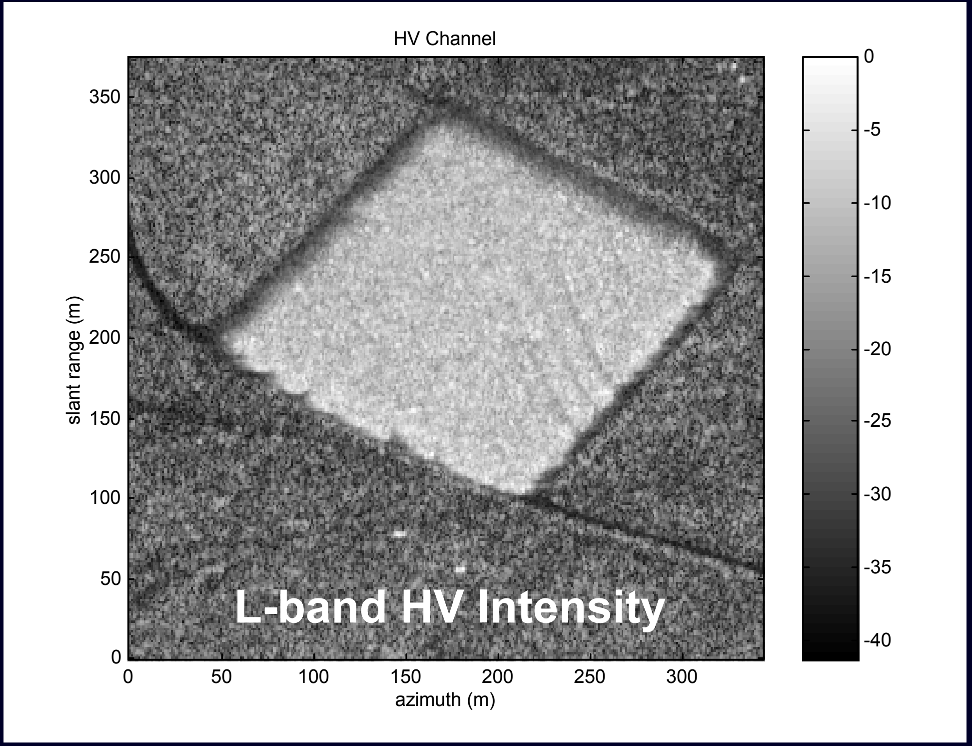

E-SAR / Test Site: Fox Covert,England

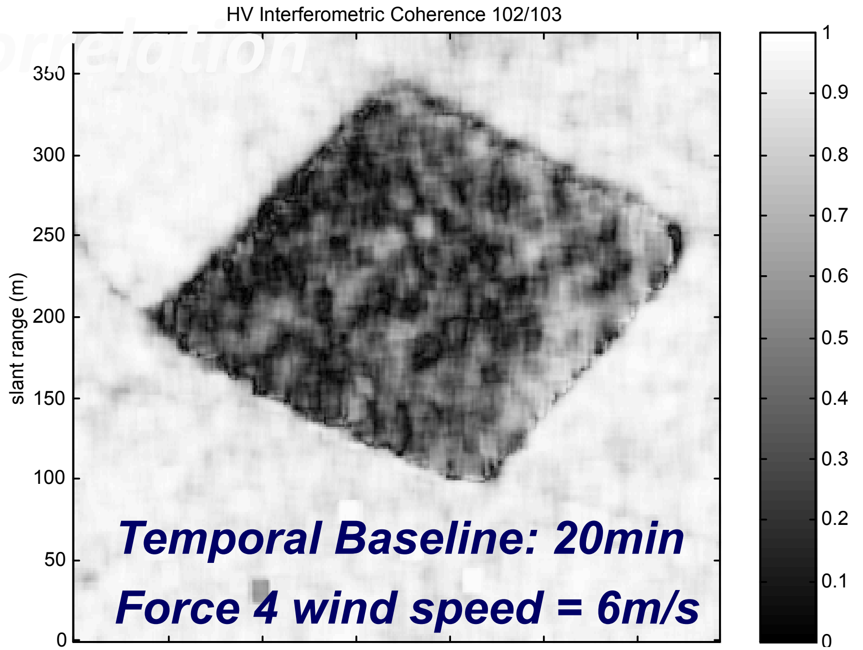

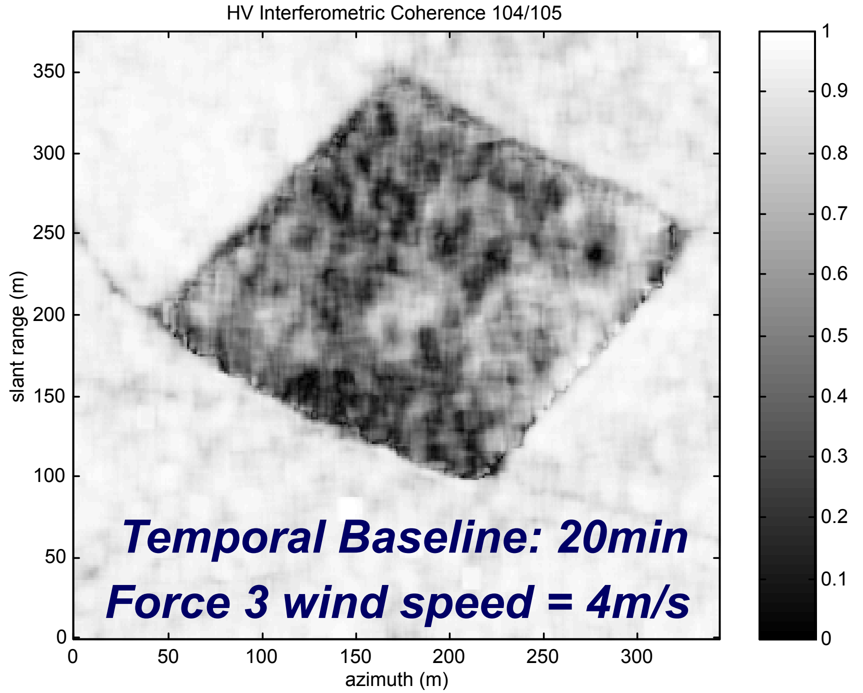

Temporal Decorrelation

E-SAR / Test Site: Fox Covert,England

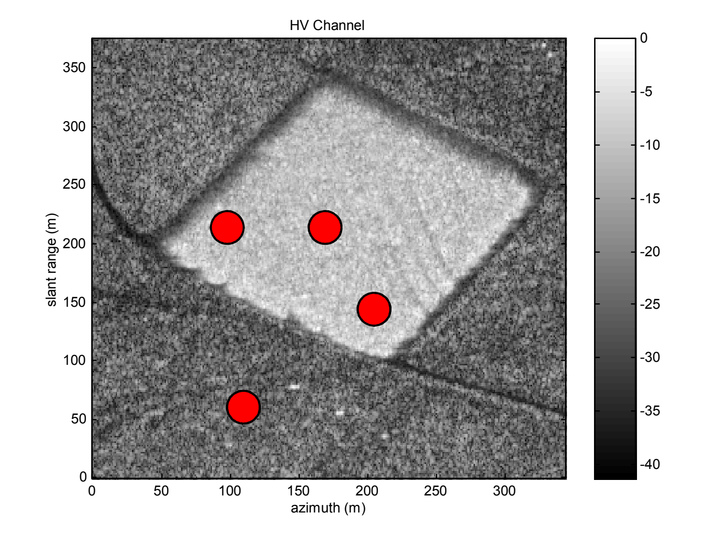

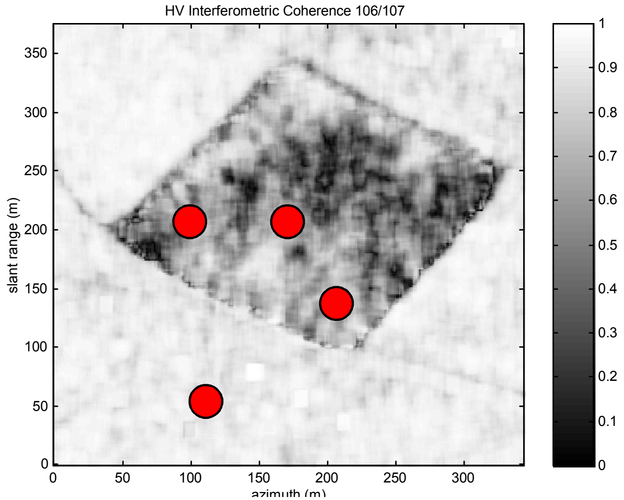

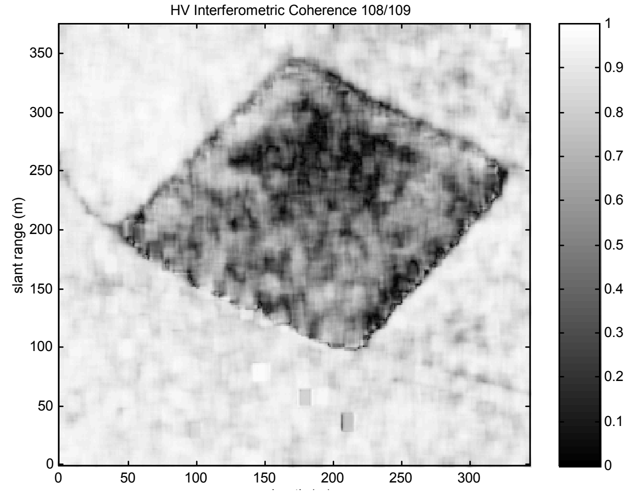

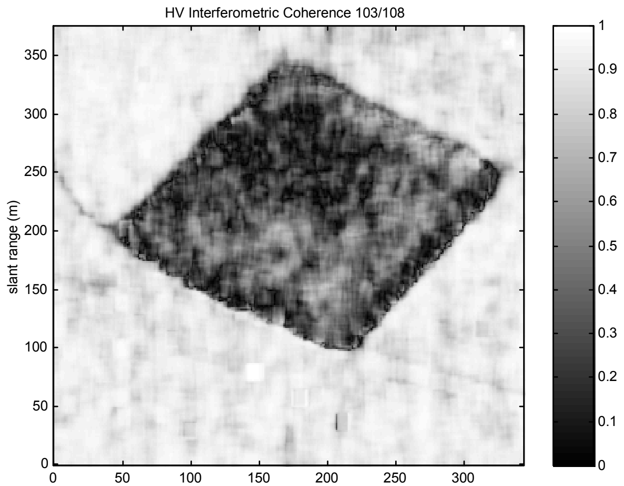

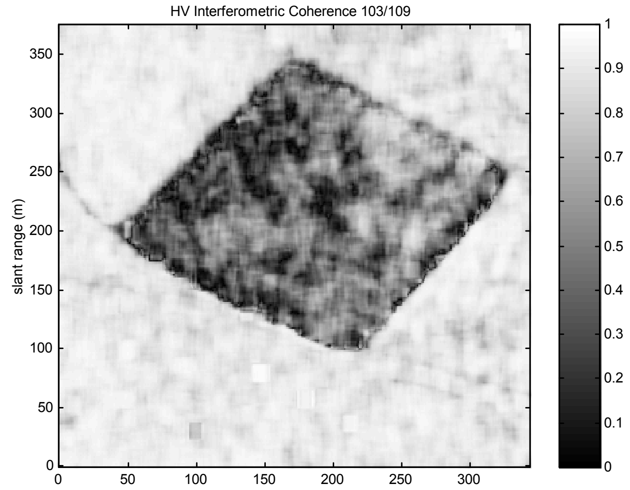

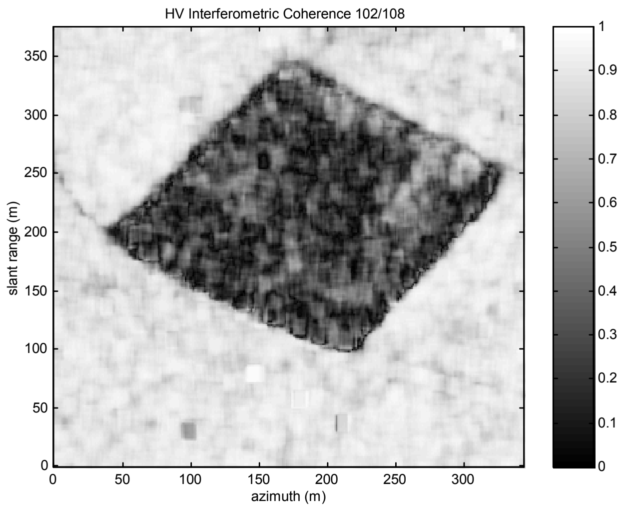

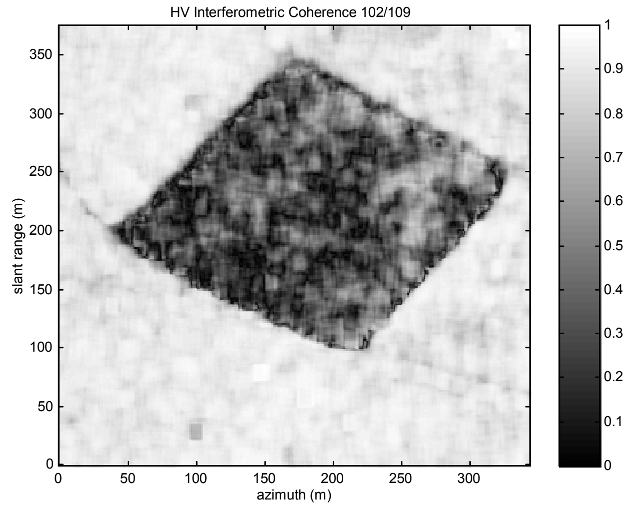

Data Courtesy QuinetiQ / UK

Forest Height Estimation – Decorrelation Effects

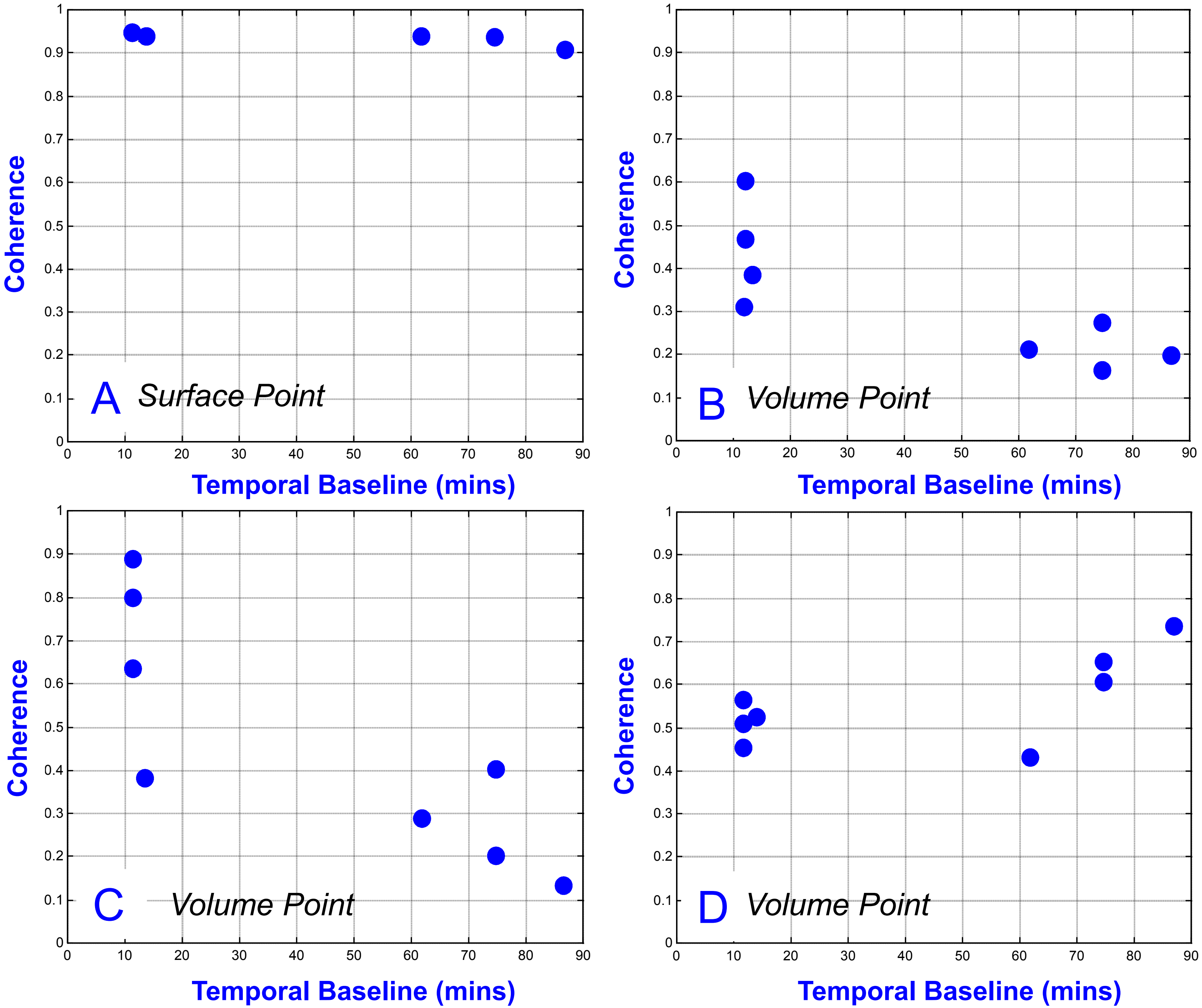

lgenössische Technische Hochschule Zürich
iss Federal Institute of Technology Zurich

TanDEM-X Data Acquisition Modes

Pursuit Monostatic

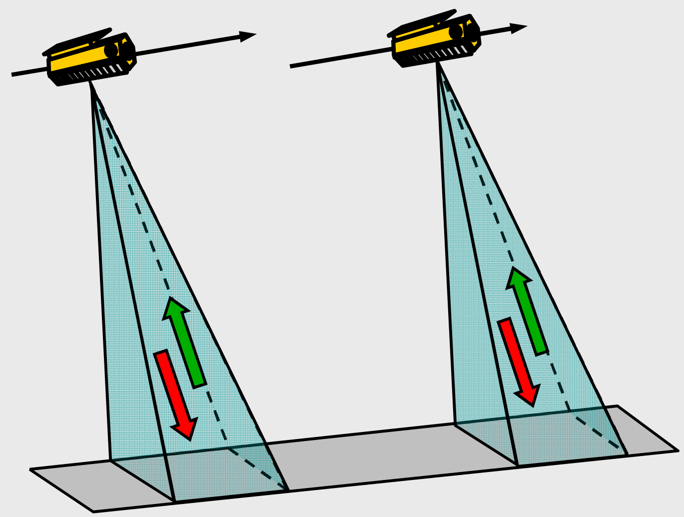

- **both satellites transmit and receive independently**
- susceptible to temporal decorrelation and atmospheric disturbances
- no PRF and phase synchronisation required (backup solution)

Bistatic

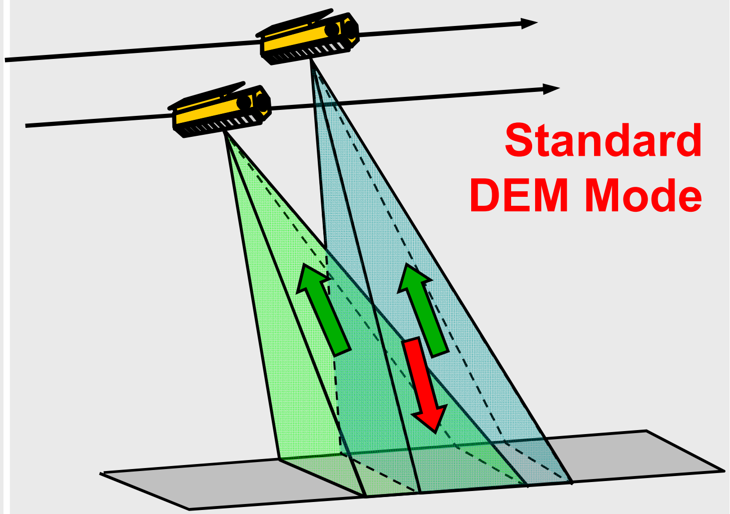

- **one satellite transmits and both satellites receive simultaneously**
- small along-track displacement required for Doppler spectra overlap
- requires PRF and phase synchronisation

Alternating Bistatic

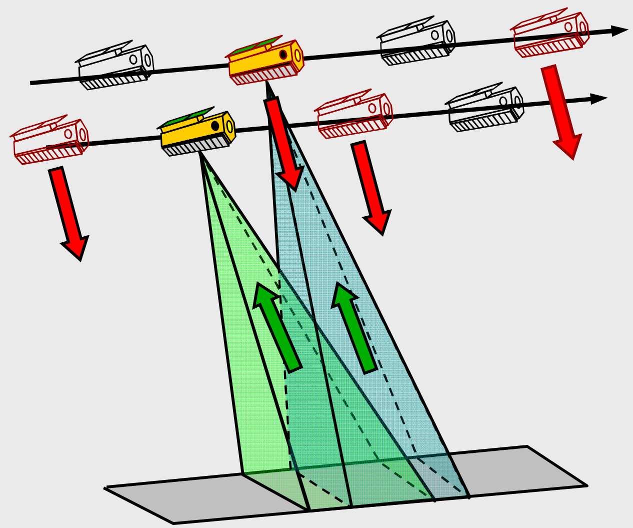

- **transmitter alternates between PRF pulses**
- provides three interferograms with two baselines in a single pass
- enables precise phase synchronisation, calibration & verification

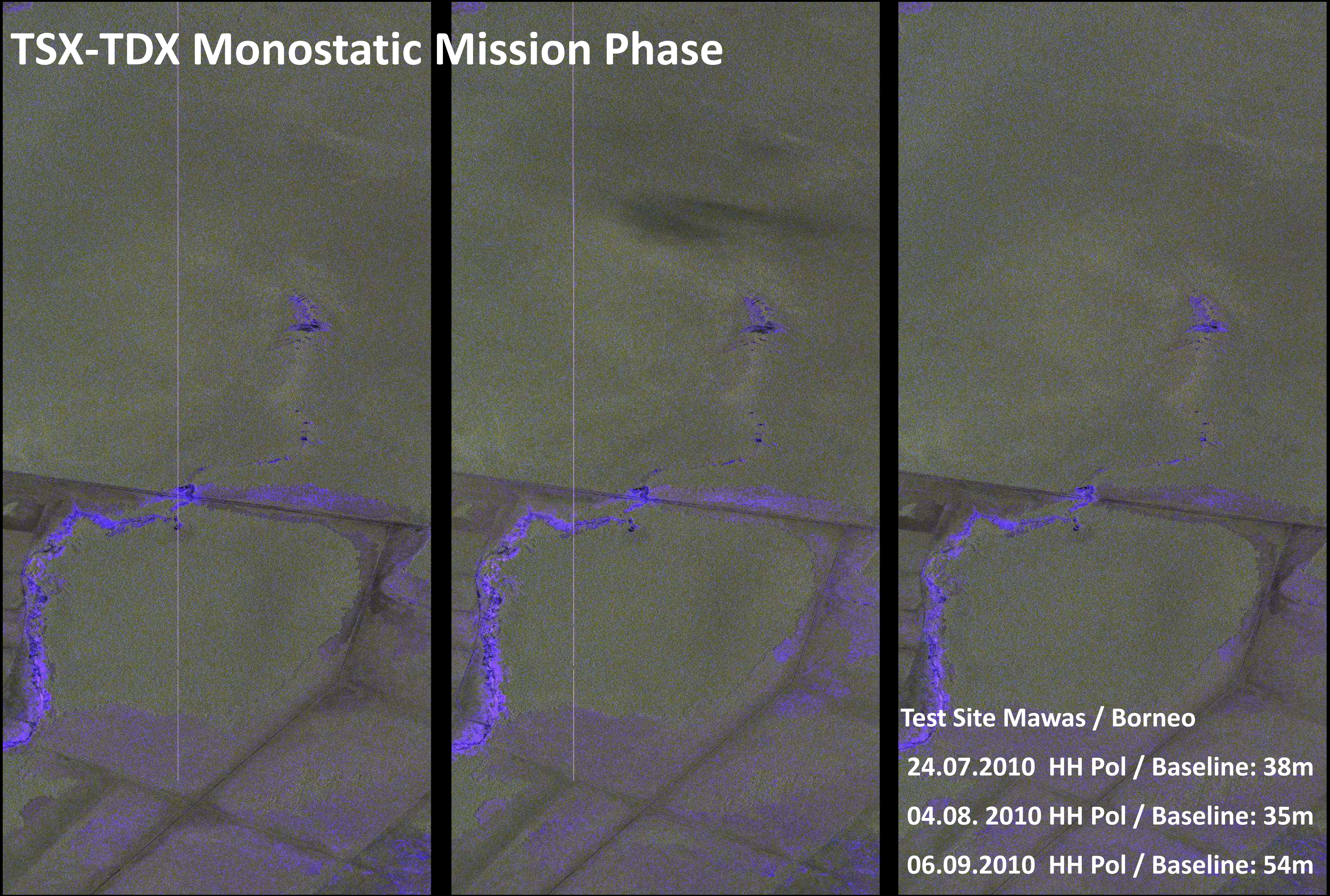
TSX-TDX Monostatic Mission Phase
Test Site Mawas / Borneo
24.07.2010 HH Pol / Baseline: 38m
04.08. 2010 HH Pol / Baseline: 35m
06.09.2010 HH Pol / Baseline: 54m

TSX-TDX Monostatic Mission Phase

Test Site Mawas / Borneo

24.07.2010 HH Pol Baseline: 38m

04.08. 2010 HH Pol Baseline: 35m

06.09.2010 HH Pol Baseline: 54m

Single-Pass SAR Interferometry

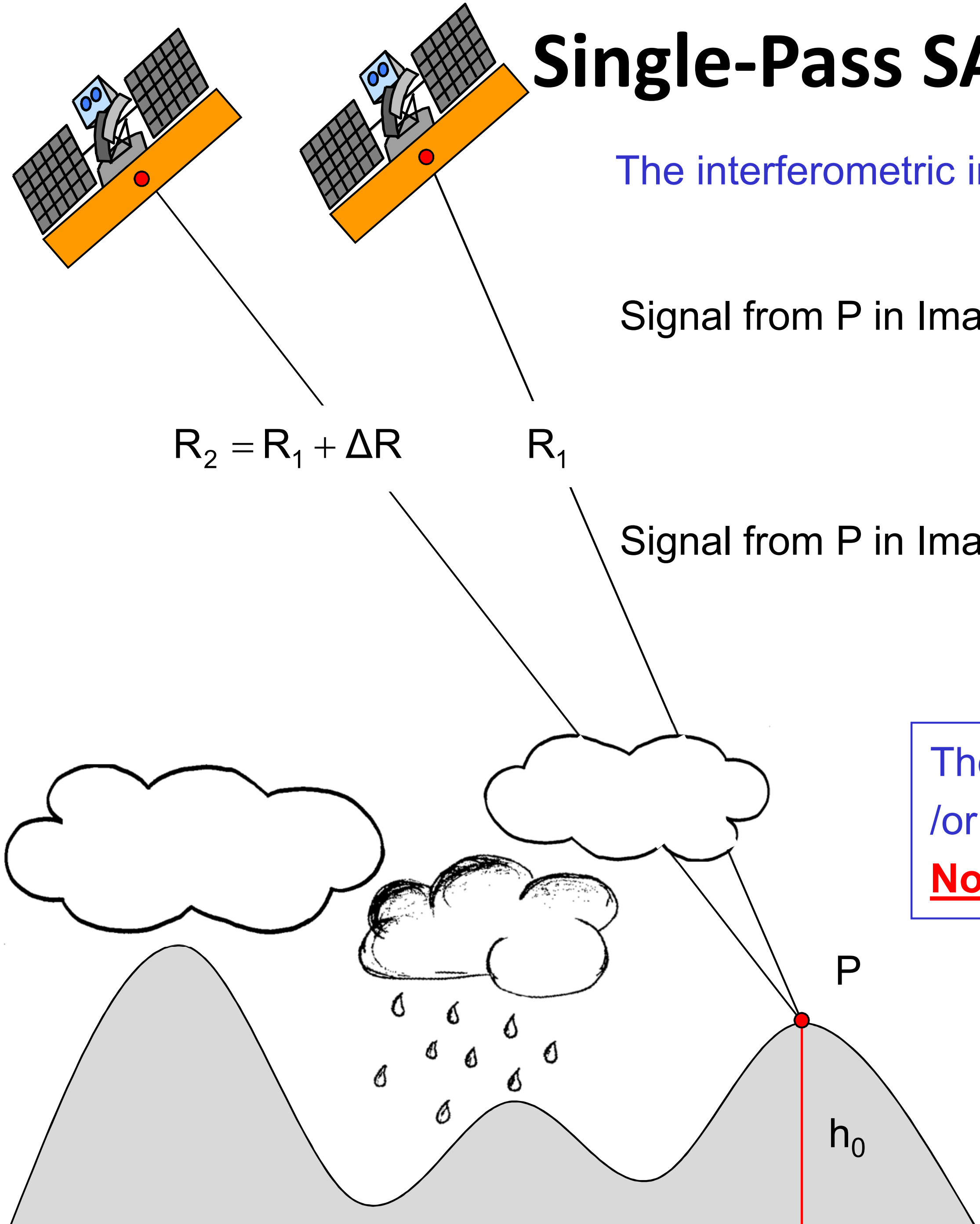

The interferometric images are acquired at the same time

Signal from P in Image 1 @ time t_1:

$$i_1 = |i_1| \exp[-i(2\frac{2\pi}{\lambda}R_1) + \varphi_{S1}(t_1) + \varphi_{Prop}(t_1)]$$

Signal from P in Image 2 @ time t_2:

$$i_2 = |i_2| \exp[-i(2\frac{2\pi}{\lambda}R_2) + \varphi_{S1}(t_1) + \varphi_{Prop}(t_1)]$$

The location of the scatterers in the resolution cell and /or their properties are the same for both acquisitions:
No temporal decorrelation

Both signals travel through the same atmosphere and ionosphere): $\varphi_{Prop}(t_1) = \varphi_{Prop}(t_1)$

hajnsek@ifu.baug.ethz.ch
irena.hajnsek@dlr.de

TanDEM-X Data Acquisition Modes

Pursuit Monostatic

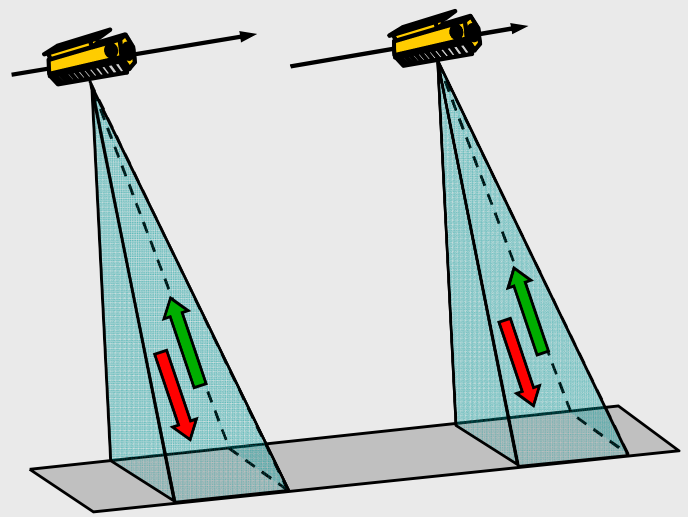

- **both satellites transmit and receive independently**
- susceptible to temporal decorrelation and atmospheric disturbances
- no PRF and phase synchronisation required (backup solution)

Bistatic

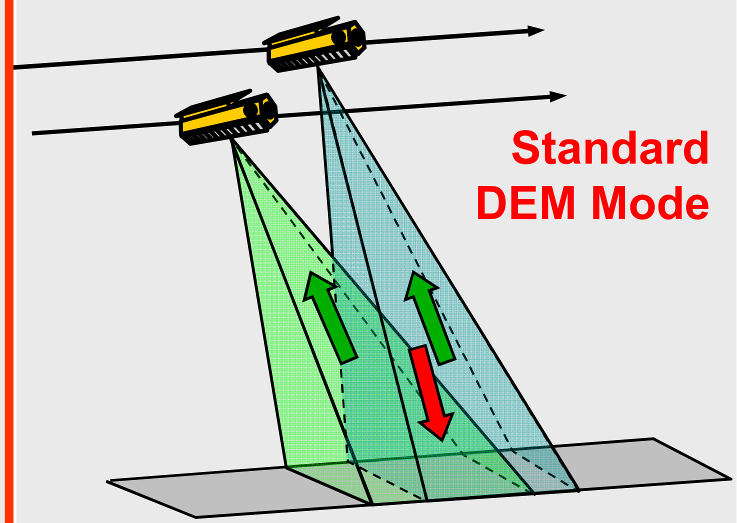

- **one satellite transmits and both satellites receive simultaneously**
- small along-track displacement required for Doppler spectra overlap
- requires PRF and phase synchronisation

Alternating Bistatic

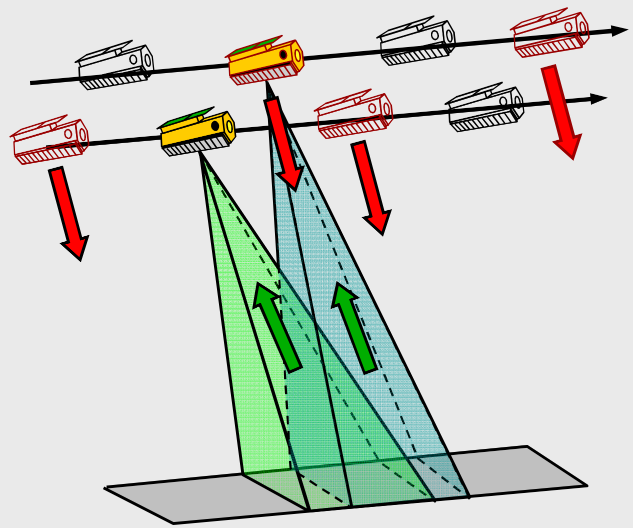

- **transmitter alternates between PRF pulses**
- provides three interferograms with two baselines in a single pass
- enables precise phase synchronisation, calibration & verification

Large Baseline DEM with TanDEM-X

- first TanDEM-X DEM (acquired before reaching 20 km formation)
- large effective baseline (~ 2 km) from Earth rotation
- squint angle ensures coherence

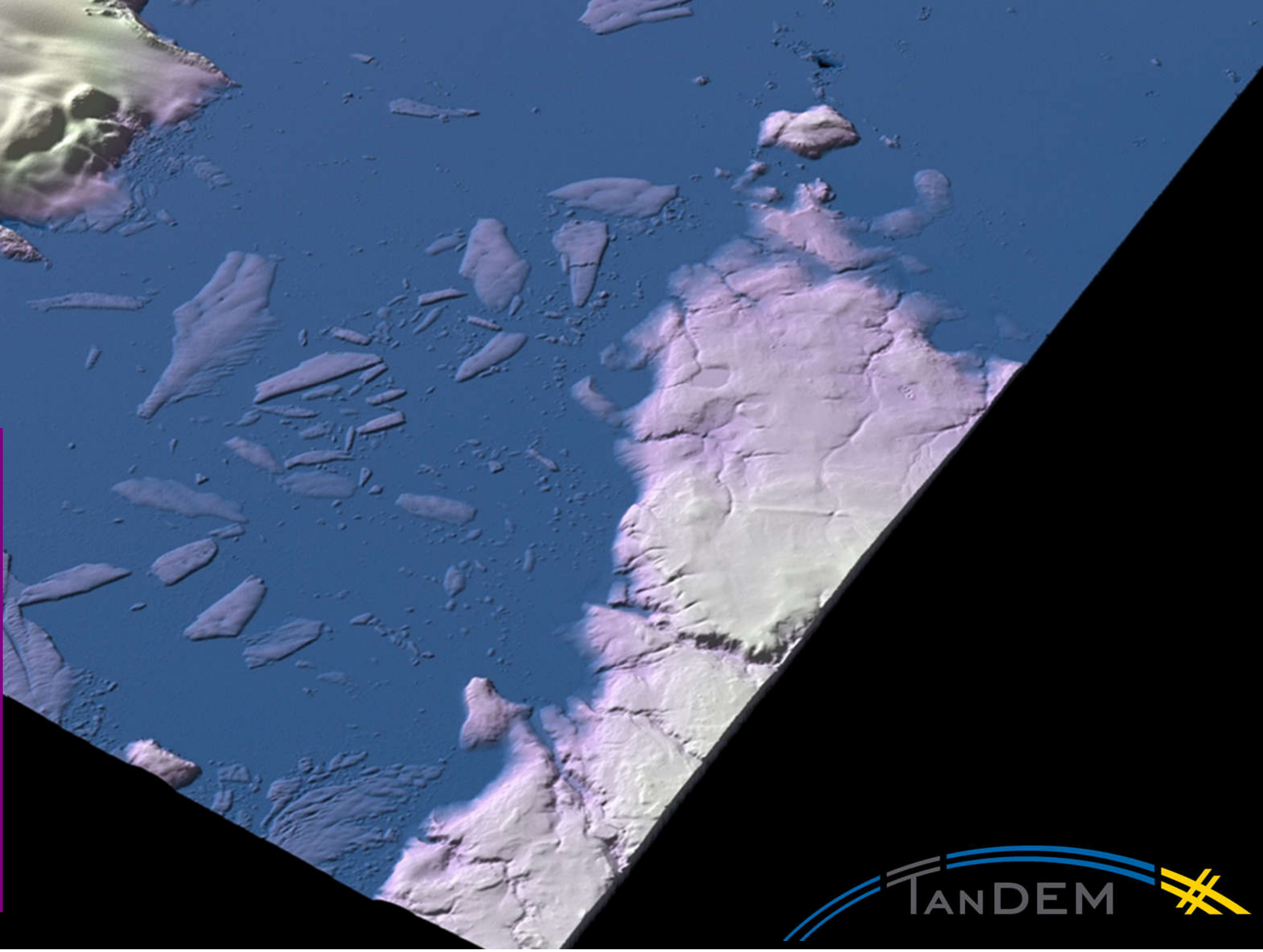

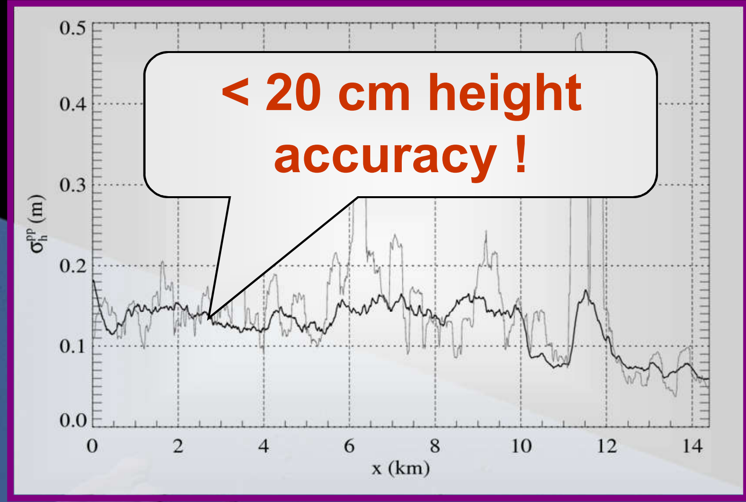

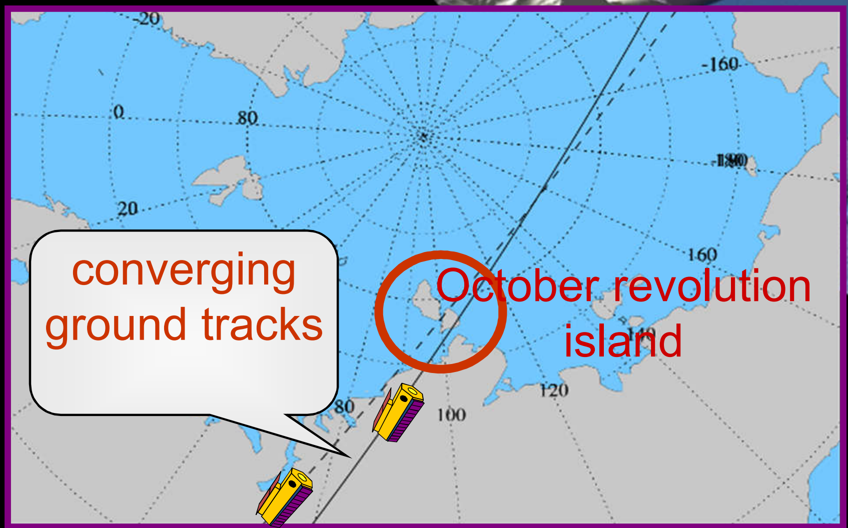

TanDEM-X: Ice loss of Aletschgletscher

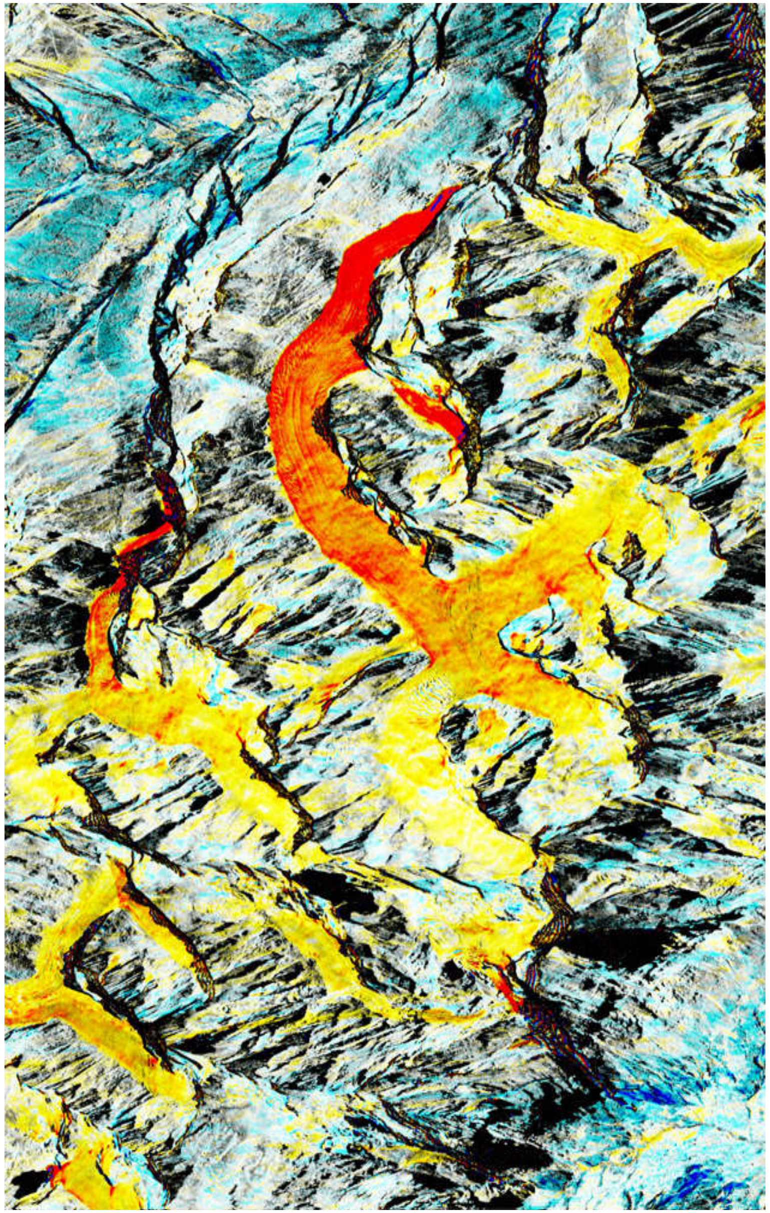

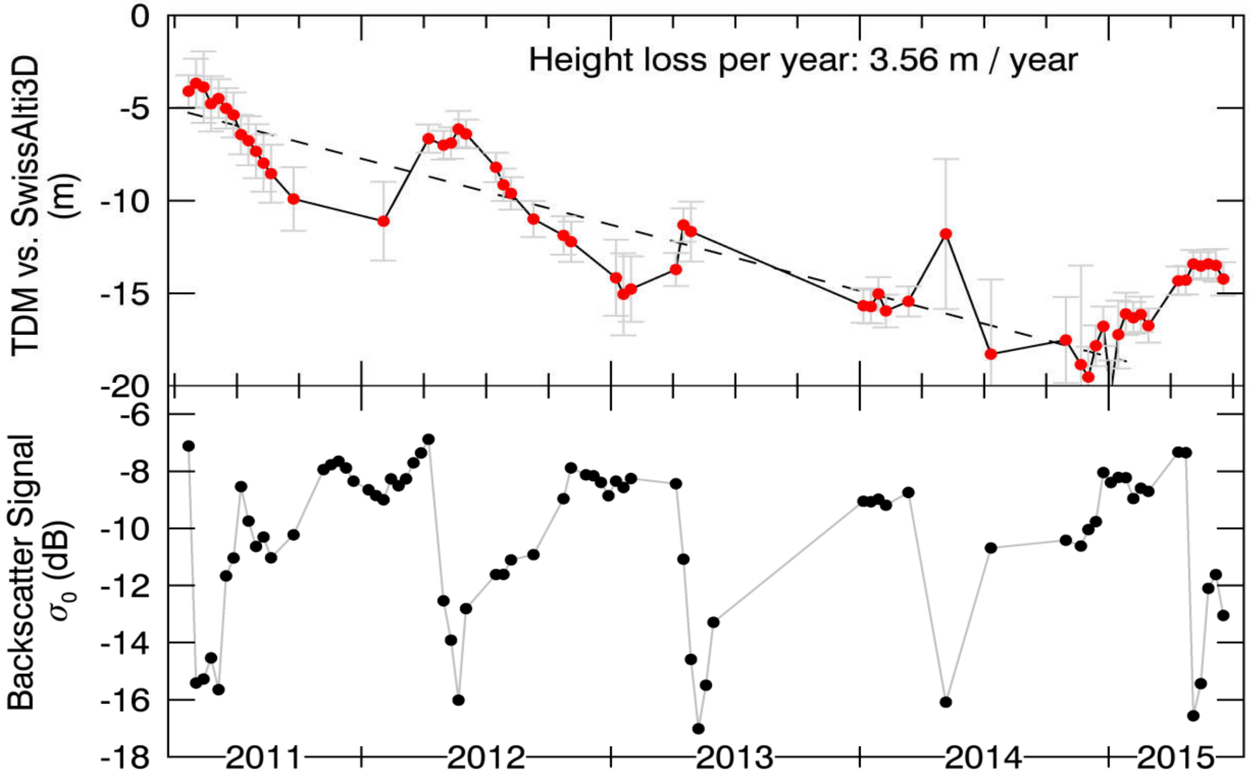

- Results consistent with IceSat data.
- In winter, the apparent elevation stays constant or even decreases(-) during snow accumulation(+) Elevation jumps up at snow melt.

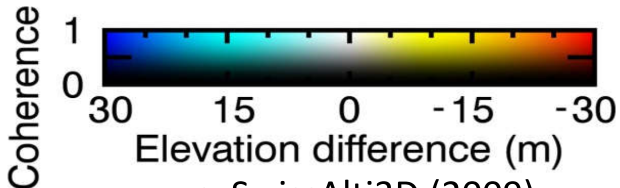

vs. SwissAlti3D (2009)

hajnsek@ifu.baug.ethz.ch
irena.hajnsek@dlr.de

Snow Depth determined by DEM Differencing I

dry snow
vs.
wet snow

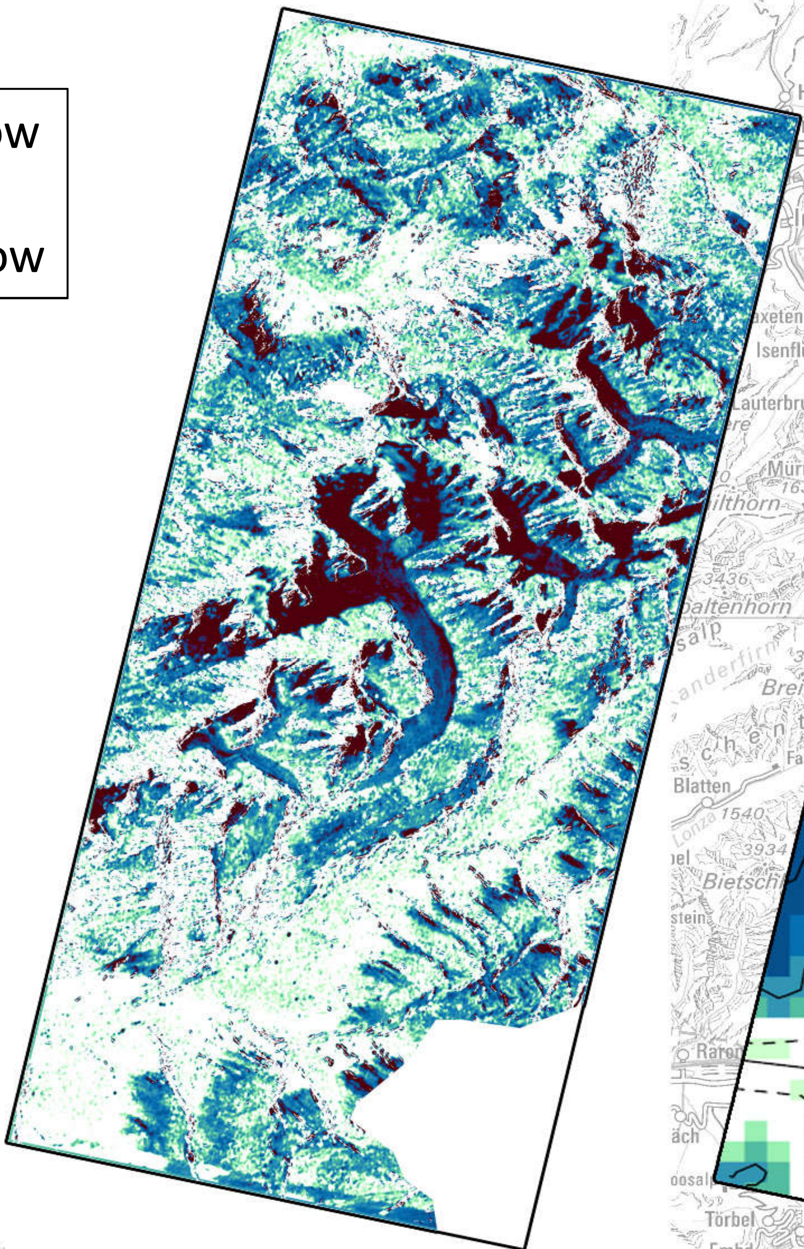

TanDEM-X elevation difference,
17.04.2013 vs. 06.04.2013

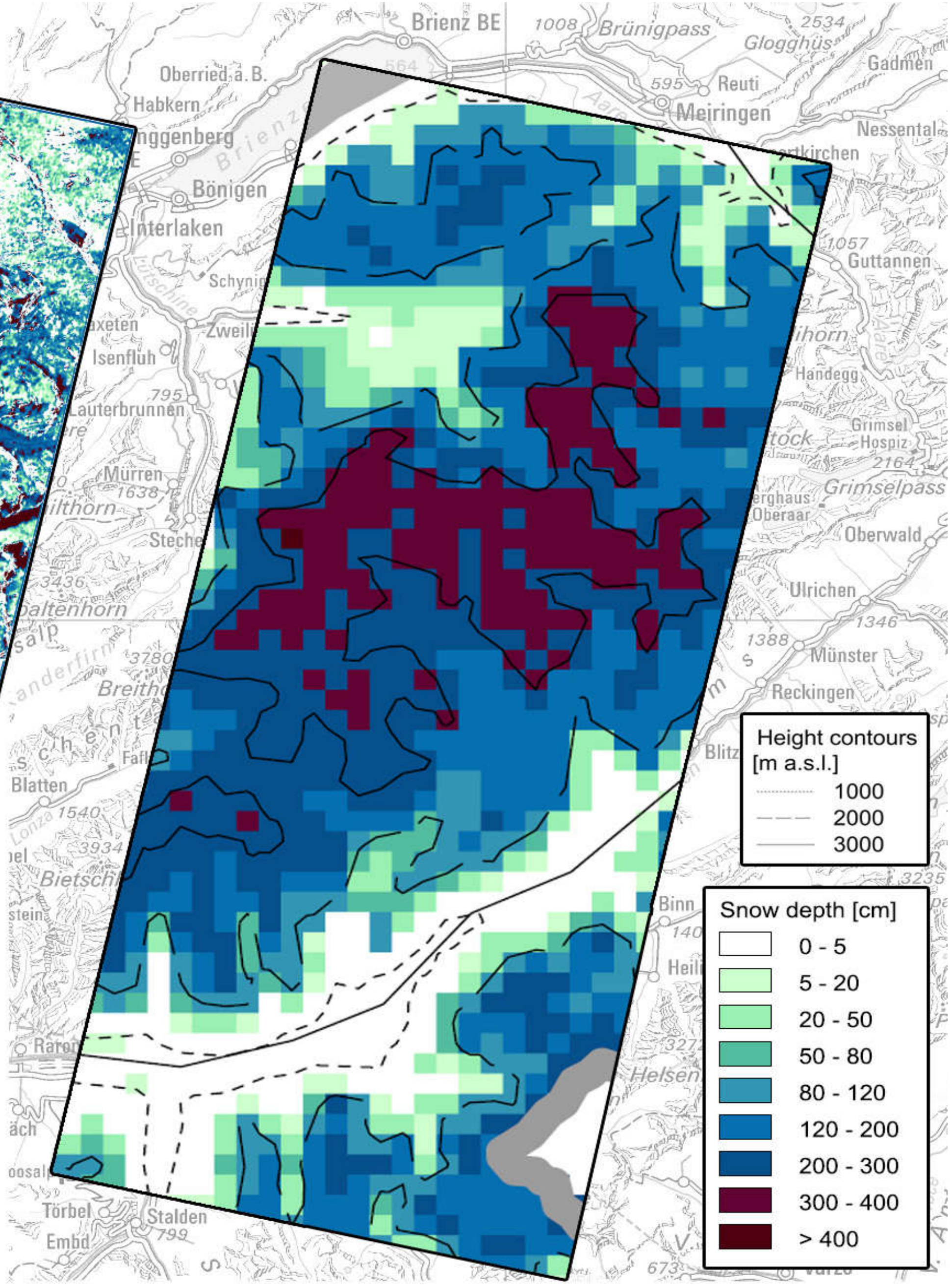

SLF, snow depth map, 18.04.2013

Snow Depth determined by DEM Differencing II

summer
vs.
wet snow
in spring

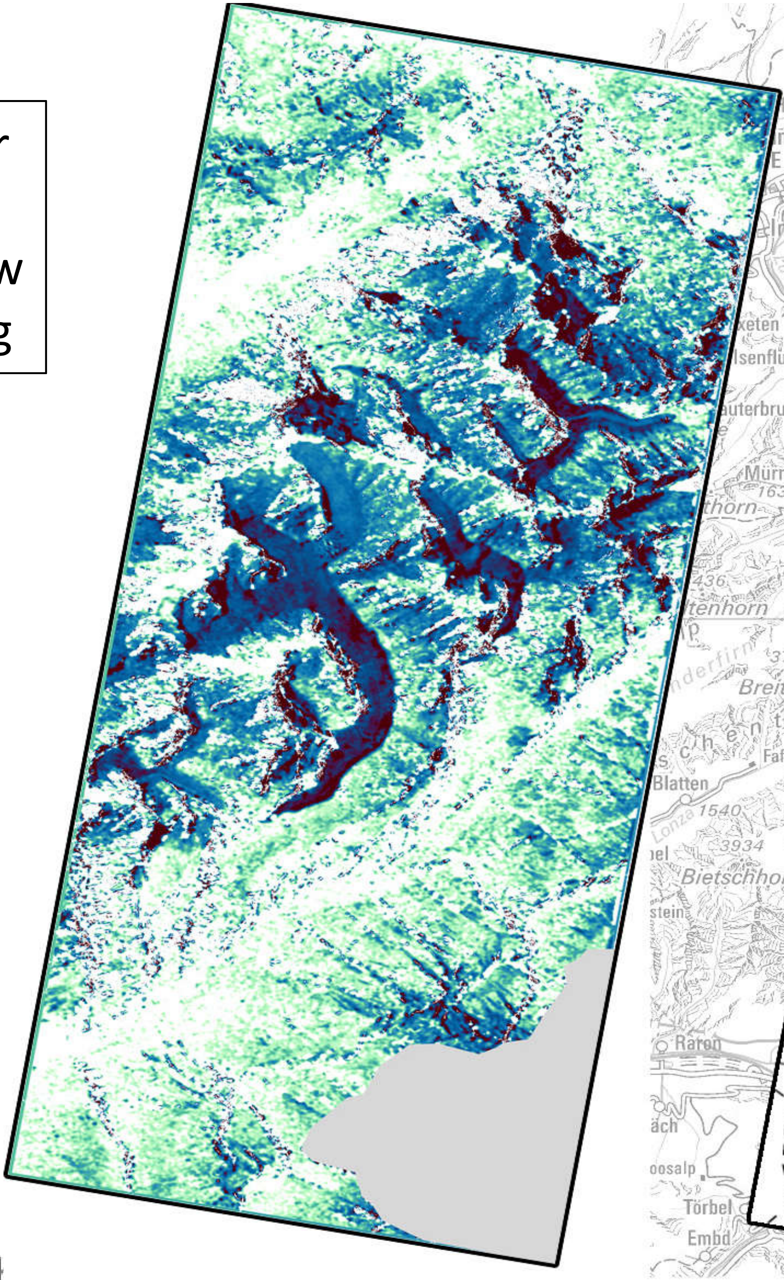

TanDEM-X elevation difference,
02.06.2012 vs. 27.07.2012

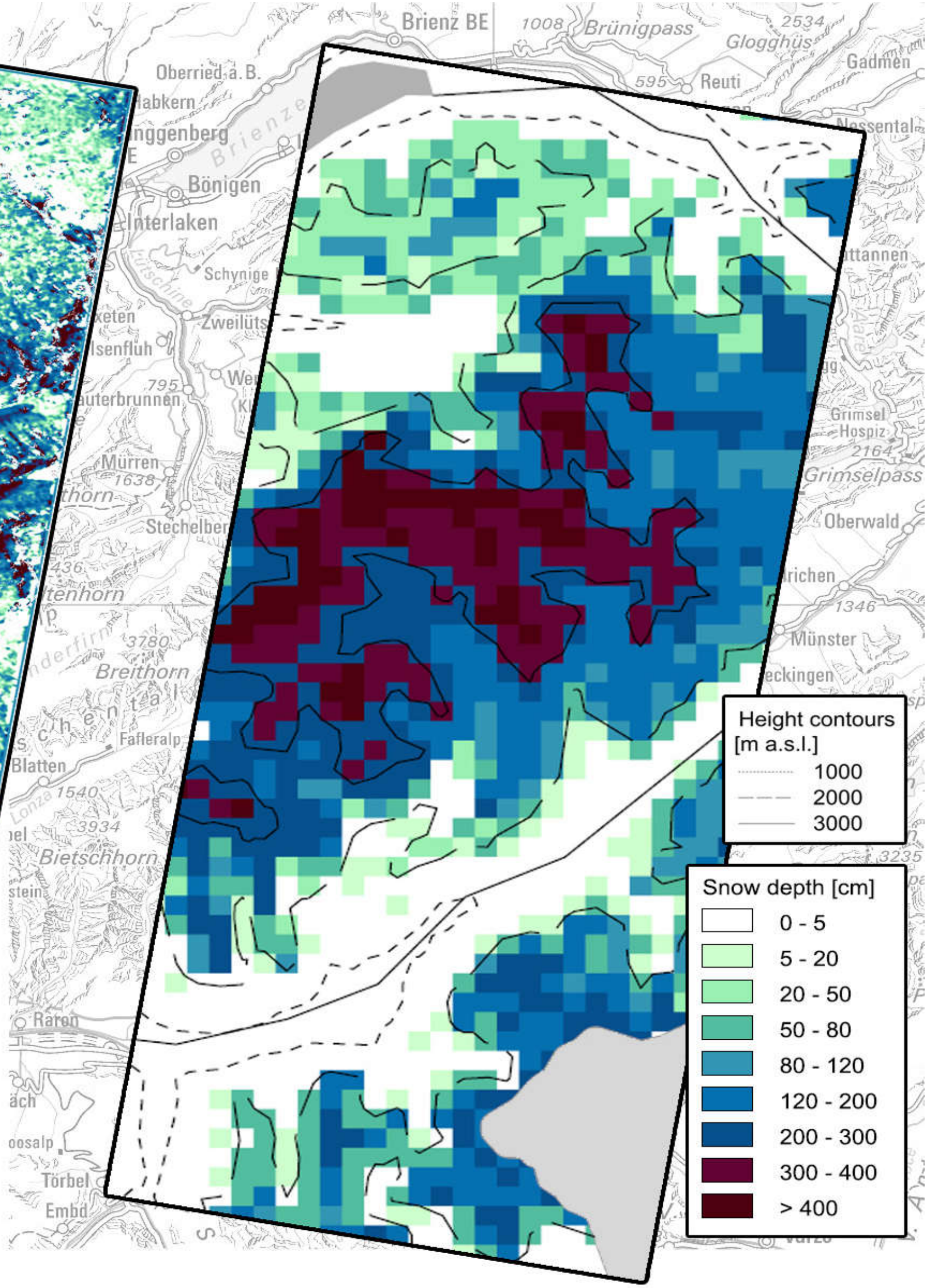

SLF, snow depth map, 31.05.2012

Earth Rem

...sche Hochschule Zürich
Swiss Federal Institute of Technology Zurich

Differential SAR Interferometry

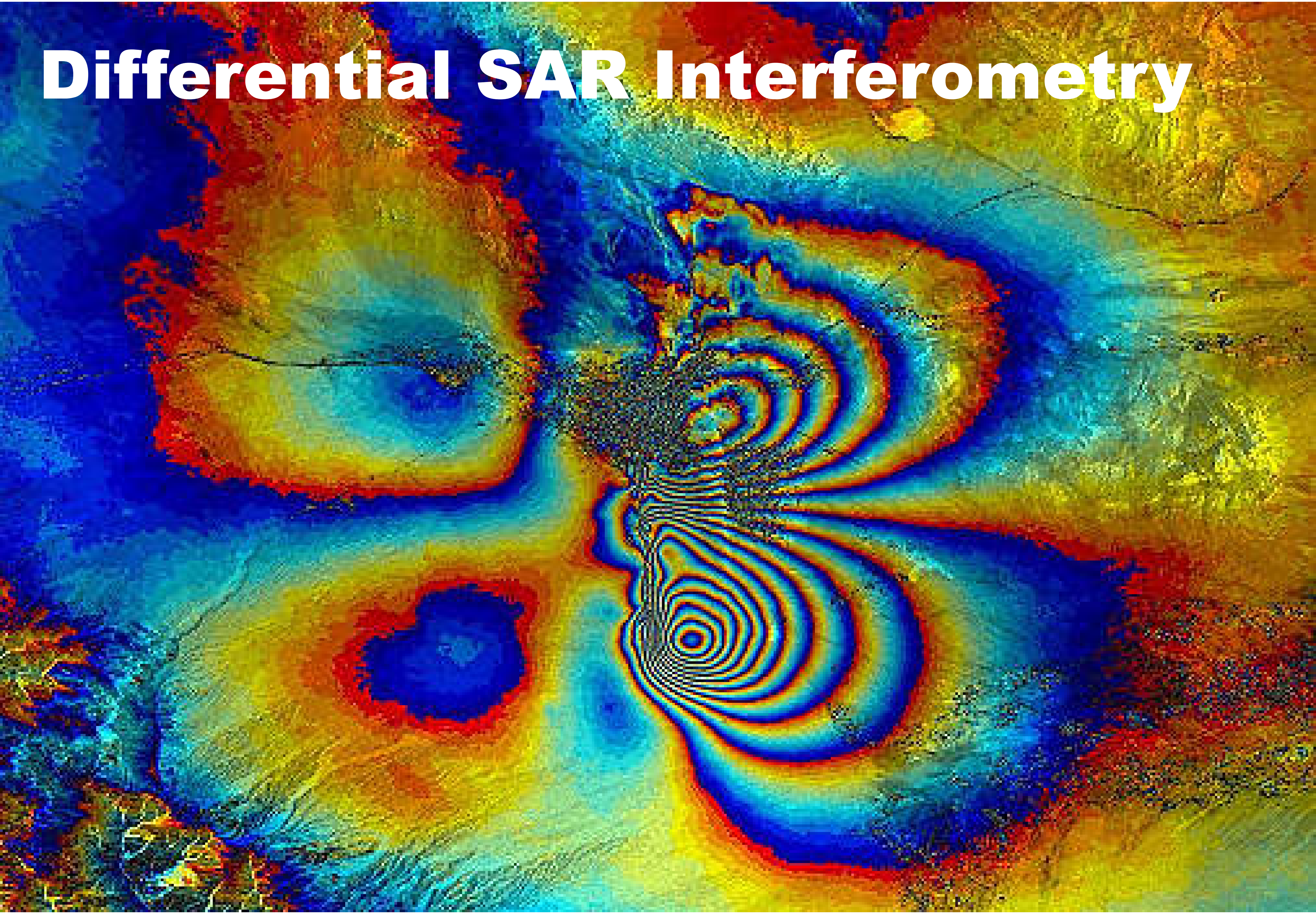

SAR Interferometry

Image 1: $i_1 = |i_1| \exp[-i(2\frac{2\pi}{\lambda}R_1) + \varphi_{S1}]$

Image 2: $i_2 = |i_2| \exp[-i(2\frac{2\pi}{\lambda}R_1) + \varphi_{S2}]$

Assuming $\varphi_{S1} = \varphi_{S2}$!!!

Interferogram: $i_1 i_2^* = |i_1 i_2^*| \exp[-i(2\frac{2\pi}{\lambda}\Delta R)]$

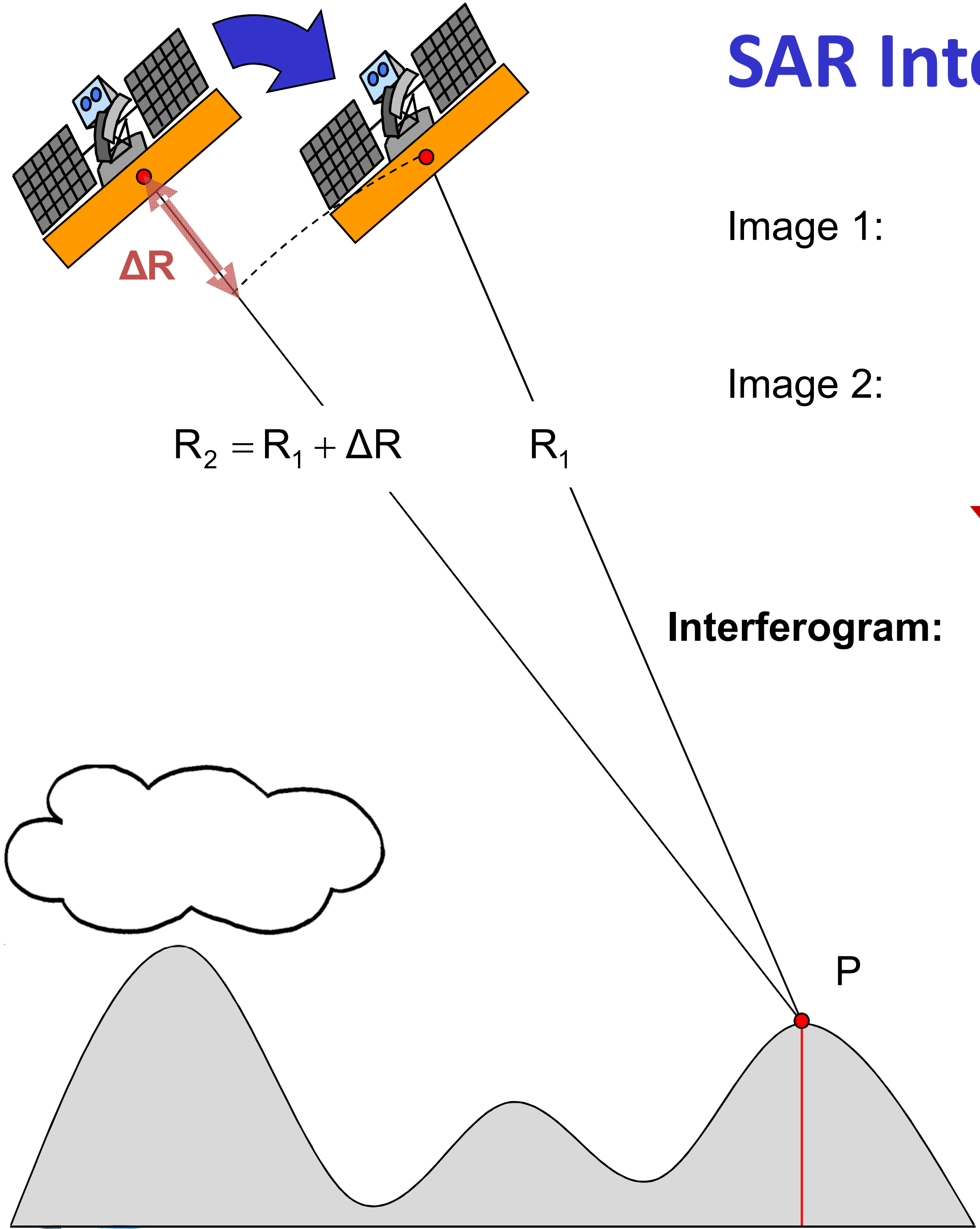

hajnsek@ifu.baug.e
irena.hajnsek@d

Differential SAR Interferometry (D-InSAR)

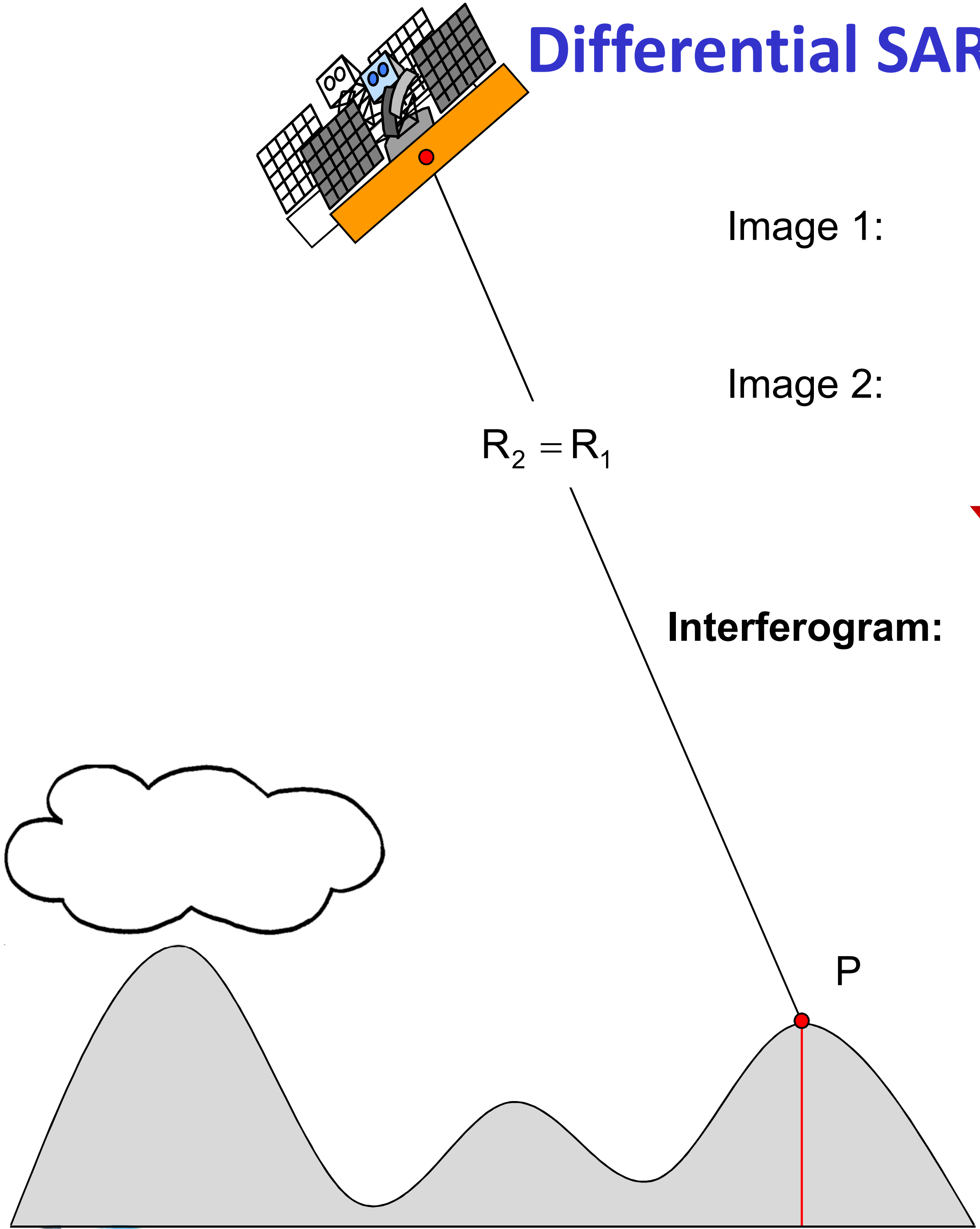

Image 1: $$i_1 = |i_1| \exp[-i(2\frac{2\pi}{\lambda}R_1) + \varphi_{S1}]$$

Image 2: $$i_2 = |i_2| \exp[-i(2\frac{2\pi}{\lambda}R_1) + \varphi_{S2}]$$

Assuming $\varphi_{S1} = \varphi_{S2}$!!!

Interferogram: $$i_1 i_2^* = |i_1 i_2^*| \exp[-i(2\frac{2\pi}{\lambda}\Delta R)] \xrightarrow{\Delta R=0} i_1 i_2^* = |i_1 i_2^*|$$

When the images are acquired from the same location i.e. the spatial baseline becomes zero, $\Delta R = 0$, and the intererometric phase loses its sensitivity to terrain elevation.

Differential SAR Interferometry (D-InSAR)

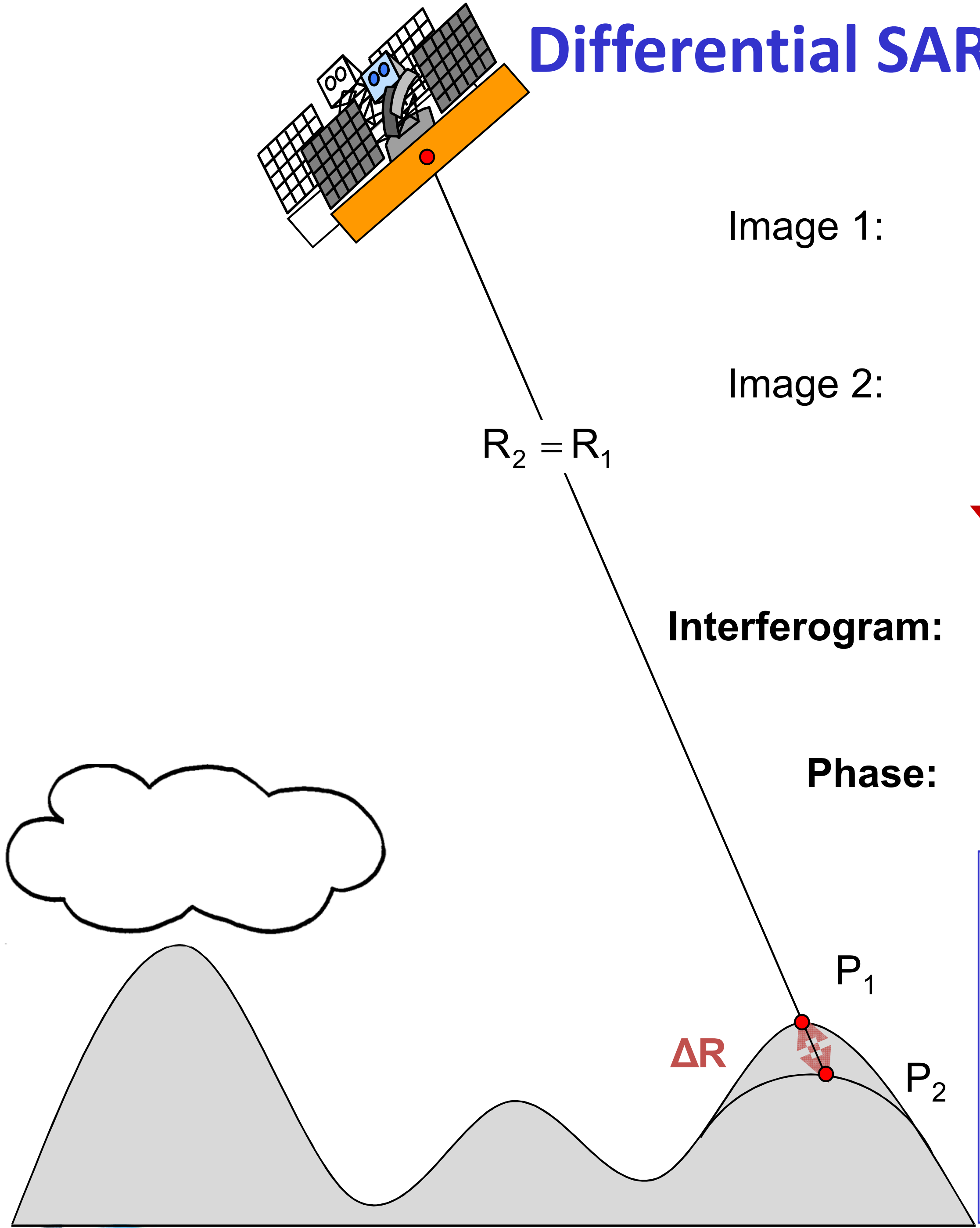

Image 1: $i_1 = |i_1| \exp[-i(2\frac{2\pi}{\lambda}R_1) + \varphi_{S1}]$

Image 2: $i_2 = |i_2| \exp[-i\ 2\frac{2\pi}{\lambda}(R_1 + \Delta R) + \varphi_{S2}]$

Assuming $\varphi_{S1} = \varphi_{S2}$!!!

Interferogram: $i_1 i_2^* = |i_1 i_2^*| \exp[-i(2\frac{2\pi}{\lambda}\Delta R)]$

Phase: $\varphi = \arg(i_1 i_2^*) = 2\frac{2\pi}{\lambda}\Delta R$

When the two images are acquired from the same location but at different times, i.e. with zero spatial & non-zero temporal baseline, **the intererometric phase** is **proportional** to the **change in the slant range distance** occurring in the time between the two acquisitions.

Differential SAR Interferometry

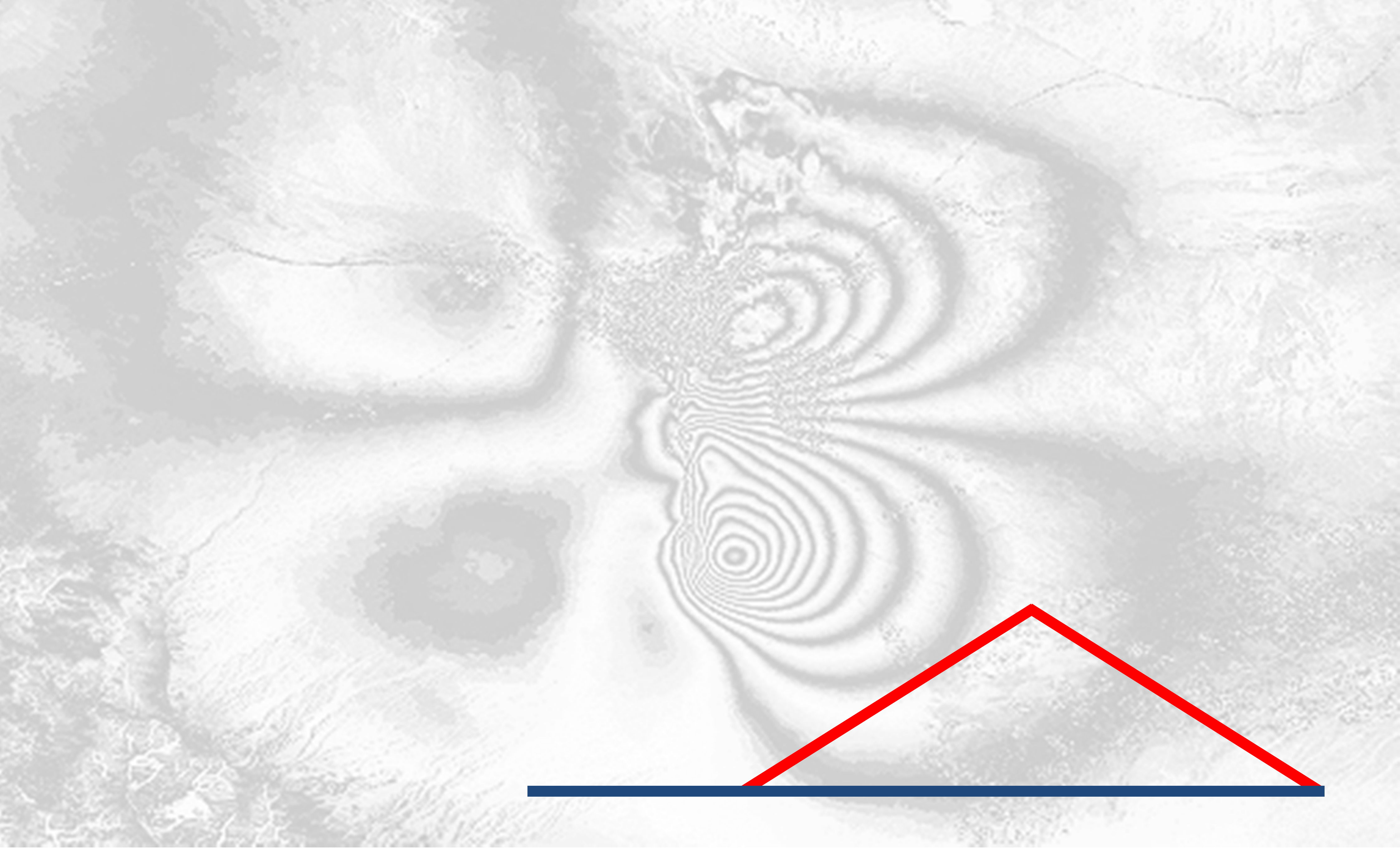

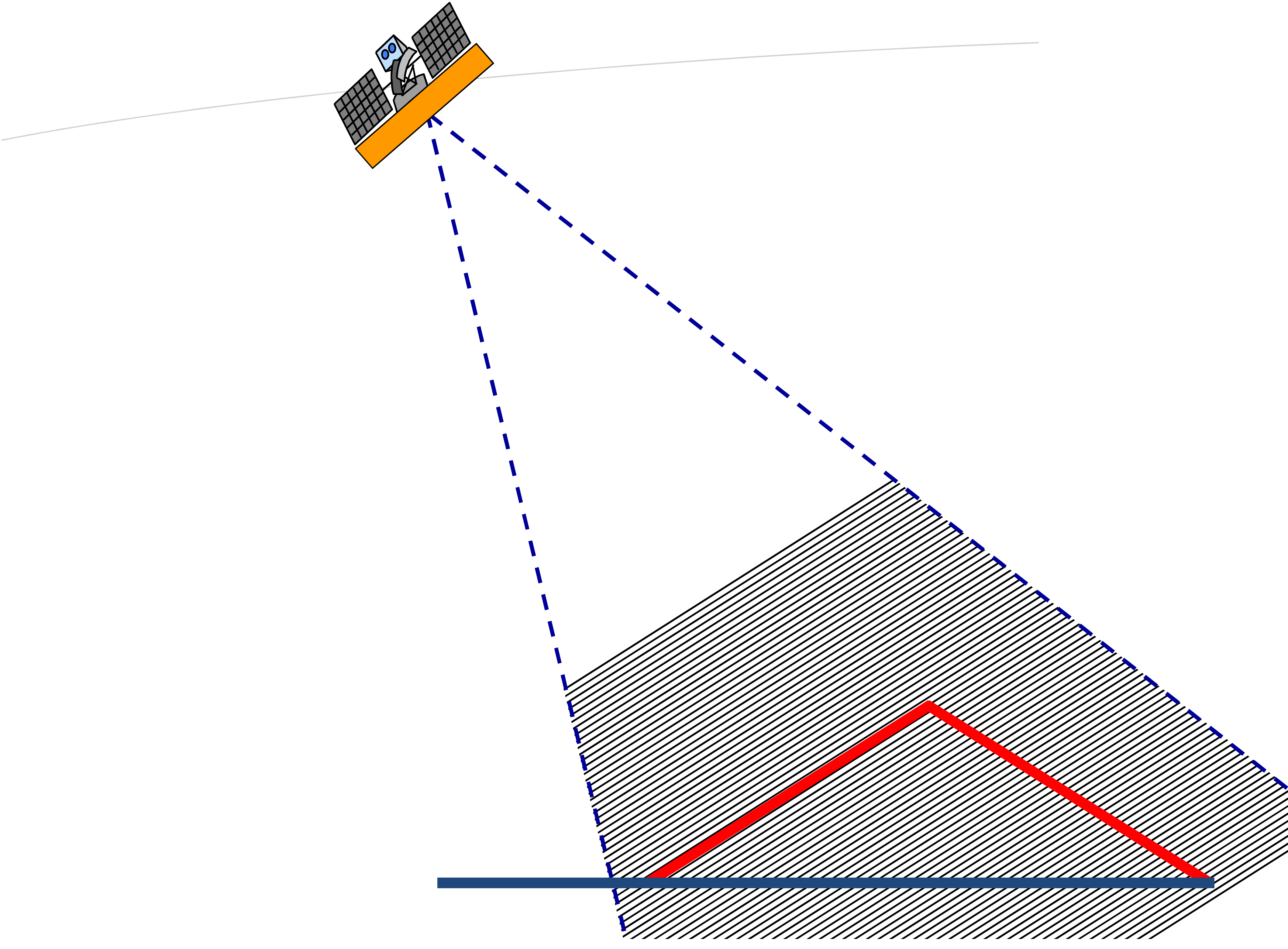

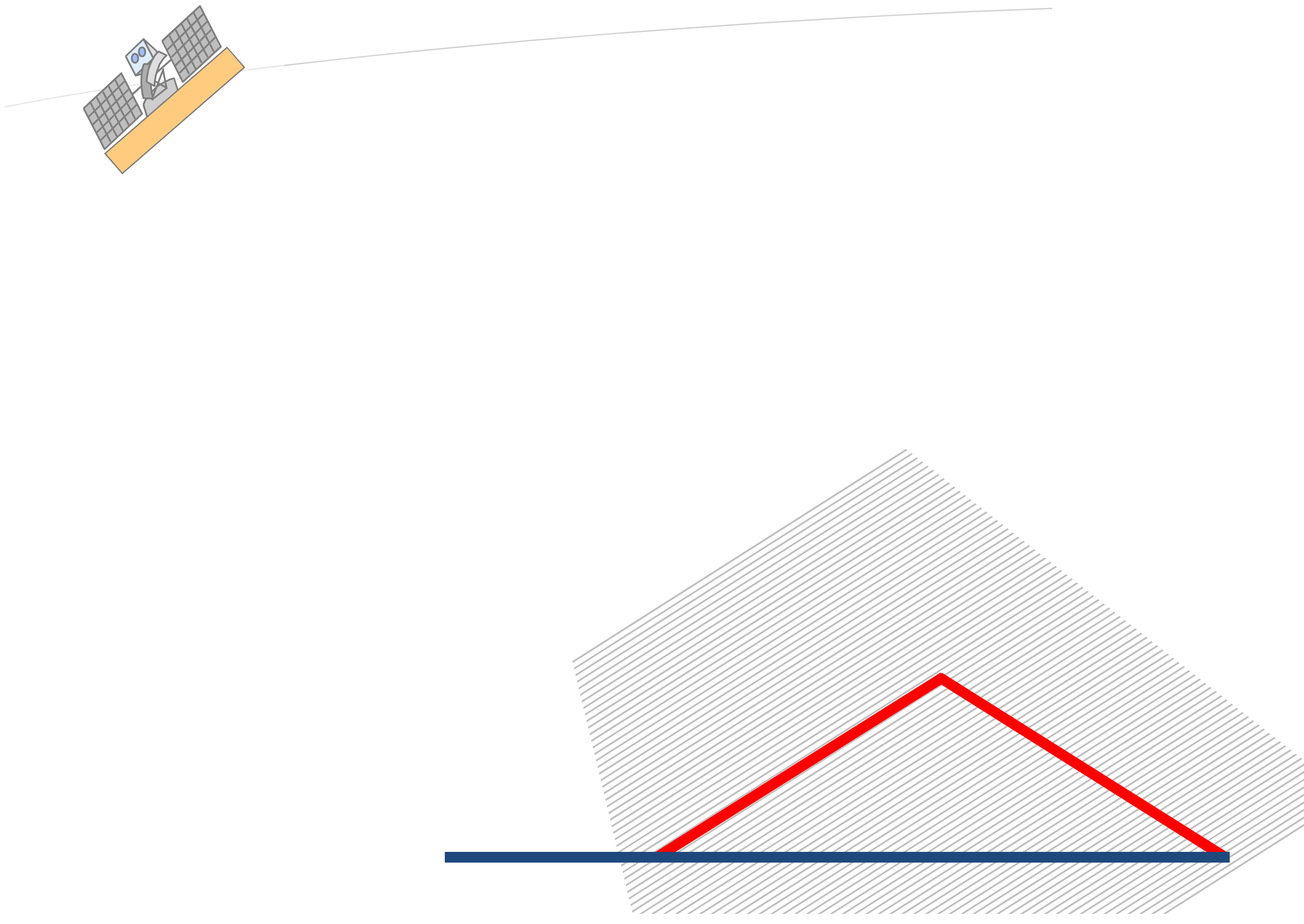

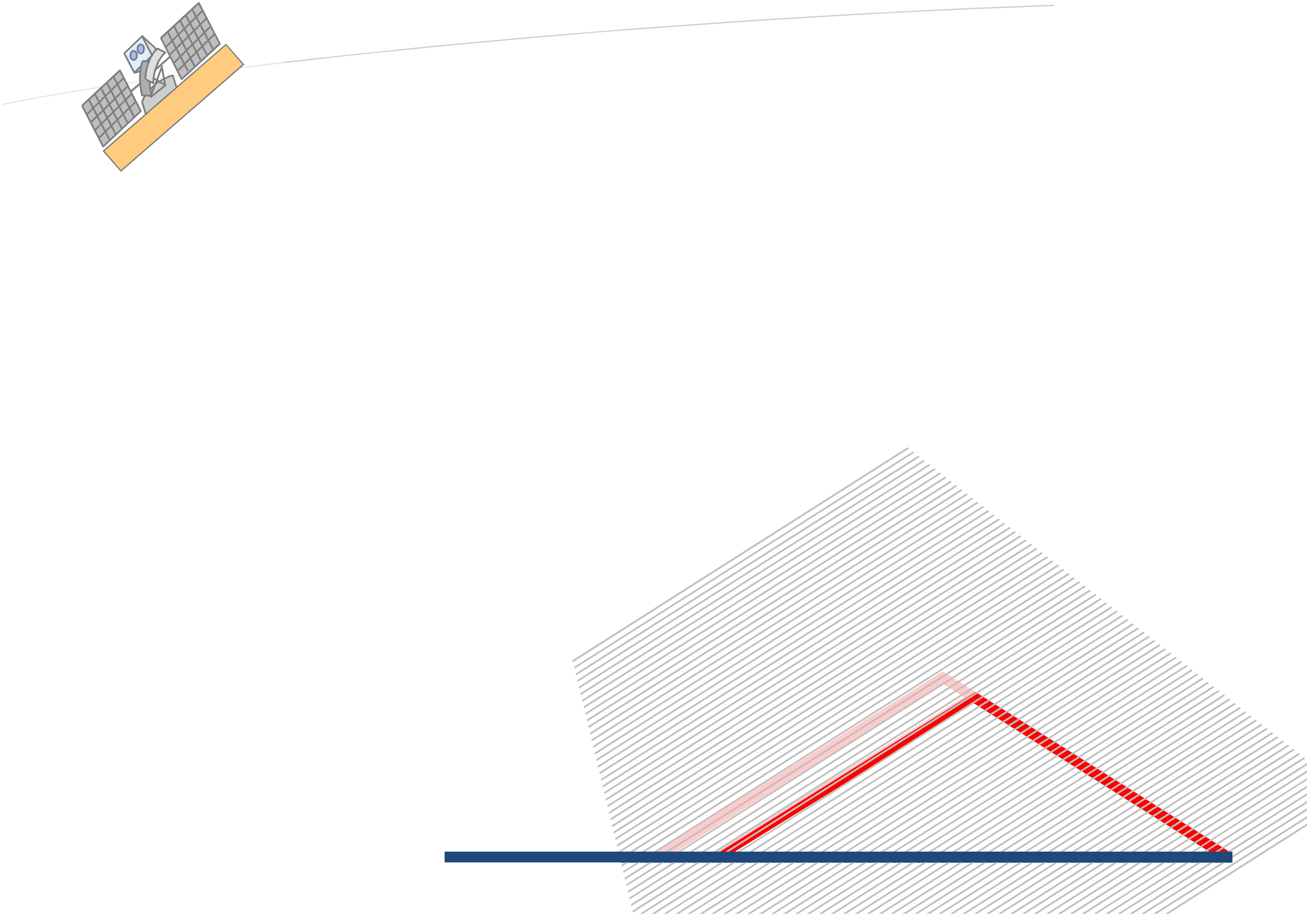

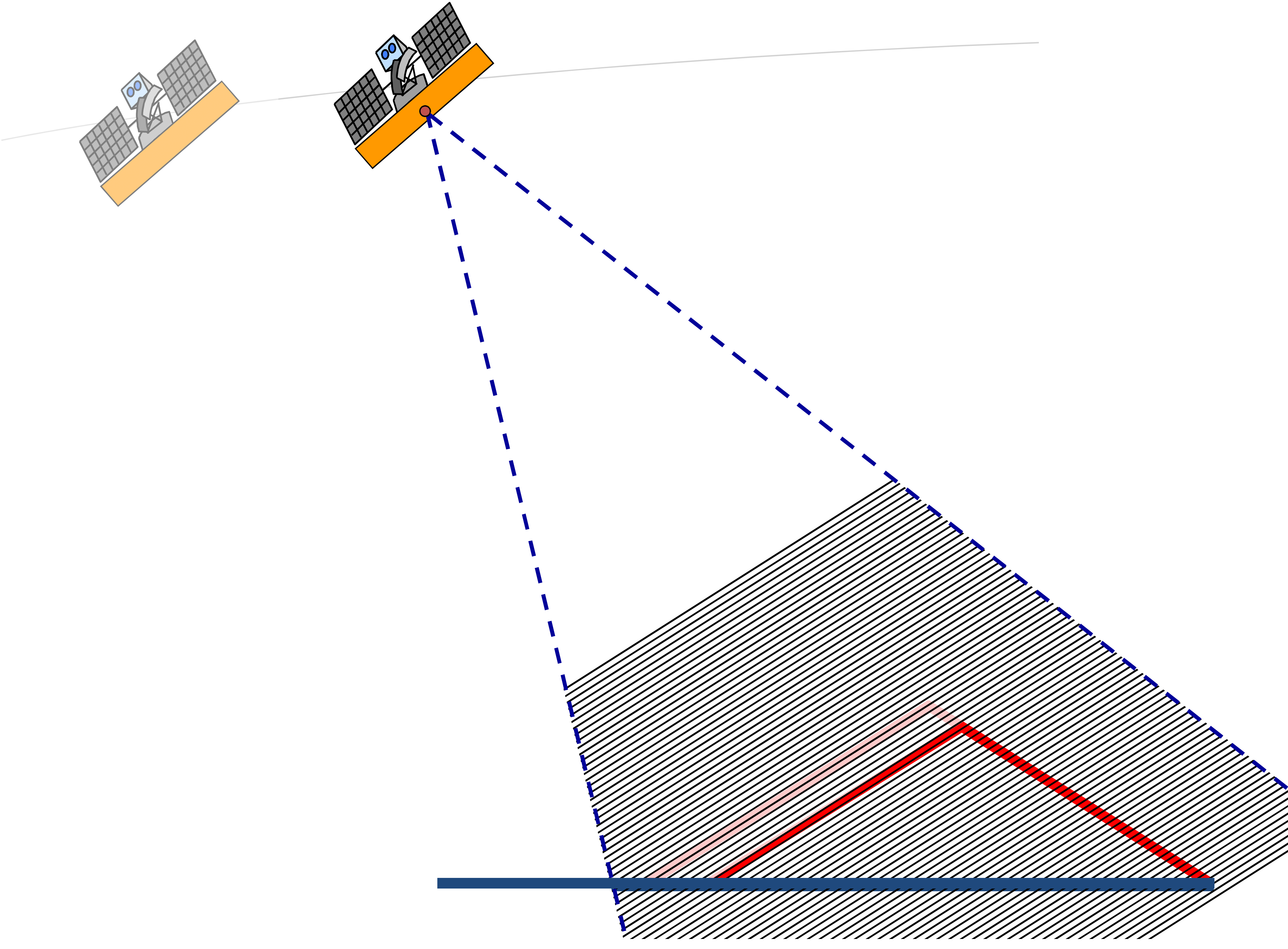

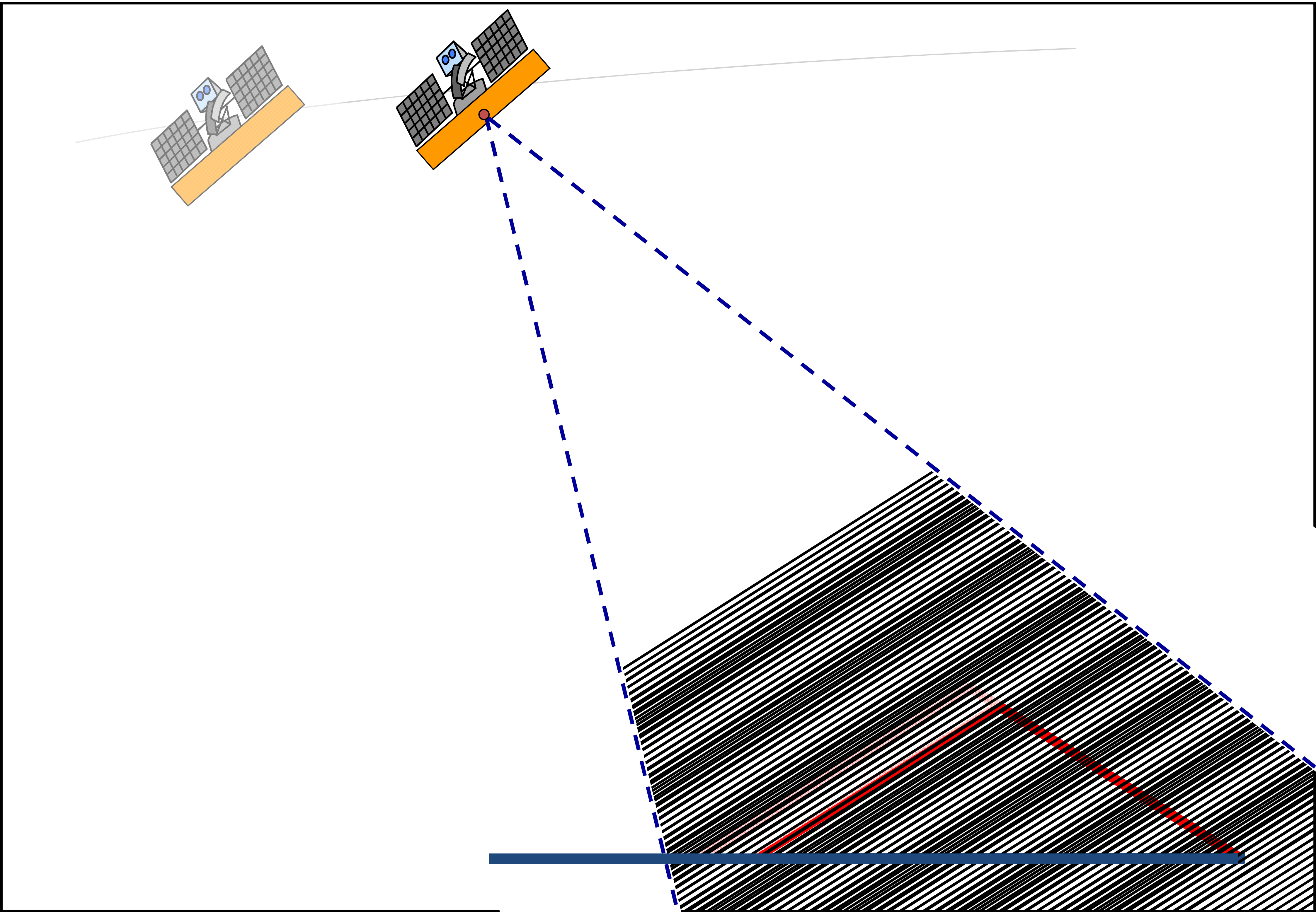

D-InSAR Phase: Height Sensitivity

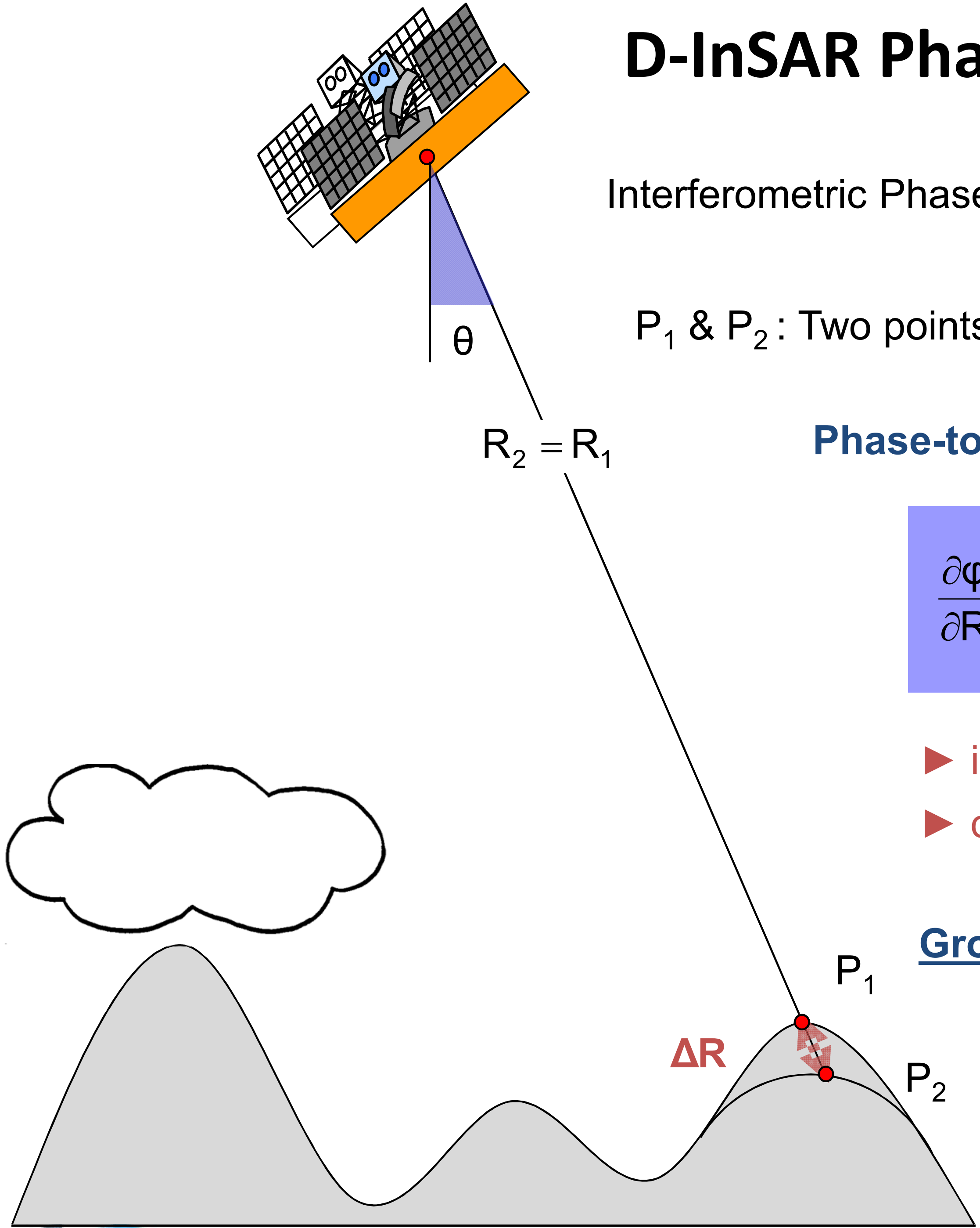

Interferometric Phase: $\varphi = 2\dfrac{2\pi}{\lambda}\Delta R + 2\pi\ N$ where $N = 0, \ \pm 1, \ \pm 2$

P_1 & P_2 : Two points at different slant range distance:

Phase-to-Slant-Range Distance Sensitivity:

$$\frac{\partial\varphi}{\partial R} := \frac{4\pi}{\lambda} \longrightarrow \sigma_R = \frac{\lambda}{4\pi}\sigma_\varphi$$

height error σ_R

► independent on the acquisition geometry

► depends only on the system wavelength

Ground range (hor.-) & **Height** (ver.- displacement):

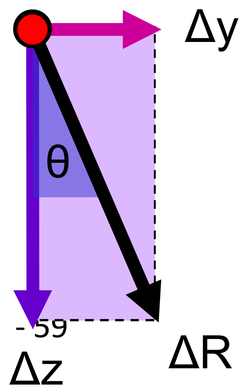

$$\Delta R = \Delta y \sin(\theta) + \Delta z \cos(\theta)$$

Earth Observation and Remote Sensing

hajnsek@ifu.baug.ethz.ch
irena.hajnsek@dlr.de

Eidgenössische Technische Hochschule Zürich
Swiss Federal Institute of Technology Zurich

InSAR vs D-InSAR

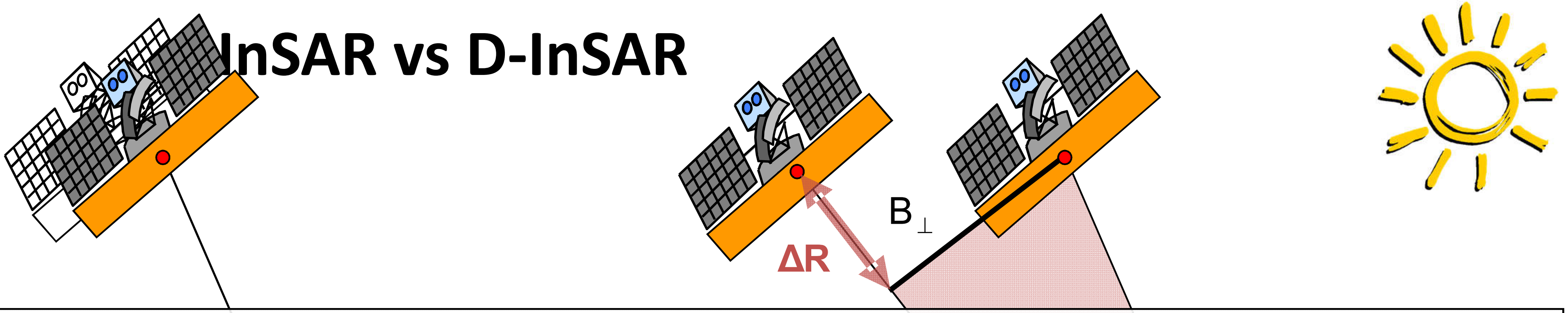

Example ERS: Space-borne C-band (λ=0.056m) interferometer with incidence θ=23° at range R=870km

1 (2π) phase cycle (i.e. 1 fringe) corresponds to:

D-InSAR

$$\sigma_R = \frac{\lambda}{4\pi}\sigma_\varphi = \frac{\lambda}{4\pi}2\pi = 0.028\ \text{m} \quad \text{(in LOS)}$$

$$\sigma_z = \frac{1}{\cos(\theta)}\sigma_R = 0.030\ \text{m} \quad \text{(vertical)}$$

$$\sigma_y = \frac{1}{\sin(\theta)}\sigma_R = 0.072\ \text{m} \quad \text{(horizontal)}$$

InSAR

$$\sigma_z = \frac{\lambda}{4\pi}\frac{R\sin(\theta)}{B_\perp}\sigma_\varphi = \frac{\lambda}{4\pi}\frac{R\sin(\theta)}{B_\perp}\frac{10}{360}2\pi$$

At perp. baseline $B_\perp$=100m: σ_z=100m terrain elevation

At perp. baseline $B_\perp$=200m: σ_z= 50m terrain elevation

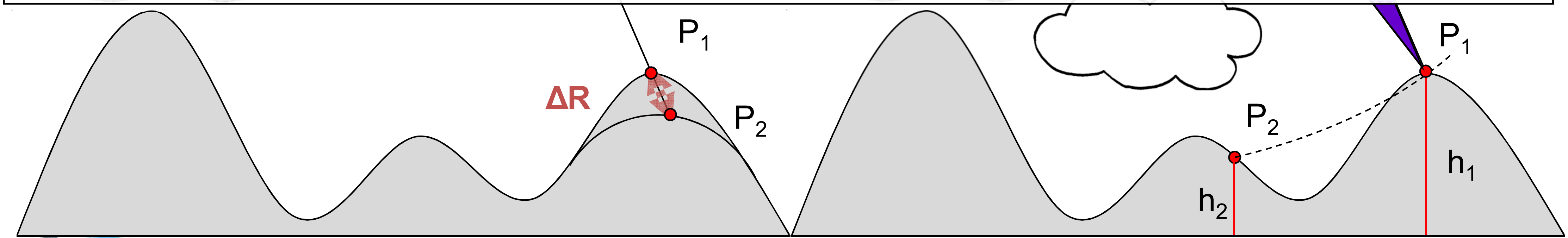

hajnsek@ifu.baug.e
irena.hajnsek@d

InSAR vs D-InSAR

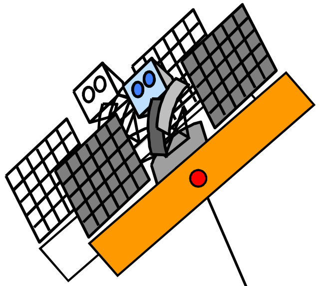

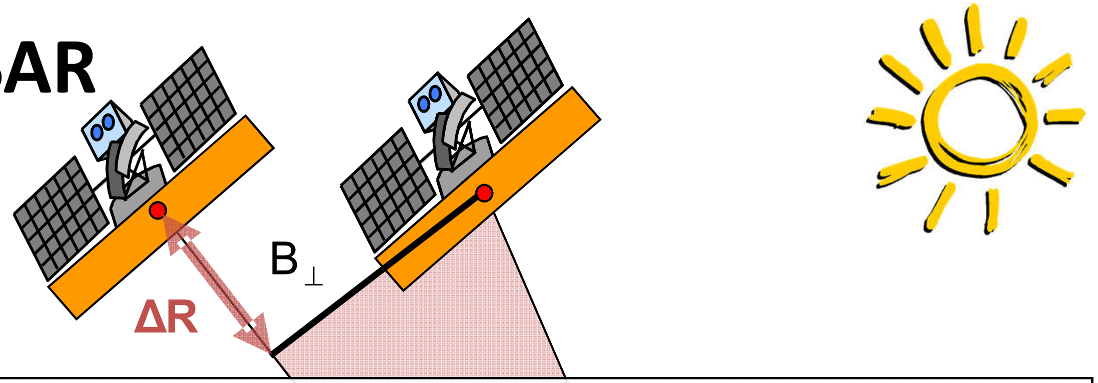

<u>Example ERS</u>: Space-borne C-band (λ=0.056m) interferometer with incidence θ=23° at range R=870Km

Assuming the ability to measure the interferometric phase with an accuracy of 20°:

D-InSAR

$$\sigma_R = \frac{\lambda}{4\pi}\sigma_\varphi = \frac{\lambda}{4\pi}\frac{20}{360}2\pi \approx 1.5\ \text{mm} \quad \text{(in LOS)}$$

$$\sigma_z = \frac{1}{\cos(\theta)}\sigma_R = 1.6\ \text{mm} \quad \text{(vertical)}$$

$$\sigma_y = \frac{1}{\sin(\theta)}\sigma_R = 4.0\ \text{mm} \quad \text{(horizontal)}$$

InSAR

$$\sigma_z = \frac{\lambda}{4\pi}\frac{R\sin(\theta)}{B_\perp}\sigma_\varphi = \frac{\lambda}{4\pi}\frac{R\sin(\theta)}{B_\perp}\frac{20}{360}2\pi$$

At perp. baseline $B_\perp$=100m: σ_z= 5.50m terrain error

At perp. baseline $B_\perp$=200m: σ_z= 2.75m terrain error

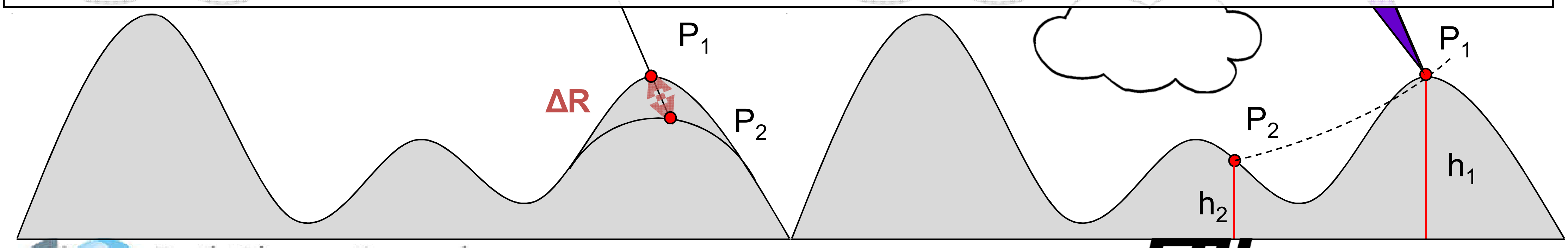

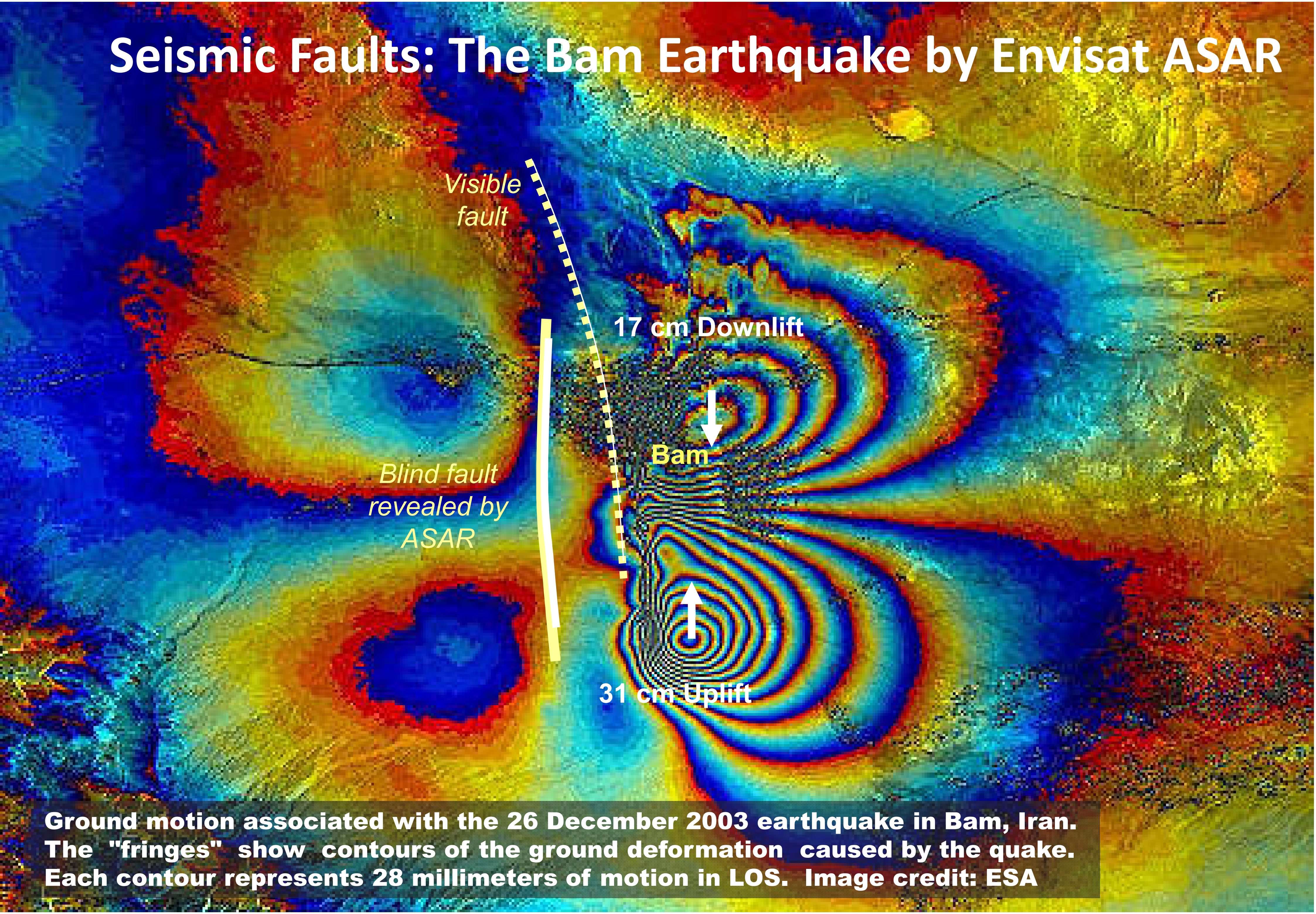
Seismic Faults: The Bam Earthquake by Envisat ASAR
Visible fault
17 cm Downlift
Bam
Blind fault revealed by ASAR
31 cm Uplift
Ground motion associated with the 26 December 2003 earthquake in Bam, Iran.
The "fringes" show contours of the ground deformation caused by the quake.
Each contour represents 28 millimeters of motion in LOS. Image credit: ESA

Ice motion of fast moving glaciers

The combination of **short repeat pass times** and a **systematic acquisition scenario** and a low SAR frequency (**L-band**) is optimum for fast ice motion.

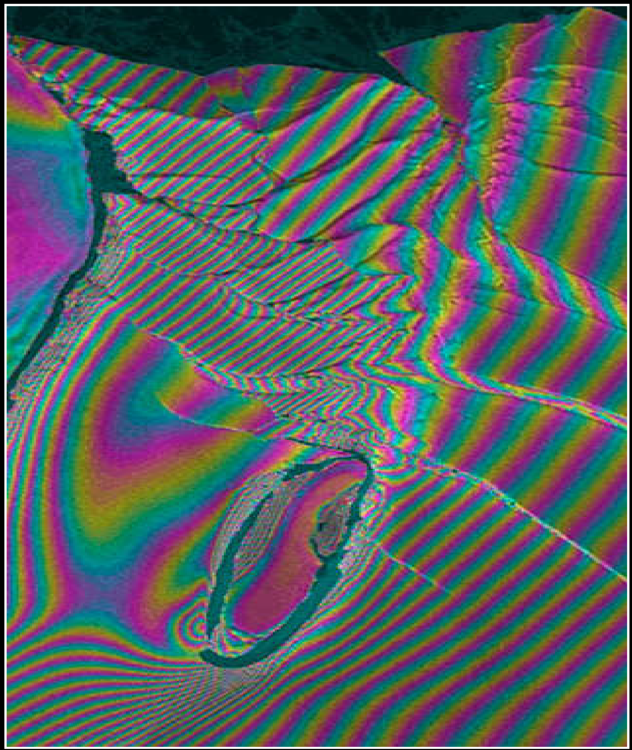

ERS Tandem 1-Day RP Time

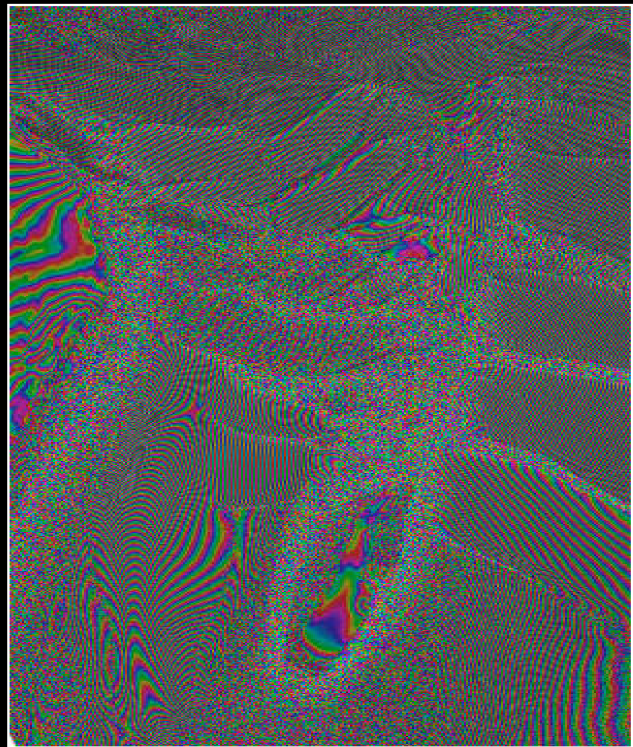

RADARSAT 24-Days RP Time

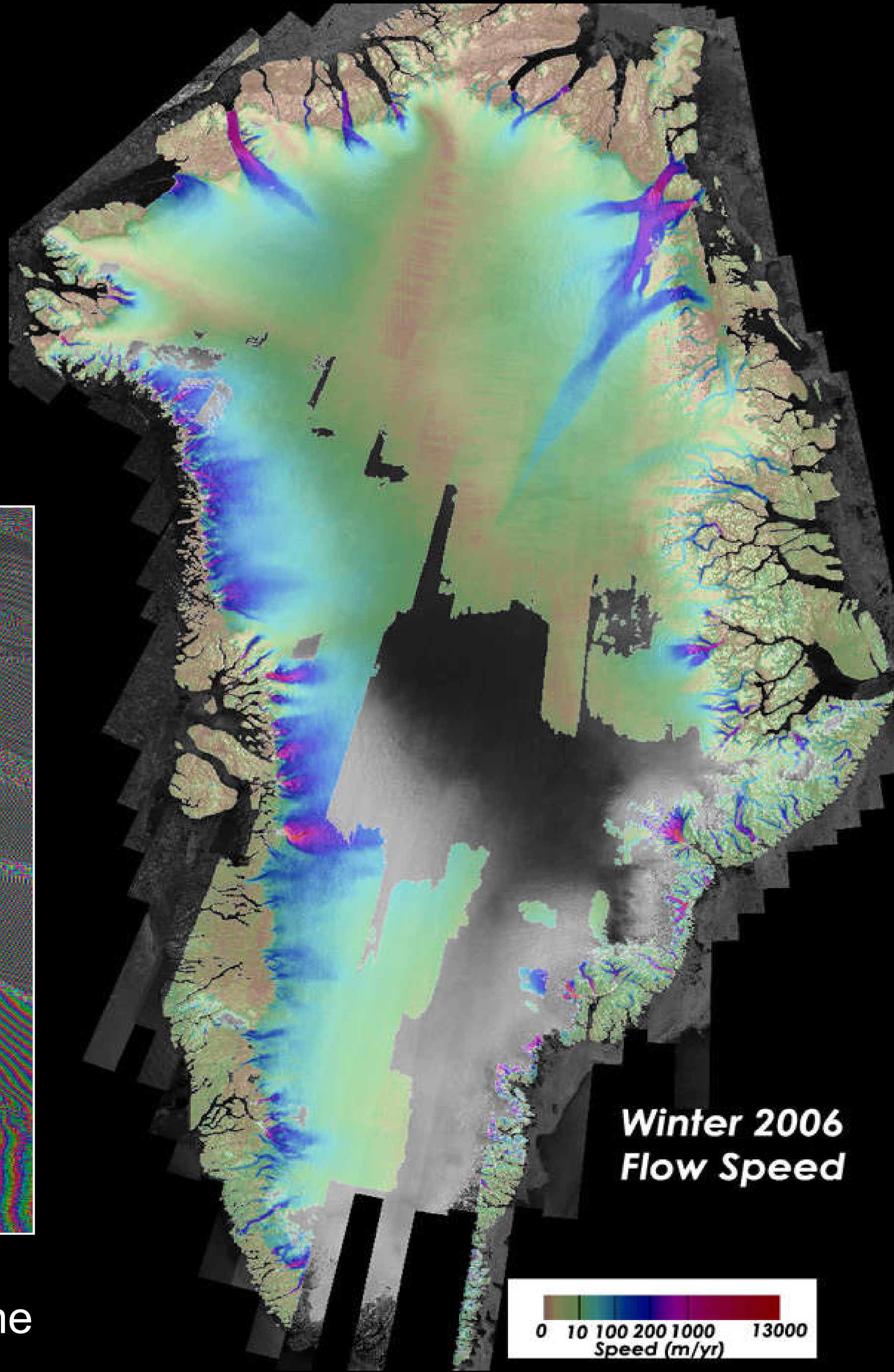

Image credit: NASA/JPL

Ice Surface Velocity from TerraSAR-X: Nimrod Glacier

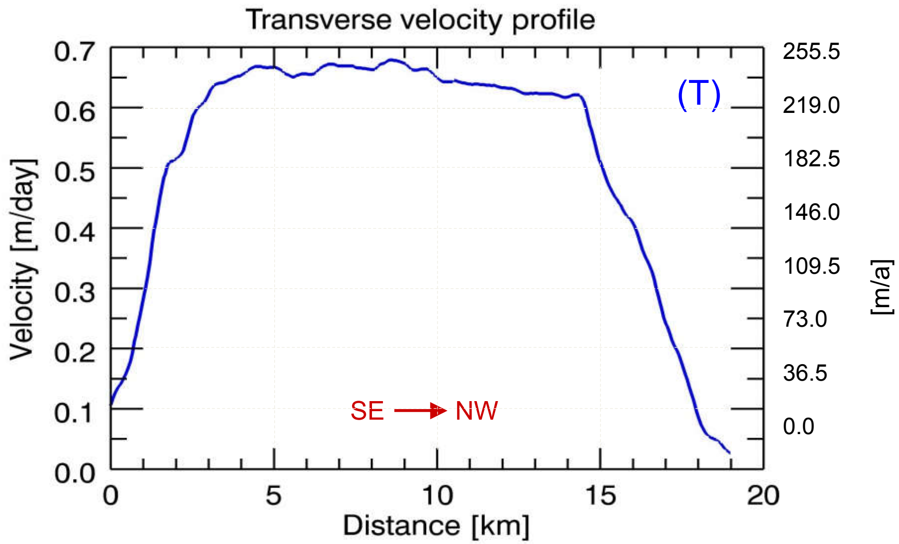

Plug-like shape: strong side drag

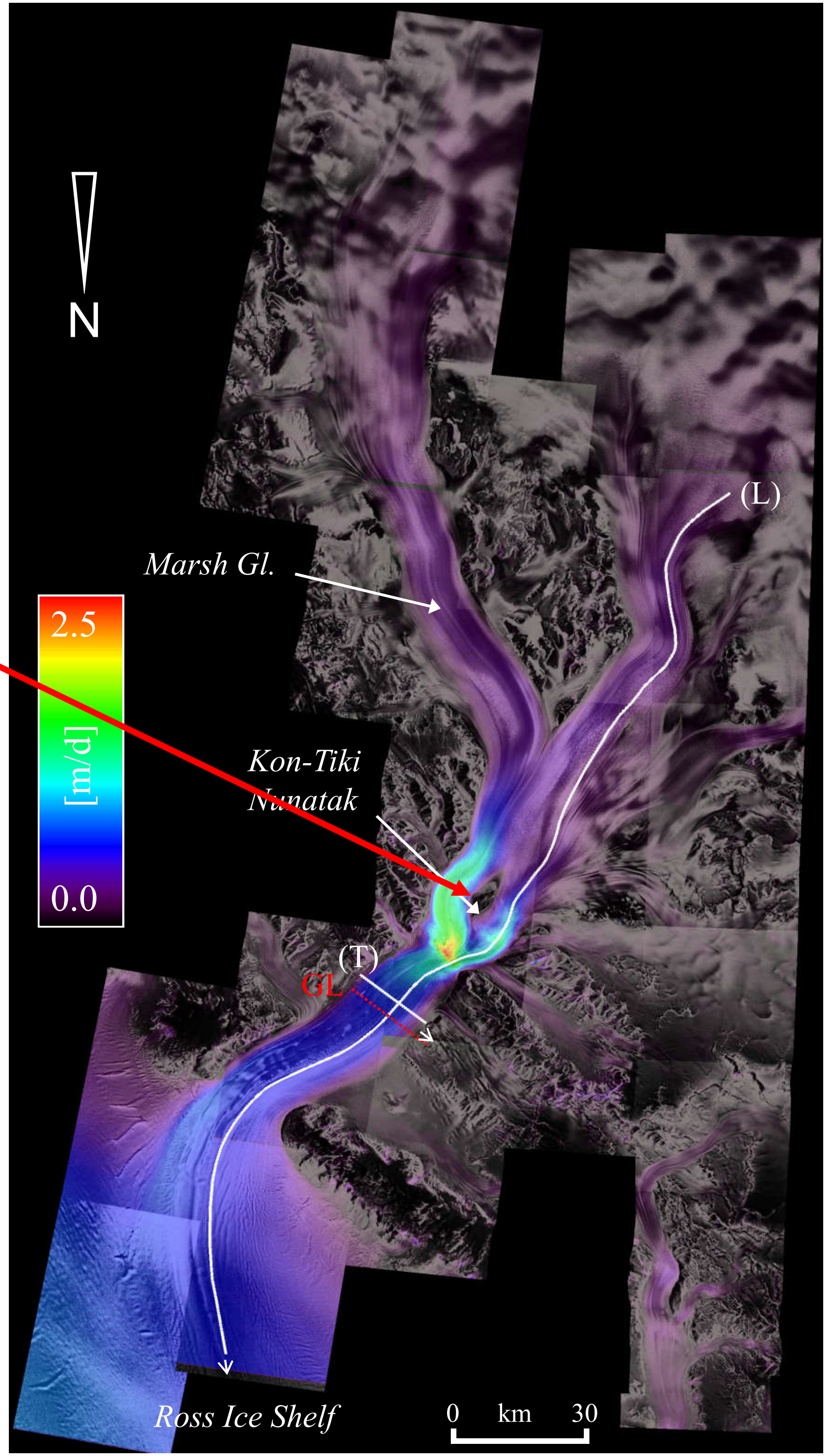

hajnsek@ifu.baug.ethz.ch
irena.hajnsek@dlr.de

Thermal Dilation: Berlin Main Train Station

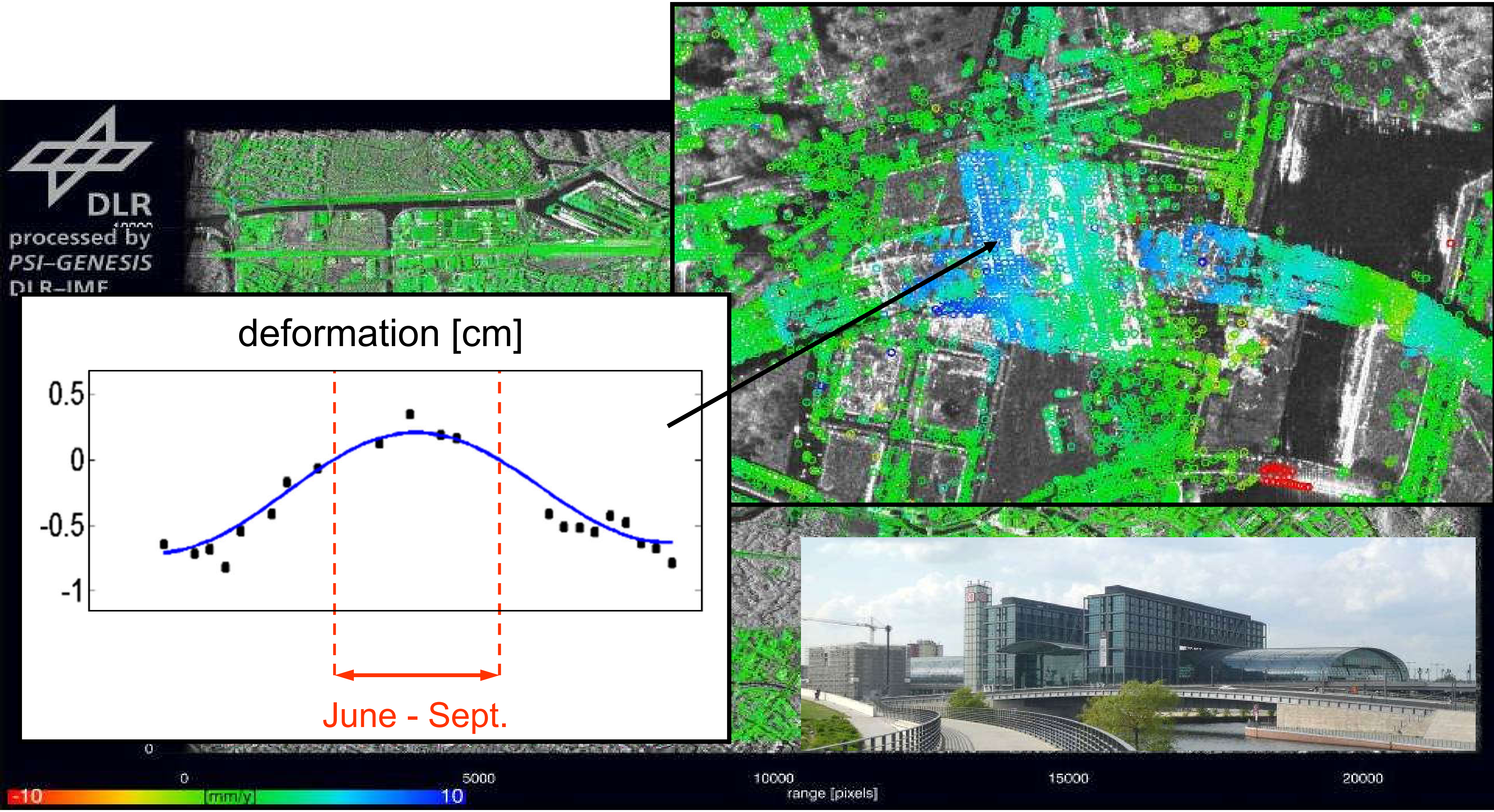

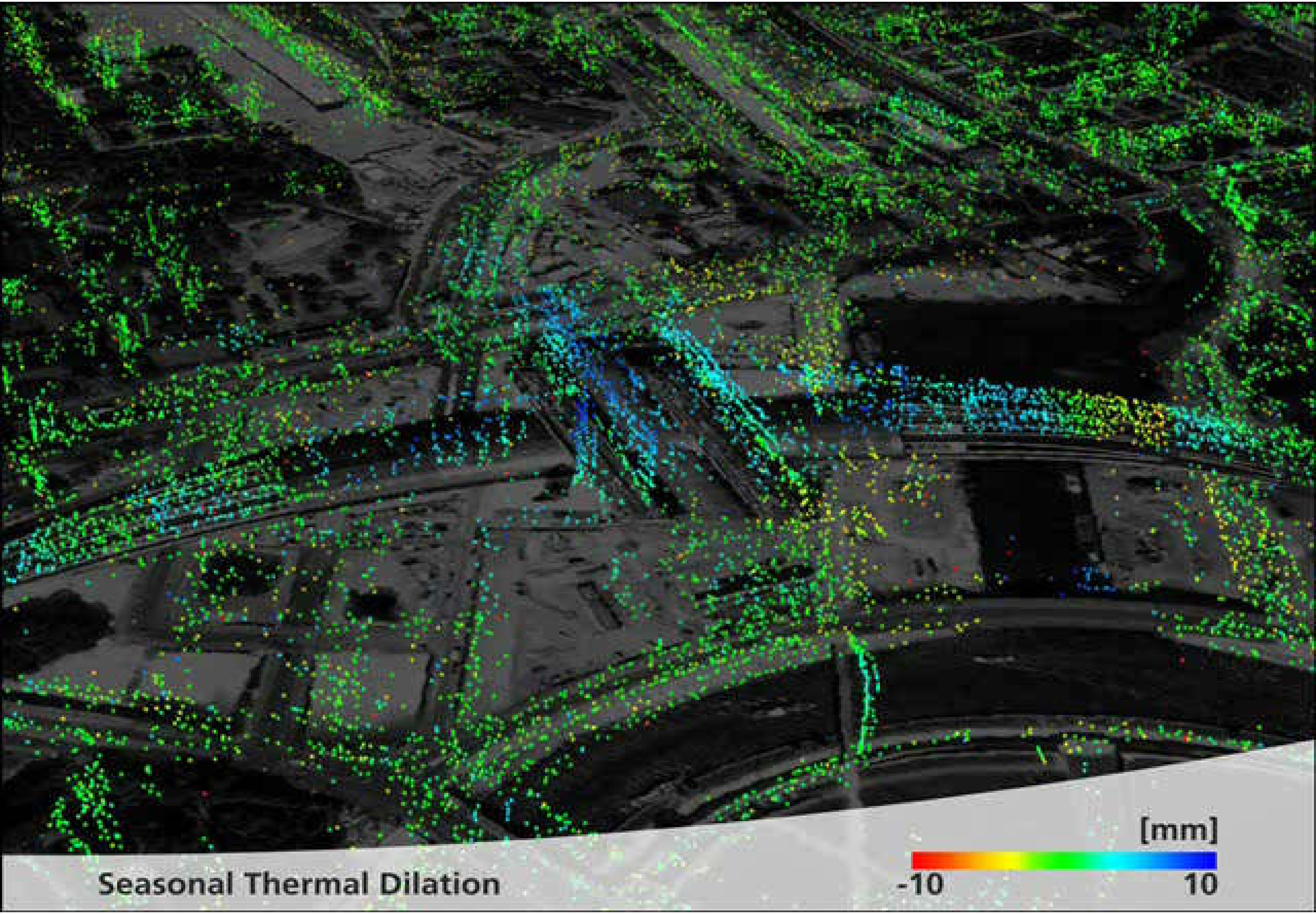

[mm]
Seasonal Thermal Dilation
-10
10

PSI Land Subsidence Monitoring

Semarang - Indonesia

27/12/02 to 23/08/06

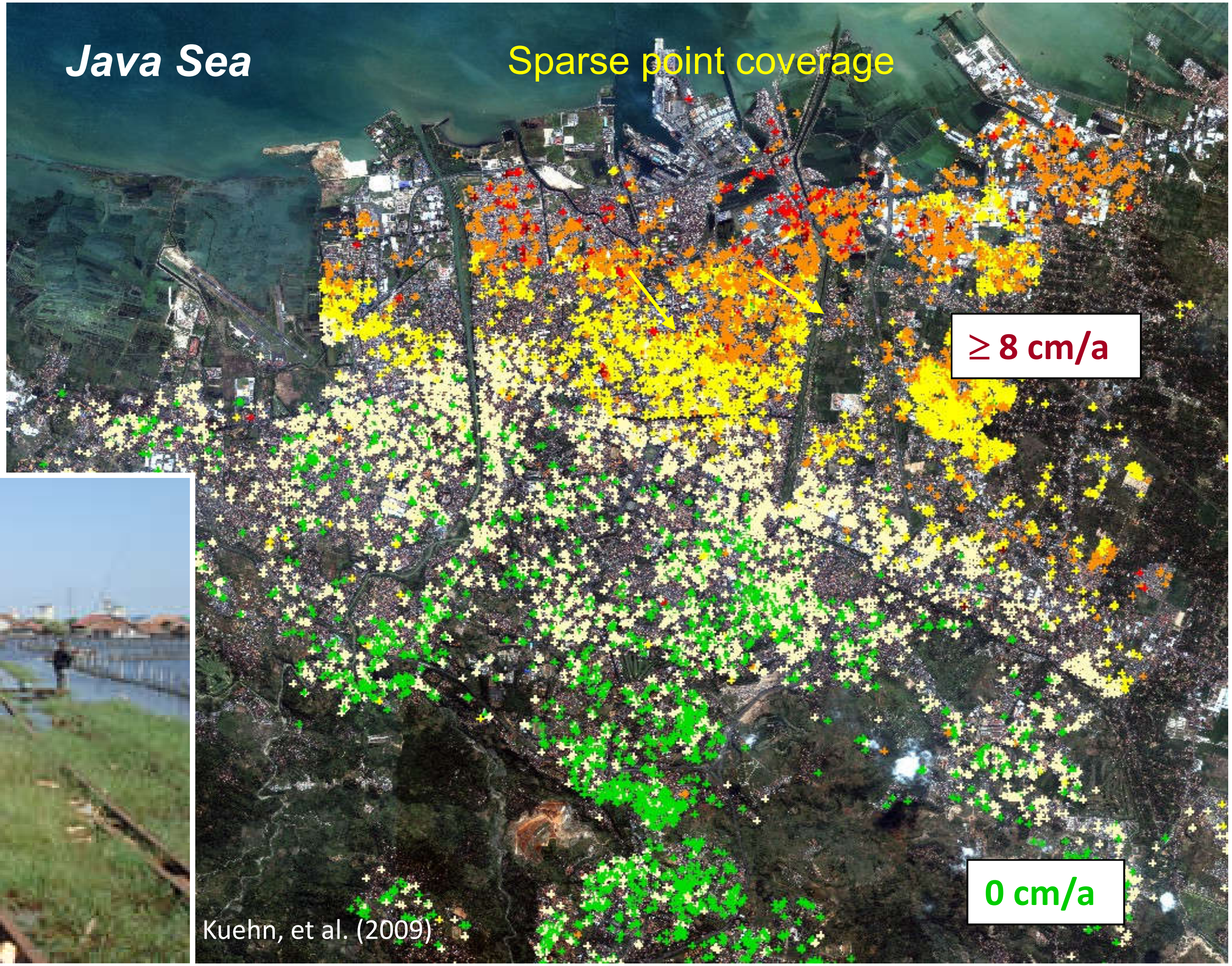

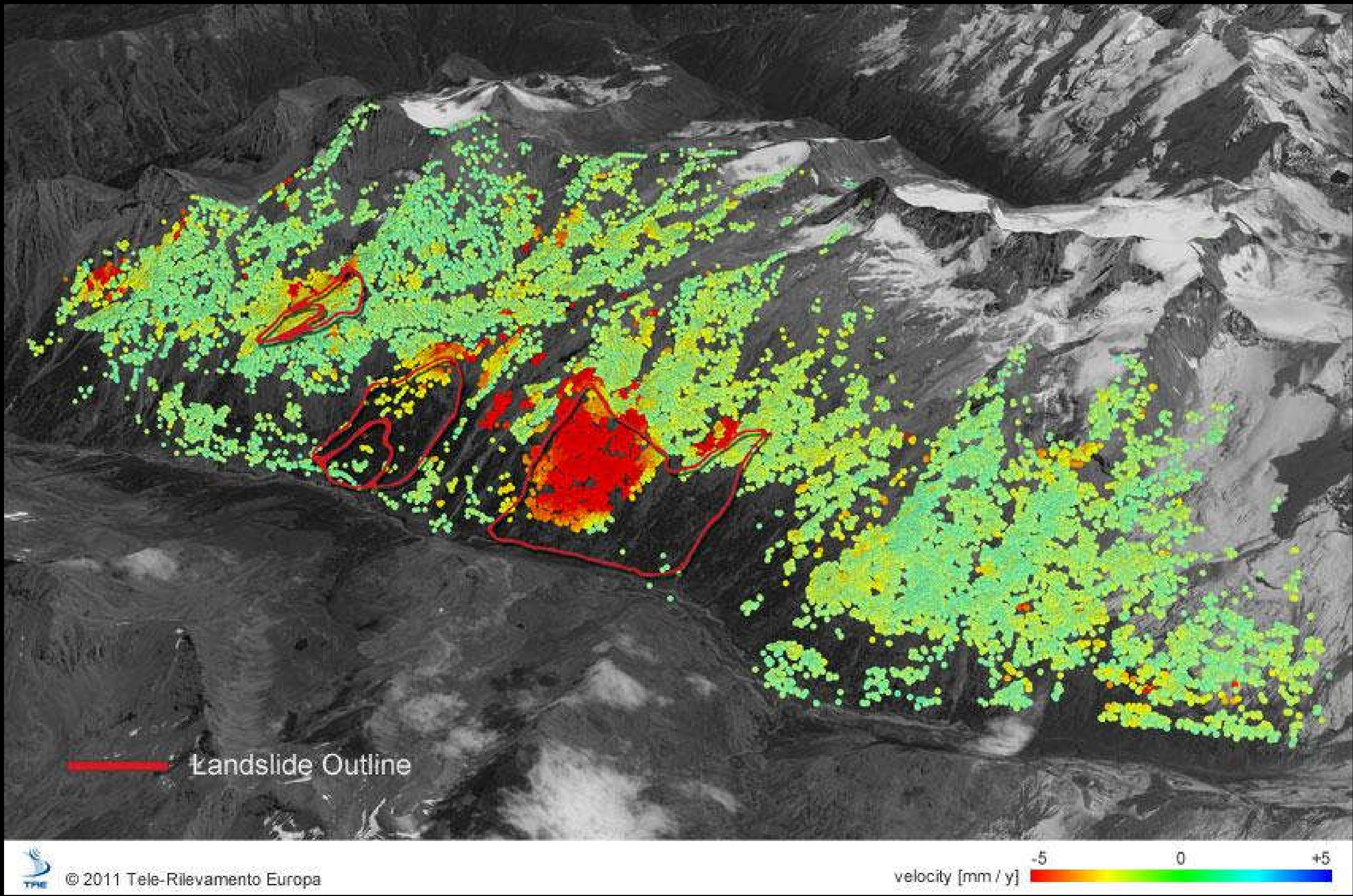

Active landslide in Valsavarenche, Italy. For each ground point identified a time-series of its deformation can be reconstructed to show its movement over the time period analyzed. Image credit: Treuropa / Sensor: Radarsat